An Air Quality Assessment of the European Nested Grid of the GEOS-Chem Model and the Influence of the Agricultural Sector

Timothy James Garstin

MSc by Research

University of York

Chemistry

December 2017

Abstract

Air pollutants have a serious influence on public health. The ability of a chemical transport model (CTM) to capture pollutant concentrations is paramount to understanding air quality issues.

For the first time the European nested (0.25° x 0.3125°) grid version of the GEOS-Chem model of chemistry and transport has been compared to European wide observations. Comparison between the model and the European Airbase monitoring network showed that the model is capturing Nitrogen Dioxide (NO_2) seasonality albeit with a negative bias. The model was found to not be capturing the observed rise in NO_2 rush hour concentrations across Europe sufficiently, suggesting that a re-evaluation of the transport NO_x source in Europe is needed. For ethane and propane the model captured seasonality in concentrations but had a negative bias which was found to be likely from a missing source. This source is potentially gas leaks from the natural gas network not being accounted for in the model. The model captures ozone European seasonal concentrations well, with a small positive (between 2-15 nmol mol^{-1} across regions), bias that is worse during the night. The afternoon peak in ozone is well represented by the model in Europe, which is important for air quality applications.

For Particulate Matter with diameter of less than 2.5 μm ($PM_{2.5}$), the model captures seasonality well, with a small positive bias (5-11 μg m^{-3} across regions), that is exacerbated during periods of elevated concentration. Comparing modelled $PM_{2.5}$ composition against the observational UK MARGA network, showed the model performed reasonably well and confirmed the modelled overestimation in $PM_{2.5}$ was likely due to an overestimation of nitrates and sulphates in the model, which is likely due to uncertainties in the ammonia emissions inventory.

The ability of the GEOS-Chem model to capture $PM_{2.5}$ short term events was assessed. The model captured the timing of these high concentrations. There was differing reasons as to why these PM events occured. Both vehicular emissions (NO_x) and agricultural emissions (NH_3) played a role. From this we conclude that the March and April 2014 events were nitrate driven, highlighting the agricultural sector was a key component in exacerbating PM levels during the pollution event.

Removing all agricultural emissions from the model has a profound impact on the european $PM_{2.5}$ with the domain-mean surface $PM_{2.5}$ concentration, with a fractional difference typically between 0.35 and 0.65 when emissions are switched off. For some regions (e.g. The Po Valley, central Europe, Turkey, and parts of north western Europe) there are large decreases in the number of days $PM_{2.5}$ exceeds the WHO 25 μg m^{-3} limit (upto ~225 days, ~125 days, ~110 days and ~90 days respectively). Policies that target the reduction in agricultural ammonia emissions are likely to result in a significant reduction in the concentration of surface $PM_{2.5}$ over Europe.

Overall the model shows many positive traits, particularly capturing in ozone and $PM_{2.5}$. However, it requires more extensive evaluation and comparison to observations before there can be confidence in its suitability for use in develop by European wide air quality policy and science.

Table of Contents

Abstract **3**

Table of Contents **4**

List of Figures **6**

List of Tables **9**

Acknowledgements **10**

Declaration **11**

Chapter 1 Introduction **13**

1.1 Air quality: What is it and why should we care? 13

1.2 Key air quality species, their formation, sinks and health impacts 13

1.2.1 Nitrogen dioxide (NO_2) 13

1.2.2 Non-methane hydrocarbons (NMHCs) 15

1.2.3 Ozone 16

1.2.4 Particulate matter 17

1.3 Air quality in Europe and the UK 21

1.3.1 EU air quality 21

1.3.2 UK air quality 22

1.4 Meteorology of pollution events 23

1.4.1 Wintertime pollution episodes in 2014 24

1.5 Thesis outline 24

Chapter 2 Observational Datasets **26**

2.1 The AQER network 26

2.1.1 Setup 26

2.1.2 AQER data management 29

2.2 The MARGA network 32

2.3 The NOAA network 33

2.4 Summary 34

Chapter 3: The GEOS-Chem Model **35**

3.1 Introduction 36

3.2 Model description 35

3.3 Emissions 37

3.3.1 Natural processes 37

3.3.2 Anthropogenic emissions 37

3.4 Deposition 38

3.5 Chemistry and transport 38

3.6 Diagnostics 38

3.7 Model simulations 39

Chapter 4: General Model Performance over regions of Europe 40

4.1 NO_2 40

4.1.1 Seasonal cycles 40

4.1.2 Point by point (hourly) comparisons 41

4.1.3 Diurnal cycles 42

4.1.4 NO_2 conclusions 45

4.2 NMHCs 45

4.2.1 Seasonal cycles 46

4.2.2 Point by point (hour) comparisons 47

4.2.3 Diurnal cycles 49

4.2.4 NMHCs comparison to Mace head Ireland 50

4.2.5 VOC conclusions 52

4.3 Ozone 52

4.3.1 Seasonal cycles 52

4.3.2 Point by point (hourly) comparisons 53

4.3.3 Diurnal cycles 55

4.3.4 Ozone Conclusions 57

4.4 $PM_{2.5}$ 58

4.4.1 Seasonal cycles 58

4.4.2 Point by point (hourly) comparisons 58

4.4.3 Diurnal cycles 61

4.4.4 $PM_{2.5}$ European conclusions 62

4.5 UK $PM_{2.5}$ composition 63

4.5.1 Stacked vs line time series and $PM_{2.5}$ composition vs total $PM_{2.5}$ plots 64

4.5.2 Comparisons with observations from the MARGA network. 66

4.5.3 Conclusions 67

Chapter 5: The Ability of the Model to Capture UK $PM_{2.5}$ Events 69

5.1 Comparison with the AQER network 69

5.2 Comparison to the MARGA Network 72

5.3 Summary 69

Chapter 6: Influence of the Agricultural Sector on $PM_{2.5}$ 75

6.1 The European agricultural burden on $PM_{2.5}$ 75

6.2 The agricultural burden on UK Spring PM episodes 80

6.3 Summary 82

Chapter 7: Conclusions 84

List of Abbreviations 86

References 87

List of Figures

Figure 1 this is the geos-fp 0.25 x 0.3125 degree resolution nested grid over europe. image from http://wiki.seas.harvard.edu/geos-chem/index.php/GEOS-Chem_horizontal_grids. 27

Figure 2 The log probability distribution function of observed NO_2, SO_2, CO and $PM_{2.5}$ and the log probability distribution function of ozone for all background sites (N = 4951) across the EU during the observation period. 32

Figure 3 Comparison of monthly median modelled and observed NO_2 concentrations for regions within Europe during the observational period. The shaded areas give the monthly standard deviation across the sites in the region. 41

Figure 4 Hourly NO_2 observed and modelled concentrations for regions within Europe during the observational period. hexagon colour shading is on a logarithmic scale which represents the density of scatter points within the hexagon area. Green line represents the line of best fit. Dashed lines represent 1:2, 1:1 and 2:1 ratios. 43

Figure 5 Comparison of modelled and observed median diurnal concentrations of NO_2 of background sites for regions within Europe during the observational period. Shaded regions give the hourly standard deviation across sites. 44

Figure 6 Comparison of monthly mean modelled and observed ethane, propane, PRPE and ALK4 concentrations in the UK over the observation period. The shaded areas is the standard deviation 47

Figure 7 Hourly A) Ethane, B) Propane, C) PRPE and D) ALK4 observed and modelled concentrations of background UK sites during the observational period. hexagon colour shading is on a logarithmic scale. Green line represents the line of best fit. Dashed lines represent 1:1, 2:1 and 1:2 ratios. 48

Figure 8 Comparison of mean diurnal modelled and observed ethane, propane, PRPE and ALK4 concentrations with for background sites over the UK in the observational period. 49

Figure 9 Comparison of monthly mean modelled and observed ethane, propane and ALK4 concentrations at mace Head for the observational period. 51

Figure 10 – Comparison of monthly mean modelled and observed ozone concentrations for regions within Europe during the observational period. The shaded areas give the monthly standard deviation across sites. 53

Figure 11 Hourly ozone observed and modelled concentrations for background sites for regions within Europe during the observational period. hexagon colour shading is on a logarithmic scale. Green line represents the line of best fit. Dashed lines represent 1:1, 1:2 and 2:1 ratios. 54

Figure 12 Comparison of modelled and observed median ozone concentrations of background sites within regions of Europe during the observational period. shaded areas are the hourly standard deviation. 56

Figure 13 Comparison of monthly mean modelled and observed $PM_{2.5}$ concentrations for regions within Europe during the observational period. The shaded areas give the monthly standard deviation. 59

Figure 14 Hourly $PM_{2.5}$ observed and modelled concentrations for background sites in regions of Europe during the observational period. hexagon colour shading is on a logarithmic scale. green line represents the line of best fit. dashed lines represents the 1:1, 2:1 and 1:2 ratios. 60

Figure 15 Comparison of modelled and observed median diurnal $PM_{2.5}$ concentrations for background sites for regions within the EU across the observational time period. Shaded areas represent the standard deviation across sites within the region. 62

Figure 16 Hourly averaged mean surface $pm_{2.5}$ concentration observed over the UK compared to modelled concentration and the model contributions across the observation period. 25 μg m^{-3} horizontal line represents the who max daily exposure limit. 65

Figure 17 The modelled stacked relative contributions of $PM_{2.5}$ against the total modelled $PM_{2.5}$ concentrations over the UK, across the observational period. 65

Figure 18 Daily averaged nitrate, ammonium and sulphate modelled and observed concentrations across the observational period where observations are from the MARGA UK network. 66

Figure 19 Mean surface $PM_{2.5}$ concentration observed over the UK compared to modelled concentration and the model contributions for 2 pollution events in march and april 2014. 70

Figure 20 Mean modelled $PM_{2.5}$ surface contributions over the UK, normalised as a percentage for the two pollution "events" march - april 2014. (events 8-14th march and 27th march - 4th april). 70

Figure 21 The modelled and observed $PM_{2.5}$ stacked relative contributions of secondary aerosol across both pollution events in the spring of 2014. 73

Figure 22 Modelled and Observed UK nitrate, ammonium and sulphate concentrations during both pollution events in the spring of 2014 (March - April 2014). 73

Figure 23 The average $PM_{2.5}$ mixing ratio across the year observational period for the "base" run (top panel), the "AgriOff" run (2nd top panel) and the difference in mixing ratio between the two runs (3rd panel). The bottom panel shows the fractional difference between the base run and AgriOff run mixing ratios (bottom panel). 76

Figure 24 The number of days $PM_{2.5}$ mixing ratios are above the WHO daily recommended maximum (25 μg m^{-3}), across the observational period for the Normal run, the AgriOff run and the delta (the difference in days between the runs). 79

Figure 25 Mean surface PM2.5 concentration observed over the UK during the two pollution 'events' compared to modelled concentration and the model contributions for the base simulation (upper) and the "agrioff" simulation. (lower). Runs are over the 2 spring pollution events between the 1st March and the 14th April 2014. 81

Figure 26 UK hourly surface levels of nitrate ammonium and sulphate for $PM_{2.5}$ for the normal run model output and agri-off model run concentrations between the 1st march and the 14th april. 82

Figure 27 The change in concentration of ammonium, sulphate and nitrate as a percentage of total change in PM2.5 between the base run and the AgriOff run between the 1st march 2014 and the 14th april 2014. 84

List of Tables

Table 1 An extract for the development in annual emissions for different pollutants in Europe, benchmarked to 2004 emissions (100%). (EEA, 2016) 22

Table 2 EU directive reference methods for species concentration measurements at AQER sites, as described in EU directive 2008/50/EC (Parliament, 2008). 26

Table 3 An example of site information for a given monitoring site, extracted from the European smonitor (Grange, 2016). 27

Table 4 Regions within Europe and the relevant countries (which have all the AQER monitoring background sites within that country for data filtering) 28

Table 5 Observational species that were selected for comparison to the model equivalent from the NOAA network at Mace Head during the observational period 34

Table 6 The EMEP emission sectors for CO, SO_2, sulphate radical, NO, ammonia, ethane, propane, PRPE (≥C3 Alkenes), ALK4 (≥C4 alkanes), acetone, formaldehyde, acetaldehyde, RCHO (>C2 aldehydes) and benzene species. 38

Acknowledgements

I would like to thank Professor Mat Evans and Dr. Tomás Sherwen for their guidance, astute criticisms and suggestions during the course of this project. I am immeasurably thankful for their unwavering patience, enthusiasm and intellect which made this project such a pleasure.

I would also like to thank Stuart Grange who build the observational network framework, allowing the data needed to be extracted from database which a large part of this project is built around.

Declaration

Declaration - I declare that this thesis is a presentation of original work and I am the sole author. This work has not previously been presented for an award at this, or any other, University. All sources are acknowledged as References.

Chapter 1 Introduction

Air Quality is one of the leading causes of death globally (WHO, 2016) and within Europe (EEA, 2015). This chapter describes the main sources, sinks and health impacts for pollutants, in relation to impacts on the EU and the UK. Focus is on the dominant chemical and physical processes which drive surface observational temporal trends.

For short term pollution events, the meteorology is often well understood, however, the pollution sources are often of debate. The latter part of this chapter describes the sources of emissions to the pollution events that will be investigated in this study.

1.1 Air quality: What is it and why should we care?

The consequence of global population and economic growth is that surface air pollution has become a significant concern, due to the detrimental effects to physical health and vegetation. Epidemiological studies have highlighted toxicity, size and concentration are the key factors that define each pollutants relative health burden (Walton et al., 2015, WHO, 2016)

A large number of premature deaths occur due to ambient air exposure in Europe. In 2012, particulate matter with diameter of less than 2.5 μm ($PM_{2.5}$), nitrogen dioxide (NO_2) and ozone were responsible for 403,000, 75,000, and 17,000 deaths respectively in Europe alone (EEA, 2015, Tegen et al., 1995). Improving air quality requires extensive understanding of the chemical processes that contribute to aerosol and other pollutant concentrations, in order to design effective legislation.

1.2 Key air quality species, their formation, sinks and health impacts

This section describes how different pollutants are emitted, how they are chemically processed and finally deposited to the earth's surface, along with their health impacts. In this study CO and SO_2 analysis are excluded as although they are being measured across Europe the data did not offer enough precision to be able to do the analysis needed so are not evaluated here.

1.2.1 Nitrogen dioxide (NO_2)

NO_2 is one part of NO_x ($NO + NO_2$). There is rapid interconversion between these species because the rapid photolysis of NO_2 leads to the production of NO (R1.1) and the reaction between NO and ozone (O_3) to produce NO_2 is also rapid (R1.2).

$$NO_2 + hv \rightarrow NO + O \quad (R\ 1.1)$$

$$NO + O_3 \rightarrow NO_2 + O_2 \quad (R\ 1.2)$$

During daytime, the equilibrium between NO and NO_2 occurs quickly (10s of minutes). NO_2 produced can react with O_3 form NO_3 and O_2. (R1.3)

$$NO_2 + O_3 \rightarrow NO_3 + O_2 \text{ (R 1.3)}$$

During the daytime the photolysis of NO_3 rapidly returns NO_3 to NO_2 and O or NO and O_2. However at night the NO_3 can react with NO_2 to form N_2O_5. (R 1.4)

$$NO_2 + NO_3 \rightarrow N_2O_5 \text{ (R 1.4)}$$

N_2O_5 can thermally decompose back to give NO_2 and NO_3, making it an important nighttime NO_x reservoir. (R 1.5)

$$N_2O_5 \rightarrow NO_2 + NO_3 \text{ (R 1.5)}$$

1.2.1.1 Sources

The emission of NO_x into the atmosphere includes both natural and anthropogenic sources. Natural sources include lightning, forest fires and soil emissions (EEA, 2015). Anthropogenic sources include combustion emitting NO_x from transport and biomass burning and industry, oxidation and fertilizer use (AQEG, 2004, EEA, 2015).

For nearly all sources, NO is the dominant emitted NO_x species. However, from automobiles there is a fraction which comes out as NO_2 directly.

1.2.1.2 Sinks

The predominant sinks of NO_2 are 1) the daytime reaction with the OH radical (R 1.6) to form HNO_3 and 2) the night time reaction between N_2O_5 and aerosol surfaces to form aerosol nitrate (NO_3^-) (R 1.7). Whether by the daytime or nighttime route, the dominant sink for NO_x is to form nitrate, whether as HNO_3 in the gas phase or NO_3^- in the aerosol phase. There is rapid partitioning between HNO_3 and NO_3^- which is highly temperature dependent. Ultimately both forms of nitrate are deposited either through wet or dry deposition.

$$NO_2 + OH \rightarrow HNO_3 \text{ (R 1.6)}$$
$$NO_2 + O_3 \rightarrow NO_3 + O_2 \text{ (R 1.7)}$$
$$NO_3 + NO_2 \rightleftharpoons N_2O_5 \text{ (R 1.4 + R 1.5)}$$
$$N_2O_5 + H_2O \text{ (aerosol)} \rightarrow HNO_3 + \text{deposition (R 1.8)}$$

Dry deposition of NO_2 to vegetation and soils occurs, although it is not as significant as the chemical sinks (Wesley, 1989).

1.2.1.3 Health impacts

NO_2 is highly oxidising. therefore it has be linked to a variety of respiratory problems. High exposure can cause inflaming of the lining in the lungs increasing the likelihood of lung infections (WHO, 2006), which can be permanently damaging to the lungs. European legislation has been implemented to reduce NO_2 (WHO, 2006) due to considerable emissions from the diesel automotive fleet.

1.2.2 Non-methane hydrocarbons (NMHCs)

Non-methane hydrocarbons (NMHCs) are a subgroup of Volatile Organic Compounds (VOCs). Ethane, propane, alkenes (PRPE) and longer chained alkanes (ALK4) are some key NMHCs that alter the chemistry in the atmosphere. Other VOCs such as benzene and toluene and poly aromatic hydrocarbons are not evaluated in this study.

Research at Mace Head (10W, 53N) highlights ethane is a long living NMHC, with an atmospheric lifetime of months (54 days), compared to propane (13 days) and longer alkanes (below 10 days) (Derwent et al., 2012).

Ethane and propane concentrations over the UK and Europe will have regional and even continental contributions due to these forementioned long atmospheric lifetimes, which allows for significant atmospheric transport. As Helmig et al., (2009) concluded, notably there are higher ambient levels of NMHCs in the more industrialised latitudes of the globe due to regional NMHC production and transport. Hence, in the northern hemisphere there are higher ambient NMHC levels than the less industrialised southern hemisphere.

1.2.2.1 Sources

NMHCs originate from a range of natural and anthropogenic sources. These sources include fossil fuel combustion, natural gas leakage, biomass burning, geochemical processes, along with vegetative and oceanic emissions (Helmig et al., 2009, Kansal, 2009).

NMHC emissions in the UK (with the exception of ethane and propane) have steadily been decreasing in recent decades (Derwent et al., 2014, Derwent et al., 2017). This reduction is mainly due to a reduction in vehicle fossil fuel emissions, which is due to the introduction of vehicle emission regulations. However ethane and propane concentrations have remained close to their 1993 values (Derwent et al., 2017). Unlike other sources it is not thought that natural gas leakages have been decreasing in this period (Derwent., 2014, Derwent et al., 2017). Derwent et al., (2014) reported that the highest observed UK Ethane concentrations between 1993 and 2012 were at London Marylebone Monitoring station, which directly sits above natural gas piping. This highlights uncertainty over the importance of petrochemical emissions against natural gas leakage as source contributors to ethane and propane.

1.2.2.2 Sinks

The major removal route of NMHCs is via the OH oxidation route (R 2.1), this ultimately forms reactive alkyl peroxyl radicals (RO_2). Smaller removal routes are reaction with NO_3 radicals and Cl atoms (Harrison, 1995). This OH removal route is attributed to the observed NMHC seasonal variation, with a

summer minima and a winter maxima. The more reactive longer chain NMHCs have shorter atmospheric lifetimes, and so a more pronounced seasonality (Derwent et al., 2017).

$$R\text{-}H + OH \rightarrow R + H_20 \quad (R\ 2.1)$$
$$R + O_2 + M \rightarrow RO_2 + M$$

1.2.2.3. Health impacts

Some NHMCS such as benzene and toluene are carcinogenic. For the smaller NMHCs, their health impacts comes from two routes. The first is that they can be oxidised to form a range of compounds such as ketones, phenols alcohols (Kansal, 2009). These have indirect health impacts are important due to their toxicity.

The second is that NMHCs are important precursors to ground level ozone and secondary organic aerosols in the troposphere both of which are health concern (Lelieveld et al., 2000). For tropospheric ozone the oxidation of NHMC leads to the production of peroxy radicals which can go on to form ozone (R 3.1) (Kansal, 2009). Secondary organic aerosol production occurs when the oxidation of the NHMC leads to the production of low volatility organic productions, which can end up condensing onto aerosols, leading to an increase in aerosol mass.

1.2.3 Ozone

1.2.3.1 Sources

Ozone is predominantly a secondary pollutant produced by hydroxyl radical driven oxidation of NMHCs, other VOCs, methane and CO in the presence of NO_x. The oxidation of these precursors leads to the production of peroxy radicals (RO_2) which can then oxidize NO into NO_2. The photolysis of the formed NO_2 formed produces an oxygen atom which can then reaction with O_2 to produce ozone. In this process (R 3.1) there is the simultaneous photodissociation of NO_2 and regeneration of NO_2. This means NO_2 is expected in a steady state in the ambient atmosphere.

$$RO_2 + NO \rightarrow NO_2 + RO \quad (R\ 3.1)$$
$$NO_2 + hv \rightarrow NO + O(3P)$$
$$O(3P) + O_2 + M \rightarrow O_3 + M$$

The concentration of ozone in a given location thus depends on a number of variables including the concentration of precursors, proximity to sources, meteorological conditions, and the strength of sunlight (Lelieveld et al., 2000).

In addition to ozone production via NO_x and VOC chemistry in the troposphere, ozone produced in the stratospheric also provides a smaller source of ozone to the troposphere, where ozone is made by the direct photolysis of O_2 (Young et al., 2013).

1.2.3.2 Sinks

Ozone typically has a chemical lifetime of several weeks (Stevenson et al., 2006, Young et al., 2013). This relatively long atmospheric lifetime allows for continental and regional transport.

Chemically, ozone is lost through many chemical pathways (Sherwen et al., 2016). The dominant sink is the photolysis of ozone and its subsequent reaction of the excited oxygen with water, which produces the hydroxyl radical (R 3.2). Only a fraction of O(1D) reacts with water, so predominantly excited O(1D) atoms relax to O(3P) ground state (R 3.3), which can react to form ozone again (R 3.1).

$$O_3 + hv \rightarrow O(1D) + O_2 \text{ (R 3.2)}$$
$$O(1D) + H_2O \rightarrow 2OH$$
$$O(1D) + M \rightarrow O(3P) + M \text{ , where M= } O_2, N_2 \text{ (R 3.3)}$$

Ozone can also be lost via the the reaction with hydrogen peroxyl radicals (R 3.4) and the direct reaction with OH radicals (R 3.5).

$$HO_2 + O_3 \rightarrow OH + 2O_2 \text{ (R 3.4)}$$
$$OH + O_3 \rightarrow HO_2 + O_2 \text{ (R 3.5)}$$

Ozone removal occurs in polluted regions by the oxidation of NO to form NO_2 (R 3.6). Nitrate radicals are formed from the subsequent reaction of NO_2 and ozone (R 3.7), which occurs during all periods of the day. During the night, the nitrate radical reacts in equilibrium with NO_2, forming N_2O_5 (R 3.8) This is not a significant equilibrium reaction during the day as the nitrate radical is rapidly photolyzed by light, but it is a significant nighttime sink of ozone.

$$NO + O_3 \rightarrow NO_2 + O_2 \text{ (R 3.6)}$$
$$NO_2 + O_3 \rightarrow NO_3 + O_2 \text{ (R 3.7)}$$
$$NO_3 + NO_2 \rightleftharpoons N_2O_5 \text{ (R 3.8)}$$

Finally ozone loss also occurs in the troposphere through dry deposition. The levels of dry deposition have been reported to account for up to a quarter of tropospheric ozone destruction globally (Lelieveld et al., 2000).

1.2.3.3 Health impacts

Tropospheric ozone is an important air quality health concern, causing respiratory problems, inflaming and increasing the likelihood of infection in the lungs (EEA, 2015, DEFRA, 2011).

1.2.4 Particulate matter

Aerosol can either be emitted directly into the atmosphere (primary), or be produced by chemical reactions in the atmosphere from their precursors (secondary). Aerosols are categorised by size into 4 modes, nucleation (<0.1 μm), aitken (0.1 - 0.5μm), accumulation (0.1 - 1 μm) and coarse modes (>1 μm). The smallest represent those aerosols which have recently nucleated, spontaneously formed from a gas

into a liquid or solid. These can grow through coagulation and vapour condensation to generate accumulation mode aerosols. Coarse aerosol are produced by mechanical processes, such as sea spray, wind blown dust and manmade processes such as quarrying and industrial processes.

Accumulation categorised mode aerosol has the longest atmospheric lifetime, as nucleation and aitken categorised mode aerosol tend to increase in mass rapidly due to coagulation and condensational growth, whereas coarse categorised mode aerosol is relatively heavy, so have a high loss rate due to gravitational settling (Monks et al., 2012).

As well as having significant health impacts, aerosols are also climatologically important as they can scatter light rays and alter the Earth's radiative balance (Cropper et al., 2013). Aerosols also act as cloud condensation nuclei which have the consequence of altering precipitation rates and altering regional albedo.

1.2.4.1 Sources and sinks

PM originates from the following environments;

Marine

In marine environments, sea salt aerosol is generated by mechanical processes from the oceans when bubbles burst from waves. Marine emission are closely linked to wind conditions. Organic material in the oceans can also be emitted by this same process, which can go on to form both primary and secondary organic PM aerosol (EEA, 2012).

Mineral dust

Mineral dust aerosol are solid particles ejected and suspended into the atmosphere through mechanical processes, naturally from winds and sandstorms and by anthropogenic processes such as construction (EEA, 2012).

The Saharan region, is the largest natural source of mineral dust aerosol, making up 55% of the global mineral dust budget (Ginoux et al., 2012). Long range transport of this dust does occur with observations of Saharan dues in Europe and the UK (Vieno et al., 2016). The north and eastern Mediterranean are highly affected by desert dust particles, but there is limited understanding of the burden on health of sustained dust exposure (WHO, 2016). A desert source of PM aerosol has been partially associated with the exceedances in PM regulations in the UK (Buckland et al.,, 2015, Vieno et al., 2016). However, a notable fraction of primarily emitted mineral dust comes from anthropogenic sources, with estimations between 10-50% globally (Ginoux et al., 2012, Tegen et al., 1995) due to agricultural emissions, deforestation, soil disturbance, and construction processes.

Much dust aerosol is coarse (> 1 μm), so deposition of shorter lived mineral dust aerosol from deserts enriches regional oceans, which alters phytoplankton productivity and therefore ocean CO_2 uptake (EEA, 2012).

Elemental carbon and organic carbon

The elemental carbon (soot) contributes to $PM_{2.5}$ composition, Soot is mainly carbon from incomplete fossil fuel combustion, with a fraction also from domestic and industrial biomass burning. Wood burning can produce high levels of fine and coarse PM aerosol, which can have a significant contribution over Europe (Saarikoski et al., 2008).

Organic carbon consists of organic compounds, which can be primarily emitted from fossil fuel, wood and industrial combustion. Organic carbon is also formed from secondary organic aerosol through natural biogenic degradation of carbon containing compounds, combustion and the oxidation of VOCs.

Sulfates

Secondary $PM_{2.5}$ is produced from reactions of their precursors e.g. NO_x, NH_3, VOCs and SO_2 which produce low volatility compounds. SO_2 is primarily produced in industry and in power generation, along with fossil fuel combustion (DEFRA, 2015). SO_2 will oxidise to form H_2SO_4 via aqueous or gas phase routes. Gas phase oxidation of SO_2 is relatively slow with a reaction lifetime of 1-2 weeks (Jacob, 1999) which occurs in the troposphere from its reaction with the hydroxyl radicals to form $HOSO_2$ (R 4.1). Without a catalyst this step is slow. $HOSO_2$ subsequently is rapidly oxidised to form sulphur trioxide SO_3 (R 4.2). Sulphur trioxide is then further oxidised, by water and hydrogen peroxide, to form sulphuric acid (R 4.3).

$$SO_2 + OH + M \rightarrow HOSO_2 + M \text{ (R 4.1)(slow)}$$
$$HOSO_2 + O_2 \rightarrow SO_3 + HO_2 \text{ (R 4.2)}$$
$$SO_3 + H_2O_{(aq)} \rightarrow H_2SO_4 \text{ (R 4.3)}$$
$$SO_3 + H_2O_2 + M \rightarrow H_2SO_4 + M \text{ (slow)}$$

However, most tropospheric oxidation of SO_2 to H_2SO_4 occurs in liquid phase on cloud droplets (Jacob, 1999) as SO_2 is readily soluble (R 4.4) and dissociates to HSO_3^- (R 4.5). Further oxidation of the bisulfite ion (HSO_3^-) with hydrogen peroxide can form sulphate ions (R 4.6) (Jacob, 1999).

$$SO_{2\,(g)} \rightleftharpoons SO_2.H_2O \text{ (R 4.4)}$$
$$SO_2.H_2O \rightleftharpoons HSO_3^- + H^+ \text{(R 4.5)}$$
$$HSO_3^- + H_2O_{2(aq)} + H^+ \rightarrow SO_4^{2-} + H_2O_{(aq)} + 2H^+ \text{ (R 4.6)}$$

The acidic aerosol condenses to aerosol phase sulphates and is commonly neutralised with ammonia or other compounds to form basic aerosols e.g. $(NH_4)_2SO_4$, $(NH_4)HSO_4$, $Fe_2(SO_4)_3$. Sulphuric acid reacts to form sulfate aerosol across a range of ammonium concentrations, as sulphuric acid is relatively nonvolatile in respect to nitrates so more readily partitions into the aerosol phase. Hence, more sulphuric acid is available to be neutralised by ammonia to form sulphates. So, typically there is enough ammonia to react all of the sulphuric acid away. Sinks of sulphates aerosol include dry deposition and wet scavenging (WHO, 2006).

Ammonium

Ammonia is primarily released into the environment through the application of synthetic fertilizers and emissions from livestock manure decomposition, urea excretion and from grazing pastures and soils

(Moran et al., 2016). It has a relatively short atmospheric lifetime of below 10 days (transport <10-100 km) which is dominated by wet and dry deposition routes (Gong et al., 2013, Morán et al., 2016).

Ammonia readily reacts with acidic aerosols to produce ammonium aerosols. Ammonium has a longer atmospheric lifetime than ammonia as it is determined by the loss rate of the parent aerosol rather than by the wet or dry deposition of the gas.

Fertilizers contain organic nitrogen compounds such as nitrates, ammonium or urea or a mixture of these. For ammonium based fertilizers, instead of nitrifying in the soil, it can be lost to the atmosphere by conversion volatilization to produce ammonia. This process occurs at a higher rate when urea is spread onto the ground and not immediately incorporated into the soil. The enzymatic hydrolysis of urea upon application produces CO_2 and ammonium, which subsequently increases the rate of ammonium volatilization (R 4.7) (Rochette et al., 2013). The uncertainties in fertilizer type, the rate of enzymatic processes and grazing levels lead to significant uncertainty in appropriation of ammonia emissions from each route (Morán et al., 2016, Skjøth et al., 2011).

$$CO(NH_2)_2 + H_2O \rightarrow CO_2 + 2NH_3 \text{ (R 4.7) (urea hydrogenation by enzymes)}$$
$$NH_3 \rightarrow NH_3 \text{ (air) (volatilization from manure)}$$

Nitrates

As mentioned earlier, nitrogen oxides (NO_x) form nitric acid (HNO_3). HNO_3 reacts with ammonia forming aerosol phase ammonium nitrate $(NH_4)NO_3$. The production of ammonium nitrate in this reversible process is typically limited by the abundance of ammonia. The oxidation lifetime of NO_x to form HNO_3 is a few days, which allows for regional NO_x transport before oxidation (Stavrakou et al., 2013).

Nitrates (esp. NH_4NO_3) from continental Europe can represent a significant contribution to $PM_{2.5}$ episodes in the UK (Vieno et al., 2014) and have a significant contribution to annual mean concentrations throughout the year (Monks et al., 2012).

The nighttime hydrolysis of N_2O_5 heterogeneously on the surface of aerosol particles is a significant night-time producer of nitrates (R 4.8) (Platt et al., 1984).

$$N_2O_5 + H_2O \text{ (on aerosol)} \rightarrow 2HNO_3 \text{ (R 4.8)}$$

Additional particulate matter sources

There has been growing interest in non-exhaust emissions from vehicles since they remain unabated whilst exhaust emissions standards are getting more stringent within the EU (WHO, 2006). These non-exhaust emissions are emitted from abrasive contact in brake systems, tyre wear and road wear along with volatilization of lubricants on abrasive systems (Grigoratos et al., 2014).

Biological

Biological aerosol particles are emitted directly into the atmosphere from their emission sources, which include viruses, bacteria, algae and fungi. The atmospheric consequences of these emissions are not well

understood, but they can play an important role contributing to $PM_{2.5}$ aerosol, being attributed to up to 25% of the atmospheric aerosol levels globally (Jaenicke, 2005).

1.2.4.2 Health impacts

The health impacts of surface PM exposure are well documented, notably causing premature death in the sickly and the old due to diseases of the respiratory and cardiovascular systems, including lung cancer (Ayres, 2010). In regions of long term high PM exposure, mortality and cardiovascular disease risk is increased. Short term exposure increases these risks, although more substantially for susceptible groups of the public (e.g. young, elderly, asthmatic, etc.) than for those not at risk (Atkinson et al., 2014).

Smaller sized aerosol particles are attributed to having a higher relative health burden than larger aerosols, due to the increased ability to pass deep into the repository system and enter the bloodstream more readily (Xing et al., 2016, WHO, 2016). More research is needed to understand the PM sources that influence health, which is in part due the lack of PM speciated measurements in monitoring networks worldwide (Monks et al., 2012).

1.3 Air quality in Europe and the UK

1.3.1 EU air quality

Current EU legislation has driven reductions in air pollution, and has been met with some success. Most primary emissions contributing to particulate matter (PM_{10} and $PM_{2.5}$) aerosol and NO_2 and ozone have reduced over the last decade (EEA, 2015). Further progress has been made on reducing emissions of CO and Benzene. However other pollutants levels, namely Ammonia (NH_3), have failed to decline at a similar rate (EEA, 2015). A partial extract of the findings in (EEA, 2015) is shown below in Table 1.

Even with these reductions in emissions, the ability of EU states to meet the EU 2004 and EU 2008 Ambient Air Quality Directives standards for pollutants has only been partially successful. In the last decade between 33-38% of the EU urban population is exposed to $PM_{2.5}$ and PM_{10} above the daily exposure limits (25 μg m^{-3}, 50 μg m^{-3} respectively) (European Parliament, 2008). More recently for O_3, between 18-65% are exposed above the 8 hourly O_3 concentration limit (100 μg m^{-3}) and for NO_2, between 5-23% are exposed above the hourly limit (200 μg m^{-3}) (Guerreiro et al., 2014).

Table 1 An extract for the development in annual emissions for different pollutants in Europe, benchmarked to 2004 emissions (100%) (EEA, 2016).

Year	SO_x	NO_x	NH3	PM_{10}	$PM_{2.5}$	NMVOC	CO	BaP
2004	100	100	100	100	100	100	100	100
2005	94.15	97.49	98.54	97.26	96.88	97.24	91.29	104.05
2006	92.05	94.97	98.95	94.99	93.95	94.65	87.27	104.49
2007	87.73	91.69	98.94	93.12	91.6	90.55	83.34	102.68
2008	68	84.93	96.9	90.8	90.39	86.55	80.49	108.12
2009	58.14	77.64	96.03	86.79	87.09	80.48	73.31	102.05
2010	54.89	76.66	94.57	89.16	89.25	81.18	76.42	110.35
2011	54.18	73.91	94.7	86.19	84.79	77.66	71.45	107.05
2012	48.83	70.95	93.8	84.14	83.36	75.04	66.6	106.32
2013	41.98	67.8	93.68	85.27	85.41	74.34	68.61	110.32

The transport sector has been subject to intense European legislation to improve air quality, but other sectors have not. The agricultural sector for example, contributes to ammonia, methane, VOCs, hydrogen sulphide and NO emissions. In Europe NH_3 abundance is often limiting $PM_{2.5}$ formation, contributing between 30 - 40% of PM concentrations across the year (Lelieveld et al., 2015, Moran et al., 2016).

1.3.2 UK air quality

In the UK, the health burden of PM and NO_2 has been of particular interest to the public (Monks et al., 2012, Defra, 2015). Anthropogenic PM has been attributed to 340 000 life years lost or 28,811 attributable

deaths and as high as 11.5 years lost from life expectancy in urban areas (Ayres, 2010). In comparison, for ambient NO_2 there were 23,500 attributable deaths (DEFRA, 2015), although there was notable health burden overlap of NO_2 with PM in this analysis and uncertainties in the associated relative risks. London has a particularly high health burden from pollution with an estimated 9418 attributable deaths from ambient levels of $PM_{2.5}$ and NO_2 in 2010 (Walton et al., 2015). This gives NO_2 a higher health burden, with 5879 attributable deaths (52630 life years lost) from NO_2 compared to the 3537 (88113 life years lost) from $PM_{2.5}$ (Walton et al., 2015).

Understanding the health impacts of short term (hourly) elevated pollution as opposed to longer term (annual) exposure is a field of growing interest. A recent study for London, attributed 787 deaths from $PM_{2.5}$ and 461 from NO_2 short term exposure in 2010 (Walton et al., 2015). These pollution episodes are often caused by a combination of low wind surface speed (stagnation), high photochemical activity and the transport of air from polluted areas. (Lee et al., 2006).

Emissions from the agricultural sector are a growing concern for air-quality in Europe, for example in 2010 89% of ammonia emissions were from this sector alone (DEFRA, 2011). The sector is highlighted as a significant contributor to UK PM pollution events, along with vehicles and industry (Vieno et al., 2016).

1.4 Meteorology of pollution events

As summarised by (Hou et al., 2016) and (Buckland et al., 2015), there are three types of meteorological events that increase the chance of a pollutional episode.

1. Temperature inversion episodes: where at ground level, air mass is at a lower temperature than the air mass above it. This cold stable air mass is trapped at ground level, hindering normal atmospheric mixing. Emissions are trapped and build up inside the cold stable air mass.

2. Atmospheric stagnation: Where an air mass holds over a region for a long period of time. Often from a high-pressure system, which reduces wind speed, subsequently reducing the ability of local emissions to be dispersed. Often regionally/continental transported emissions are held over the region along with a build-up of local emissions which pollute the stagnant air mass.

3. Heatwaves: Between spring to autumn, for a period of time an air mass is exposed to a higher temperature than normal, which increases the rates of certain chemical processes and increases emission rates of certain pollutants. This is due to increased energy demands from increased anthropogenic evaporative emissions and increased biogenic emissions.

PM events typically occur in the winter and/or spring period in the UK (Vieno et al., 2016). As these episodes are more likely with a temperature inversion and atmospheric stagnation, which occur more frequently in winter and spring. In 2014 there were two significant UK PM pollution events, the first between the 12-14th of March and the second between 28th March to the 3rd April. (Buckland et al., 2015). Pollutants in both episodes were circulating from north western Europe and drawn across into the UK, elevating pollution concentration. For periods of the pollution episodes air mass from the African continent

was drawing up Saharan dust which also contributed to PM concentrations. They are good examples of the type of PM pollution events that occur in the UK and so will be discussed now in more detail.

1.4.1 Wintertime pollution episodes in 2014

During the spring of 2014 there were multiple PM pollution events breaching the European Commision and World Health Organisation air quality standards (25 μg m^{-3} for $PM_{2.5}$ over a 24 hour period), two of these were recorded by the MET office as severe. The media highlighted that the causes of these UK episodes were from a combination of Saharan dust and continental pollution (BBC, 2014, Independent, 2014).

These pollution events have been reported in DEFRA's annual pollution report (Buckland et al., 2015). The mid-march pollution episode began on the 8th of March and was most severe between the 12-14th. On the continent, in Benelux and France there were severe PM concentrations, along with the southern UK. DEFRA (Buckland et al., 2015) determined the cause was due to a stagnant high-pressure weather system. Local and regional transport hindered dispersion, contributing to severe ground level PM levels on the 13th. During the nights, low wind speeds, brought dry, cold nights, reducing PM loss and dispersion which kept pollution close to ground level until westerly airflow ended the PM event on the 14th (Buckland et al., 2014).

The second severe pollution episode occured between the 28th March and 3rd April with DEFRA (Buckland et al., 2014) highlighting that it had a similar nature to the mid march episode. This march-april episode was most severe across most of the UK and southern Wales. This pollution event had a less common component, with the additional long range of transport of pollution from central Europe and Africa. (Buckland et al., 2015, Vieno et al. 2014, Buckland et al., 2014).

On the 28th of March light easterly winds transported polluted air masses from central Europe over the UK. On the 29th, stagnant conditions led from moderate to high PM levels. The combination of local and central European pollution air masses led to the initial episode. On the 30th, PM levels reduced due to a change in the wind's direction, with a south wind, bringing in less polluted air. However, the following day, slower moving air mass from France, which contained continental urban and industrial pollution combined with long range transported Saharan dust, caused high pollution levels across the UK which the media partially misdiagnosed as a Saharan dust event. On 3rd April, westerly winds blew the air mass from the UK to end the pollution event (Buckland et al., 2015).

The 2015 Defra Report (Buckland et al., 2015) attributed the major component of the mid march event as typical of winter event episodes highlighting vehicle and heating sources as large contributors. For march-april event they also concluded that exhaust emissions locally and from mainland Europe was a major component. In contrast, (Vieno et al., 2014) highlighted a substantial contribution of ammonium nitrate driving high PM levels. They concluded a reduction in ammonia would have benefits in reducing the march-april PM event, indicating that the agricultural sector and not vehicular emissions was the major component.

1.5 Thesis outline

Understanding the processes which control the concentration of pollutants over the UK or more widely is central to formulating effective policies to reduce human exposure. Computer models which try to simulate the emissions, deposition, chemistry and transport are an important tool to help assess our understanding and to develop scientifically rigorous policies. This thesis will evaluate one such model (GEOS-Chem) against the observations collected by the EU and UK air quality networks to evaluate its performance. Initially the general performance of GEOS-Chem is evaluated over Europe, then with more specific interest taken over the UK for certain pollutants. It will then investigate the sensitivity of the model to one emissions source (agriculture) to evaluate the impact of emissions controls on that source.

Chapter 2 discusses the observational datasets that will be used, whilst Chapter 3 discusses the model. Chapter 4 discusses the model's general performance over Europe and the UK, and Chapter 5 focuses on the models performance for pollution events described in this chapter over the UK. Chapter 6 evaluates the role of agricultural emissions of European pollution and Chapter 7 draws conclusions from all chapters.

Chemical Transport Models (CTMs) are important tools for our understanding of atmospheric pollution and so, for developing effective policies to reduce human and ecosystem exposure. These models are discussed in more detail in Chapter 3. They can simulate ground level distributions of pollutants such as nitrogen dioxide (NO_2) and volatile organic compounds (VOCs). Determining the levels primary emitted pollutants and their relative contributions to secondary pollutants is critical in capturing the levels of species like ozone and $PM_{2.5.}$ Here, the GEOS-Chem model (a CTM) is used to get a general perspective on European pollution levels and determine model strengths and weaknesses, which would benefit the GEOS-Chem modelling community. The model is evaluated for all primary and secondary species mentioned above over the period of a year (spring 2013 – spring 2014).

There has been interest in the modelling of species that impact episodic pollution events, with the aim to improve forecasting of future events. Such modelling focus is more common in China (Wang et al., 2014, Streets et al., 2007) and the US (Rieder et al., 2015, DeBell et al., 2004). However, in comparison there is less focus on modelling UK wide pollution events (Vieno et al., 2016). Evaluating the GEOS-Chem model's ability to simulate pollution events will be investigate, with focus is on two major UK springtime pollution events. Then, the model's ability to capture the composition of $PM_{2.5}$ aerosol is evaluated, with comparison to observations. The model is compared to results in Europe from the Airbase network and in the UK from the Airbase, the Monitor for AeRosols and Gases in Air (MARGA) and National Oceanic and Atmospheric Administration (NOAA) networks.

The effective burden of the agricultural sector is then assessed. Initially, the impact of sectors on pollution levels is investigated, with comparison investigated between the model run with emission from agricultural sector are included and then excluded. The assessment of the agricultural sector is run over the same time period, with particular focus on PM levels. The sectors that contribution to the exacerbating pollution events are assessed, with further analysis on the consequence the sector has on PM composition.

Chapter 2 Observational Datasets

Assessing the European nested grid version of the GEOS-Chem model (see Chapter 3) against observations is a focus of this thesis. Three sources of of observational data were used in this study: the the Air Quality E Reporting (AQER) network (EEA, 2017), the Monitor for AeRosols and Gases (MARGA) network (MARGA, 2017) and the hydrocarbon analysis of the National Oceanic and Atmospheric Administration (NOAA) canister system (NOAA, 2013). This chapter highlights how relevant data was extracted from these data sources and the subsequent processing that occurs.

2.1 The AQER network

The Air Quality E-Reporting (AQER) database (EEA, 2017) was setup to incorporate monitoring data and site metadata from participating EU countries for a range of air quality pollutants. Data from ground level monitoring sites across Europe were accessed, which are then used to compare to the model, as seen in Chapter 4.

2.1.1 Setup

The sites in the AQER databased have met the criteria for reference methods and standardisation as legislated by the European Union directive (Parliament, 2008) and is in accordance with reference method procedures from the EU directive as shown in Table 2, as of 11th June 2010.

Table 2 EU directive reference methods for species concentration measurements at AQER sites, as described in EU directive 2008/50/EC (Parliament, 2008).

Pollutant	**EU reference method: as described in:**
NO_2 and NO_x	EN 14211:2005 'Ambient air quality — Standard method for the measurement of the concentration of nitrogen dioxide and nitrogen monoxide by chemiluminescence'.
CO	EN 14626:2005 'Ambient air quality — Standard method for the measurement of the concentration of carbon monoxide by non-dispersive infrared spectroscopy'.
SO_2	EN 14212:2005 'Ambient air quality — Standard method for the measurement of the concentration of sulphur dioxide by ultraviolet fluorescence'.
O_3	EN 14625:2005 'Ambient air quality — Standard method for the measurement of the concentration of ozone by ultraviolet photometry'.
$PM_{2.5}$	EN 14907:2005 'Standard gravimetric measurement method for the determination of the $PM_{2.5}$ mass fraction of suspended particulate matter'.
PM_{10}	EN 12341:1999 'Air Quality — Determination of the PM_{10} fraction of suspended particulate matter — Reference method and field test procedure to demonstrate reference equivalence of measurement methods'.

The AQER data was extracted by Dr Tomas Sherwen via the smonitor framework, consists of packages (Grange, 2016) and the technical report (Grange, 2017). Data from a total of 9,388 monitoring sites was extracted from the database between the dates of 15th Feb 2014 - 1st December 2014. A full year of observational data could not be collected for this study due to data cleaning re-extraction and cleaning

issues. Typical metadata from each monitoring site is shown in Table 3. Th sites selected for comparison to the model, were the AQER sites that sit within the model boundaries of the GEOS-Chem 0.25° x 0.3125° nested grid which is shown in Figure 1.

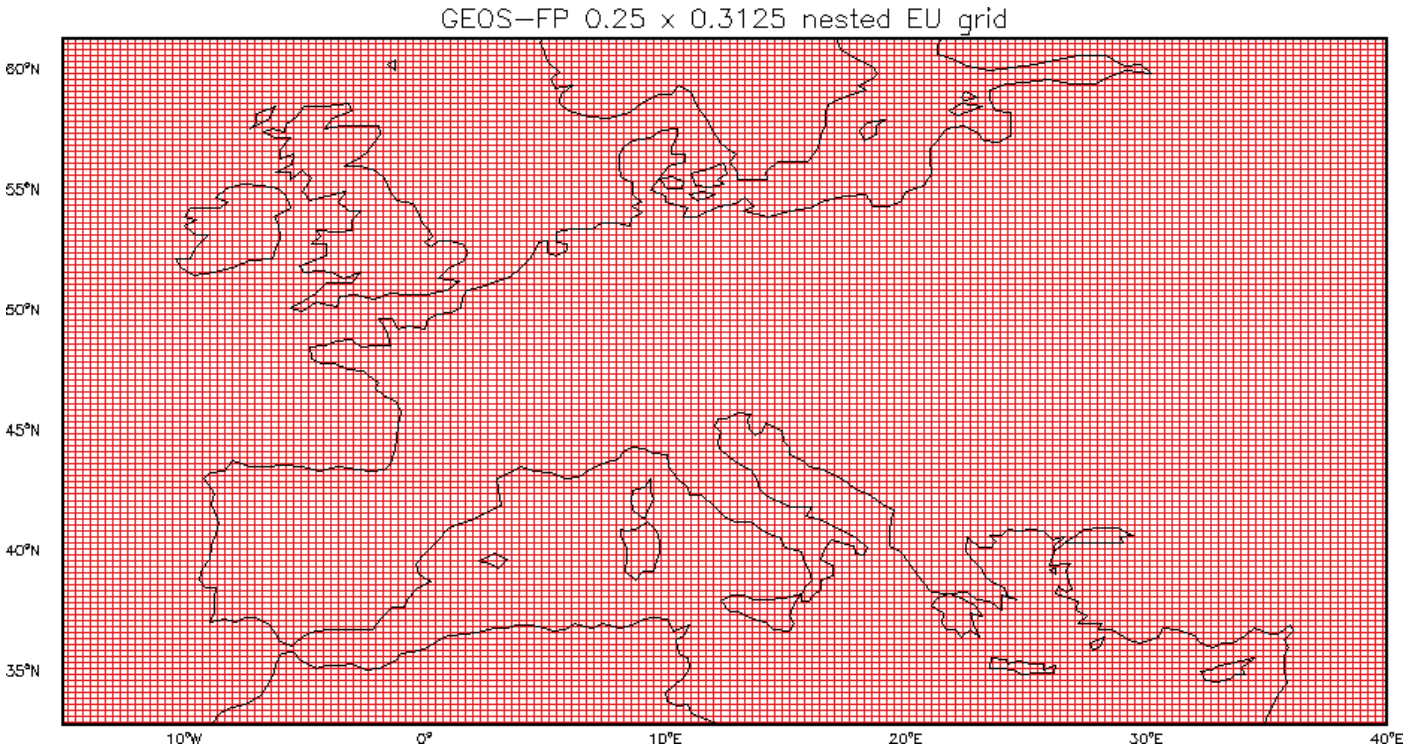

Figure 1 this is the GEOS-FP 0.25 x 0.3125 degree resolution nested grid over Europe. Image from http://wiki.seas.harvard.edu/geos-chem/index.php/GEOS-Chem_horizontal_grids.

European observations outside of the model domain above were excluded. Observational sites that were thought to be unrepresentative on the gridscale of the model (urban sites) were excluded. Thus only sites which were classified as rural, background, suburban background or rural background were included in this study. This led to the exclusion of sites types of industrial, road and urban background classification, along with sites without classification. Of the the 9388 potential sites in the monitoring network, only 4951 were suitable site types, which are referred onwards as “background sites”.

Table 3 An example of site information for a given monitoring site, extracted from the European smonitor (Grange, 2016).

site_name	site	site_type	country	longitude	latitude
Market Harborough	GB0838A	rural background	united kingdom	52.55	-0.77

In order to identify regional scale trends in model performance. Europe was split into 5 regions shown in Table 4.

Table 4 Regions within Europe and the relevant countries (which have all the AQER monitoring background sites within that country for data filtering).

Region	Countries within Region

UK and Ireland	United Kingdom, Ireland
West EU	Spain, France, Portugal, Andorra
Benelux	Netherlands, Belgium, Luxembourg
Central-Eastern EU	Austria, Czech Republic , Denmark, Estonia, Germany, Hungary, Latvia, Lithuania, Norway, Poland, Slovakia, Sweden, Switzerland
Southern EU	Albania, Bosnia and Herzegovina, Bulgaria, Croatia, Cyprus, Greece, Italy, Kosovo, Macedonia, Malta, Montenegro, Romania, Serbia, Slovenia, Turkey

The AQER network measures a number of air pollutant compounds (NO_2, CO, SO_2, NMHCs, ozone, and PM). The number and spatial coverage of sites measuring these compounds is discussed below.

2.1.1.1 Nitrogen dioxide (NO_2)

For all regions there is good spatial coverage for NO_2 observations with 81, 86, 555, 492 and 298 background sites reporting in the regions of the UK and Ireland, Benelux, Central-Eastern Europe, West and Southern Europe respectively. Data was extracted for the period between the 15th Feb 2014 until 1st December 2014.

In the UK and Ireland region, there is potential for the spatial analysis to be skewed due to the density of sites in certain counties (i.e. Greater London). Of the 149 sites reporting over UK, 40 are in Greater London. If a more balanced set of observations based on population or area was undertaken, there would be a number of London observational site more like 17 (population) or 1 (areas). Thus the model's performance in simulating the UK and Ireland region is likely biased by its performance for London.

2.1.1.2 Carbon monoxide (CO) and sulphur dioxide) (SO_2)

There is a much smaller number of CO observations compared to say NO_2, yielding much poorer spatial coverage. Such were issues with the precision of data and non standardisation of reporting that meant the data extracted could not be used in this study. There are 9, 14, 133, 91 and 90 background sites in the regions of the UK and Ireland, Benelux, Central-Eastern Europe, the West and Southern Europe respectively that were reporting.

This reflects the typical low concentrations relative to the EU Air Quality limits of carbon monoxide in the regions (DEFRA, 2015). Thus, CO isn't a priority air quality issue in Europe.

The CO instruments have been chosen to detect air quality violations rather than provide model assessment, so have observed limited precision at the low concentrations. Thus CO concentrations are often below the detection limit of the AQ network. This is due to the precision of the analysers which are specified by the EU directive reference methods (Table 2). Data processing for CO was made more complicated by countries reporting in different units (μg m^{-3}, mg m^{-3}, ppm) or incorrectly reporting units. This issue appears to be particularly apparent for the year of this study (2014). Where possible correction factors have been applied to correct the data but it is likely that not all reporting errors have been captured. Observations are made for CO but they are designed for compliance activities and/or the data was not good enough to be used in this analysis. Similar issues with non standardised reporting of SO_2 data meant that not all the errors could be captured in this study. Therefore due to time limitations the data for SO_2 and CO so was not good enough to be used in this analysis.

2.1.1.3 Non-methane hydrocarbons (NMHCs)

In this study, NMHC observations were selected for only the UK where data for the few sites was extracted separately for a whole year (15th Feb 2014 - 14th Feb 2015). The evaluation in this study is an aspect of this analysis, but not the primary focus. So for simplicity data was initially collected just for the UK.

The NMHC network across the UK has poor spatial coverage. There are 3 background sites reporting during the observation period. These are Auchencorth Moss (Midlothian, Scotland, 55.79N, 3.24W), Harwell (Oxfordshire, England, 51.57N, 1.32W) and Eltham (Greater London, England, 51.5N, 0.07W).

Eltham is excluded in this study, due to local influences affecting NMHC concentrations. This suburban background was previously classified as an “urban background” site (Derwent et al, 2014), and was found to have local emissions influences in this study.

2.1.1.4 Ozone

There is good spatial coverage for ozone reflecting concerns about it as an air quality pollutant. There were 79, 71, 557, 546 and 287 background sites reporting in the regions of UK and Ireland, Benelux, Central Eastern Europe, West and Southern Europe respectively. Southern Europe has poor spatial coverage in the eastern countries (Turkey, Greece, Cyprus), meaning the region is more representative to South-Western Europe in analysis. Data was extracted for the period between the 15th Feb 2014 until 1st December 2014.

2.1.1.5 Particulate Matter with a diameter less than 2.5 um ($PM_{2.5}$)

$PM_{2.5}$ also had good spatial coverage in all regions but southern Europe, again reflecting concern about it as an air quality pollutant. 45, 61, 158, 139 and 21 background sites were reporting in the regions of UK and Ireland, Benelux, Central Eastern Europe, West and Southern Europe respectively. Data was extracted for the period between the 15th Feb 2014 until 1st December 2014.

2.1.2 AQER data management

For all sites, observational hourly concentrations were extracted. Probability distribution functions (PDFs) of the observed species concentrations in Europe are shown in Figure 2. For species with a small dynamic range (ozone) a linear PDF is shown. For species with a larger dynamic range (NO_2, CO, SO_2, $PM_{2.5}$) a natural logarithmic PDF is used.

For NO_2, SO_2 and $PM_{2.5}$, a proportion of sites only report hourly measurements to 1 decimal place. This leads to a significant rounding error. This is represented by the “zigzag” nature of the lower logged concentrations of all species other than ozone in the PDF plots.

The PDF of NO_2 shows a log normal distribution with zig-zagging occurring at lower concentration due to the issues with the number of decimal places in the reporting. The PDF of ozone shows a generally normally distributed, so the mean value sits relatively near to the maximum frequency, but with a high frequency of observations at very low (< 3 μg m^{-3}) concentrations. This reflects the titration of ozone in regions with high NO emissions (Jhun, 2015).

The PDF of CO shows that a significant proportion of the sites are reported in the different sets of units (being mg m^{-3} and µg m^{-3}) than specified in the meta-data.

For $PM_{2.5}$ and SO_2 there is significant spiking in the data again reflecting issues with the precision of the data reporting.

NO_2

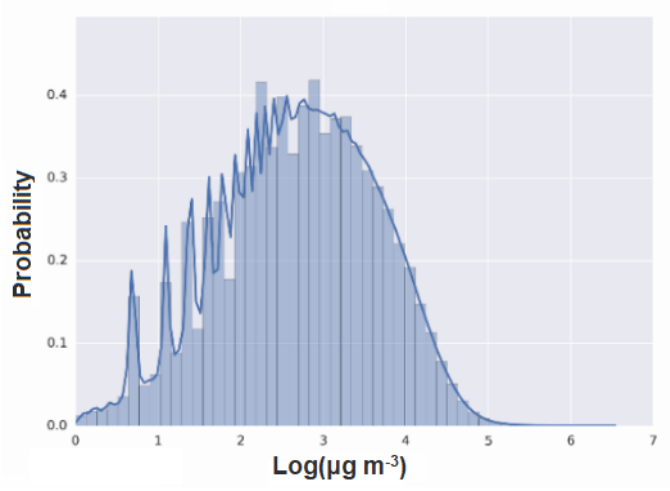

CO

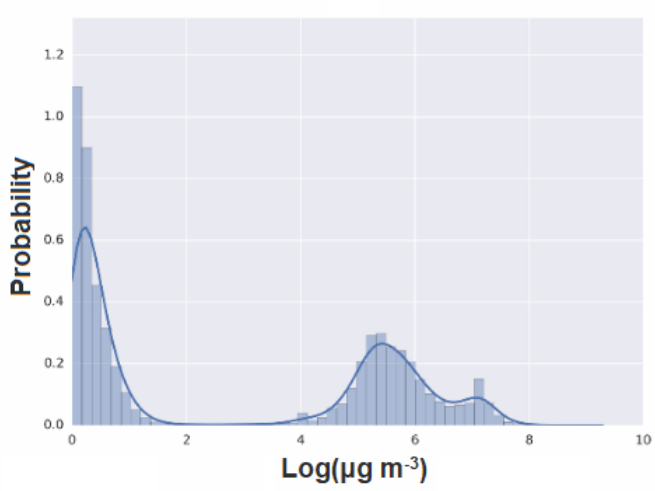

SO_2

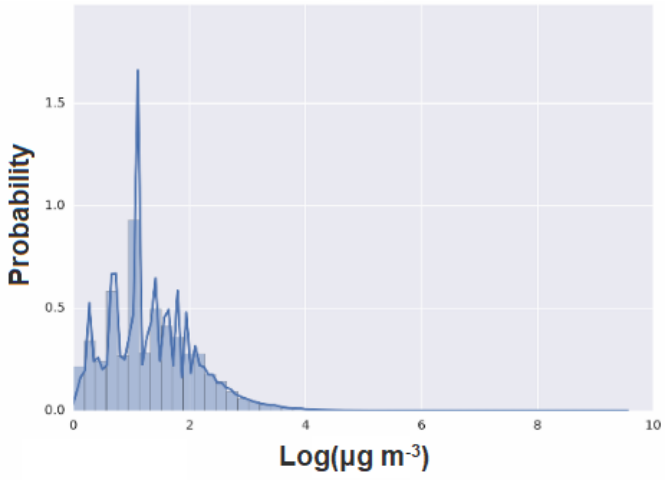

Ozone

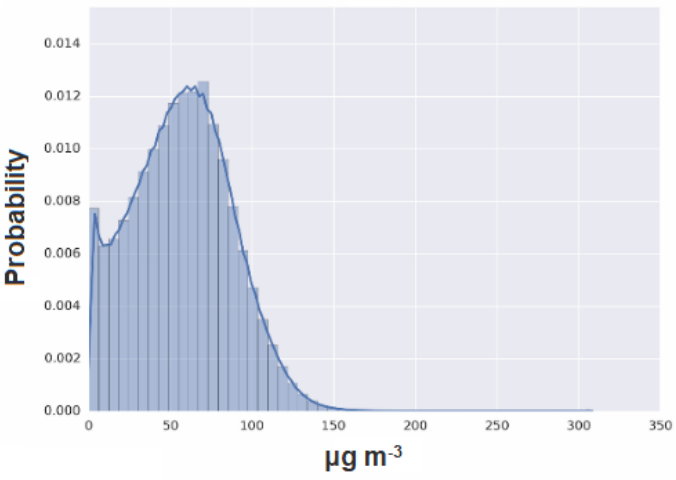

$PM_{2.5}$

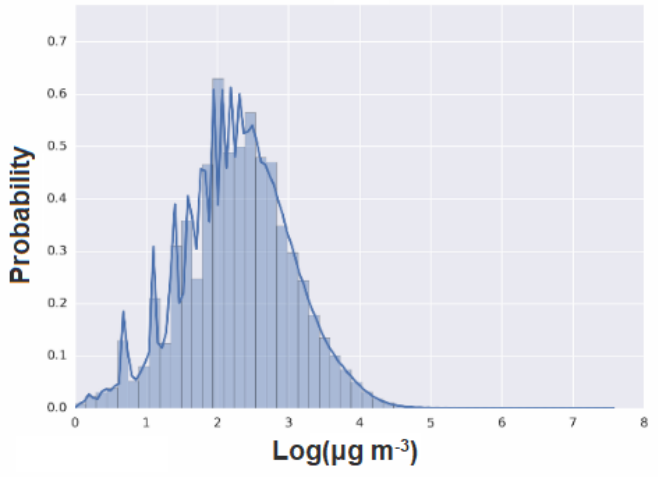

Figure 2 The log probability distribution function of observed NO_2, SO_2, CO and $PM_{2.5}$ and the log probability distribution function of ozone for all background sites (N = 4951) across the EU during the observation period.

The quality of the raw data was sufficient for $PM_{2.5}$, NO_2 and ozone for the european dataset for a viable comparison to be made to the GEOS-Chem model. It does however highlight differences in precision amongst the same type of observation as seen in the spiking. The differences in reporting for SO_2 and CO meant that these observations could not be used for comparison to the model.

2.2 The MARGA network

Data from the Monitor for AeRosols and Gases (MARGA) network was used when specifically looking into the model performance for the composition of $PM_{2.5}$ over the UK.

The MARGA instrumentation has two “super sites” in the EMEP network, within the UK; Auchencorth Moss (55.79N,-3.24W) and Harwell (51.57N, 1.32W). MARGA instrumentation takes hourly measurements of aerosol ions, such as ammonium (NH_4^+), nitrate (NO_4^-) and sulphate (SO_4^{2-}). This provides insight into the contribution of components to the annual and episodic sources of PM. The model needs to capture the UK observations in the UK of these ions to accurately predict air quality events. Current health metrics just use $PM_{2.5}$ burden. However speciation is needed to understand sources and therefore where effective policies should be directed at to reduce $PM_{2.5}$ effectively. Thus we compare the measured ion concentrations with those modelled.

Previous long term analysis of PM composition at Auchencorth Moss by Twigg et al., (2015) concluded that between 2007 and 2012, $PM_{2.5}$ was primarily composed of secondary aerosols. The research showed nitrate and ammonium and sulphate ions contributed to 26,16 and 21 percent of $PM_{2.5}$ composition respectively. These contributions at Auchencorth Moss are inline with (Malley et al., 2016), which PM contributions which investigated between 2010 and 2013.

At the Harwell site, Malley et al., (2016) concluded that PM composition was dominated by secondary aerosols. PM composition was between 16-27%, 8-13%, 11.8-14.7% for nitrates, ammonium and sulphates respectively. These contributions are relatively similar to at Auchencorth Moss, showing secondary aerosol contributions are dominant contributors to background PM composition, at different latitudes across the UK.

Recent research by (Buckland et al., 2014) and (Vieno et al., 2016) has highlighted the importance of understanding sources of PM better over the UK. The limitation of PM observed composition spatial coverage is an issue. However, the role of nitrates has been highlighted of particular importance by the Yin et al., (2008) study on road and urban background sites, which attributes 46% of PM composition to nitrates during PM episodes.

2.3 The NOAA network

For NMHC compounds with a long lifetime, model discrepancies may be due to the emission in the European domain or due to the transport of the global background into the domain. In order to separate these two possibilities the National Oceanic and Atmospheric Administration (NOAA) flask sampling system is used (NOAA, 2013). Of specific interest is its measurements of NMHCs at Mace Head. The Mace Head monitoring station is situated on the west coast of Ireland, with direct exposure to the Atlantic Ocean. It is representative of the background marine air (rural background) arriving into the British Isles from the Atlantic. The predominant wind is from the Atlantic (W, SW ~52% of the time) (Jennings et al.,1996). Mace Head sometimes receives European air mass arriving from the south-east, with pollution transported from the UK and mainland Europe..

The monitoring site sampling regularity at Mace Head reported by NOAA ranged from multiple times per week to biweekly sampling. It operates a dual sampling method, so for any given observation, there are 2 concentrations of given species at that time. The average of the dual observations are used to make a singular observation. Data for ethane and propane was directly available to compare to the model at Mace Head.

To simplify its chemistry the GEOS-Chem model uses a “lumped” NMHCs, approach for larger VOCs (version 10 of the model). Lumped alkenes (PRPE) and a lumped longer alkanes (ALK4) tracer is used. The modelled PRPE tracers represents all alkenes with 3 carbons or longer, and ALK4 is all alkanes with 4 carbons or longer. The required combination of direct observational measurements to the model for certain species is seen in Table 5. Difficulties arise with the measurement of alkenes from canisters due to loses. Thus they are not reported and so can not be directly used to from the NOAA network to compare to the model.

Data measured over the observational period was between 09:00 and 18:00, meaning only daytime observations are compared to the model at Mace head, meaning any comparison to the UK NMHC AQER network is a daytime comparison. Data collected in this analysis was the same period as for the NMHCs in the AQER network (15th Feb 2014 - 14th Feb 2015).

Table 5 Observational species that were selected for comparison to the model equivalent from the NOAA network at Mace Head during the observational period.

Model VOCs	**NOAA Mace head species used in comparison**
Ethane	Ethane
Propane	Propane
PRPE	No Comparable observations
ALK4	2- Methyl Butane, 2- Methyl Propane, n- Butane, n- Propane

2.4 Summary

For NO_2, $PM_{2.5}$ and ozone there is a reasonable AQER observational network in Europe. For a minority of sites there are issues with reporting. However, the network does provides a good observation network for comparison to a model. For CO and SO_2 there are regions of poor spatial coverage due to the lower relative risks these species are on public health in Europe. There is also an issue with the quality of the observations being made which meant subsequent analysis could not be performed. Comparison of NO_2, $PM_{2.5}$ and ozone species in this chapter to a chemistry transport model, will highlight currently how well European pollution is understood.

An evaluation of raw network observations has been covered in this chapter, highlighting issues with published units of measurements of species, a lack of PM speciation observations and issues with finding direct comparables for modelled longer NMHCs. Suitable spatial and temporal comparables are required from the model to the site observations which is the purpose of Chapter 3.

Chapter 3: The GEOS-Chem Model

3.1 Introduction

Chemistry transport models (CTMs) are used to evaluate the biological, chemical and physical processes that determine the composition of the atmosphere in both time and space domains. The performance of the models are then assessed by comparison to observations (Hu et al., 2017, Yan et al., 2016, Sofen et al., 2016). These models can then be used to predict future or explore past composition, or to understand the processes controlling the composition in the present. They are key in understanding the chemistry of the atmosphere and providing policy solution to problems such as air pollution and climate change.

The spatial and temporal domain of a CTM is dependent on the problem being investigated. For climate change a global domain is used, with simulations run over time periods spanning from years to centuries. Urban air pollution requires a regional or city scale domain which usually results in simulations run over a time period between hours and months (Maione et al., 2016). This allows the model to assess smaller scale processes and evaluate model performance against different meteorological conditions, which in turn affects species concentrations and subsequent chemistry.

To simulate atmospheric concentrations, CTM's can be run online or offline. Offline simulation occur when a model uses previously calculated meteorological information. Online simulation occur when the chemistry and meteorology are integrated together to allow for two way interactions such as chemical feedback on physical processes (e.g. aerosol effects on radiative forcings) (Zhang et al., 2015).

A range of atmospheric chemistry models exist (GEOS-Chem, EMEP, CMAQ, LOTOS EUROS, MOZART, CAMx, CHIMERE, WRF-Chem, etc.). They all have different histories reflecting institutional, management and personal decisions. For the studies described in this thesis the GEOS-Chem model has been used (www.geos-chem.org). The model was described by Bey et al., (2001). Since then the model has been used for a number of studies of atmospheric photochemistry globally (Martin et al., 2003, Read et al., 2008) and regionally (Lee et al., 2006) The model can also be used to study the atmospheric processing

or mercury (Holmes et al., 2010), CO_2 (Nassar et al., 2013), isotopes (Alexander et al., 2005), polycyclic aromatic hydrocarbons (PAHs) and persistent organic pollutants (POPs) (Friedman and Selin, 2012, Friedman et al., 2014).

GEOS-Chem is can be used on a global scale (Bey et al., 2001) or a regional scale. Regional examples have investigated pollution over China (Chen et al., 2009, Gao et al., 2014, Wang et al., 2014) and the USA (Zhang et al., 2011). In Europe there has been less coverage with the GEOS-Chem model reflecting the mainly US and Chinese user groups for the model

Pollution mitigation policies have typically been assessed once implementation of that policy has occurred. Examples of these are; the vehicle emission reduction within the London Congestion Charging zone (Atkinson et al., 2009), following similar success in Singapore (Chin, 1996). However more recently, pollution mitigation policies have been evaluated within CTMs before implementation. Particular recent focus has been on Beijing's pollution levels with studies assessing the CMAQ model for the effectiveness of pollution mitigation policies during the Olympic games 2008 (Wang et al., 2010), and the GEOS-Chem model for the APEC meeting in Beijing (Zhang et al., 2016). Similar methodology has been used elsewhere, such as in the Chimere model which has been used to assess emission control in northern Italy (De Meij et al., 2009).

This chapter will describe how the GEOS-Chem model is setup for this study, enabling it do be used for evaluating air pollution over Europe and to assess the role of agricultural emissions in determining that pollution.

3.2 Model description

The GEOS-Chem model (http://www.geos-chem.org, Bey et al., 2001) is driven by archived meteorological data assimilated by the Goddard Earth Observation System model (GEOS-5) by the NASA Global Modelling and Assimilation Office (GMAO). The GEOS-Chem model used in this study was version 10-0 which describes VOC, NO_x, HO_x and O_x chemistry (Mao et al., 2013) but also recent updates to the halogen chemistry (chlorine, bromine and iodine) (Sherwen et al., 2016).

This model has the capacity for being run globally (Bey et al., 2001, Holmes et al., 2010, Sherwen et al., 2016, Martin et al., 2003, Read et al., 2008) or on a regional scale (Chen et al., 2009, Wang et al., 2009, Zhang et al., 2011, Zhang et al., 2016 de Meij et al., 2009). The regional simulations are one-way nested into the global model so that the global model provides the initial boundary conditions to the smaller grid nested within it. Nested simulations for North America, China, Africa, and Europe (Wang et al., 2004, Chen et al., 2009, Zhang et al., 2015, Zhang et al., 2011, Travis et al., 2016) are available.

The purpose of the nesting is to allow regional or continental scale modelling at a higher spatial resolution than is possibly globally. This allows for finer spatial modelling for pollutant sources. The nested grid has typically a higher spatial resolution grid (e.g. 0.25° x 0.3125°) embedded into a lower resolution (4° x 5°) global model (Wang et al., 2004). One way coupling as described by Wang et al., (2004), the domain boundary conditions are defined from the global model. No information flows from the nested grid to the

global grid. In two way coupling, as described in Yan et al., (2014), the nested domains results which influence the global domain.

The model simulates the atmospheric composition by splitting the Earth's surface into columns which are regular in longitude and latitude. The columns then have 47 vertical layers extending from the surface to the top of the stratosphere. The surface layer is selected in this study for comparison to surface observations.

In this study the model was run globally at 4° x 5° spatial resolution to generate boundary conditions required to run a "nested" finer resolution grid (0.25° x 0.3125° ~25 km) over Europe for the observation periods.

3.3 Emissions

A large number of different emissions datasets are used in the model. These cover both natural and human driven processes.

3.3.1 Natural processes

Emissions are included from global and regional emission inventories, with higher resolution in the latter inventories considered in preference to coarser emissions where available (Keller et al., 2014). For biogenic isoprene emissions, we use the Model of Emissions of Gases and Aerosols from Nature (MEGAN) which can be run on both a regional and global scale (~1 km horizontal resolution) (Guenther et al., 2006). For biomass burning emissions of SO_2, NH_3, EC and OC the GFED4 (http://globalfiredata.org) inventory is used.

Mineral dust is accounted for in the model through the implementation of two dust mobilisation schemes (algorithms) i) the GOCART CTM (Ginoux et al., 2004) Scheme and ii) the dust entrainment and deposition scheme (DEAD) as explained comprehensively in Fairlie et al., (2007). Sea-emission are accounted in the model based on the Jaeglé et al., (2011) setup which accounts for wind and sea surface temperature dependence emissions.

3.3.2 Anthropogenic emissions

On a global scale, the Emission Database for Global Atmospheric Research (EDGAR v4.2) is used for NO_x, CO, SO_2 and ammonia anthropogenic emissions (http://edgar.jrc.ec.europa.eu). For anthropogenic VOCs, a combination of the Global Emissions Inventory Activity (GEIA) and the Reanalysis of the Tropospheric chemical composition (RETRO) is used (Reinhart and Millet, 2011).

However, in this study, a regional anthropogenic emission inventory is used, which replaces certain global emissions over Europe. The Monitoring and Evaluation of Long-range Transmission of Air Pollutants (EMEP) is used in Europe, which reports emissions by sector level (Torseth et al., 2012) as seen in Table 6. Sector emissions of CO, SO_2, sulphate radical, NO, ammonia, ethane, propane, PRPE (≥C3 Alkenes), ALK4 (≥C4 alkanes), acetone, formaldehyde, acetaldehyde, RCHO (>C2 aldehydes) and benzene replace

Edgar emissions. EMEP ship emissions of CO, NO, SO_2 and ammonia were switched off in this study. The EMEP inventory (http://www.emep.int) for the year of 2014 is used. The inventory also includes diurnal and seasonal scaling of emissions for NO_x, CO, NH_3 and SO_2 and VOCs.

Table 6 The EMEP emission sectors for CO, SO_2, sulphate radical, NO, ammonia, ethane, propane, PRPE (≥C3 Alkenes), ALK4 (≥C4 alkanes), acetone, formaldehyde, acetaldehyde, RCHO (>C2 aldehydes) and benzene species.

EMEP Sectors	
Combustion in energy and transformation industries	Road transport
Non-industrial combustion plants	Waste treatment and disposal
Combustion in manufacturing industry	Other mobile sources and machinery
Production processes	Waste treatment and disposal
Extraction and distribution of fossil fuels and geothermal energy	Agriculture
Solvents and other product use	Other Sources and Sinks

3.4 Deposition

In the model, deposition of species to the surface occurs after the previously mentioned atmospheric chemistry processes. In the model, deposition occurs through both wet and dry deposition. The wet deposition scheme used includes the washout of soluble aerosols and scavenging in convection updrafts (Liu et al., 2001). The dry deposition scheme used is predominantly based on the “Wesley” resistance-in-series scheme as described in Wang et al., (1998) where gravitational settling is dependent on the size of the dust aerosol (Johnson et al., 2012). Wet deposition of mineral dust is also accounted for via scavenging and rainfall washout as described in Liu et al., (2001). For sea salt aerosol a size dependant dry deposition scheme is used according to hygroscopic growth which is described in Zhang et al., (2001). A more comprehensive overview sea-salt deposition scheme is found in Jaegel et al., (2011).

3.5 Chemistry and transport

Transport of chemical species emissions in the model is driven by assimilated meteorological fields from the NASA GEOS-5 system (Suarez et al., 2008). The native resolution of the meteorological fields is 0.25°

x 0.25^{o} which is also the resolution of the European regional grid. The global model is forced by data averaged onto a 4^{o} x 5^{o} grid. The meteorological fields includes information about the 3D large scale winds, temperatures, pressures, water vapour concentrations, vertical diffusion coefficients, convective mass fluxes, cloud properties, surface types, etc. (Liu et al., 2006). The model internal timestep was set at 10 minutes for transport and 20 minutes for chemistry.

3.6 Diagnostics

Hourly values of surface ozone, NO, NO_2 , PAN, ethane, propane and the aerosol tracers were output each hour of the simulation for all surface locations in the European nested grid.

In order to calculate a $PM_{2.5}$ that could be comparable to those measured. All 'fine mode' aerosol components were summed, together with factors to account for the liquid water associated with each component. A relatively humidity of 50% was assumed across the European domain which is the standard relative humidity typically used for model simulations.

Regulatory observations of NO_2 are made by converting NO_2 to NO and then by measuring the additional NO formed from this process. This conversion is typically made using a Molybdenum converter. This has the tendency of also converting other species which contain NO_2 into NO (Steinbacher et al., 2007). So for example a fraction of the PAN in the air may be converted and so the instrument may measure an artificially high value. In order to evaluate this as a problem a NO2* diagnostic is calculated in the model which is composed of NO2 + HNO3 + PAN + PMN.

3.7 Model simulations

The model "base" run was setup as described in Sherwen et al., (2016), with the EMEP diurnal and seasonal scaling updates. The model has halogen chemistry switched on and secondary organic aerosol chemistry switched off.

The observational period of interest for running the model is between 15th Feb 2014 – 1st December 2014, although in some of the analysis of the year model run is used (15th Feb 2014 - 14th Feb 2015). For the two weeks prior to the 15th Feb 2014 the model is "spun up", with these two weeks output is disregarded.

In order to evaluate the impact of agriculture on European pollution loads the ("AgriOff") model simulation was ran. This switched off the agricultural sources of pollution (see Table 6) but otherwise was simulated identically to the base run. From the EMEP emissions the emission sectors for i) Manure Management ii) Crop Production emissions and agricultural soils iii) Agriculture other including the use of pesticides and iv) Field burning of agricultural wastes sectors were switched off. Fertilizer NO_x was switched off but soil NO_x emission was left on.

Chapter 4: General Model Performance over regions of Europe

In comparison to the US or China nested grids available in the GEOS-Chem model (Travis et al., 2016, Zhang et al., 2011, Rieder et al., 2015, DeBell et al., 2004, Chen et al., 2009, Zhang et al., 2015, Zhang et al., 2016), there has not been large studies evaluating model performance using the Europe nested domain (see Figure 1). This section aims to give an evaluation of the European nested domain against observations of surface air quality pollutants.

For simplicity, the European domain is split into five regions: UK and Ireland, Benelux, Central- Eastern EU, West and Southern Europe, as described in Chapter 2.1 (see Table 3). For each region, the relevant Air Quality e-Reporting (AQER) site data was extracted as described in Chapter 2.1. Observed data at each site is compared to the nearest GEOS-Chem grid box species at the same hourly time-step. Model performance is assessed in terms of a regional monthly trends, diurnal trends and point-for-point comparisons. This will gives an assessment of the spatial and temporal performance of the model.

4.1 NO_2

The model was compared to 1512 background sites reporting NO_2 over Europe, as explained in Chapter 2.1, for a between February and December in 2014.

4.1.1 Seasonal cycles

Figure 3 shows the modelled and observed regional monthly median NO_2 concentrations. Both the model and measurements show a generally minimal observed seasonality in observations which peaks in winter and has a summer minimum. In general the model is bias low by around 5 to 10 ppbv or 50-150%. A smaller bias is seen for the UK and Ireland region and the Benelux region relative to the other regions.

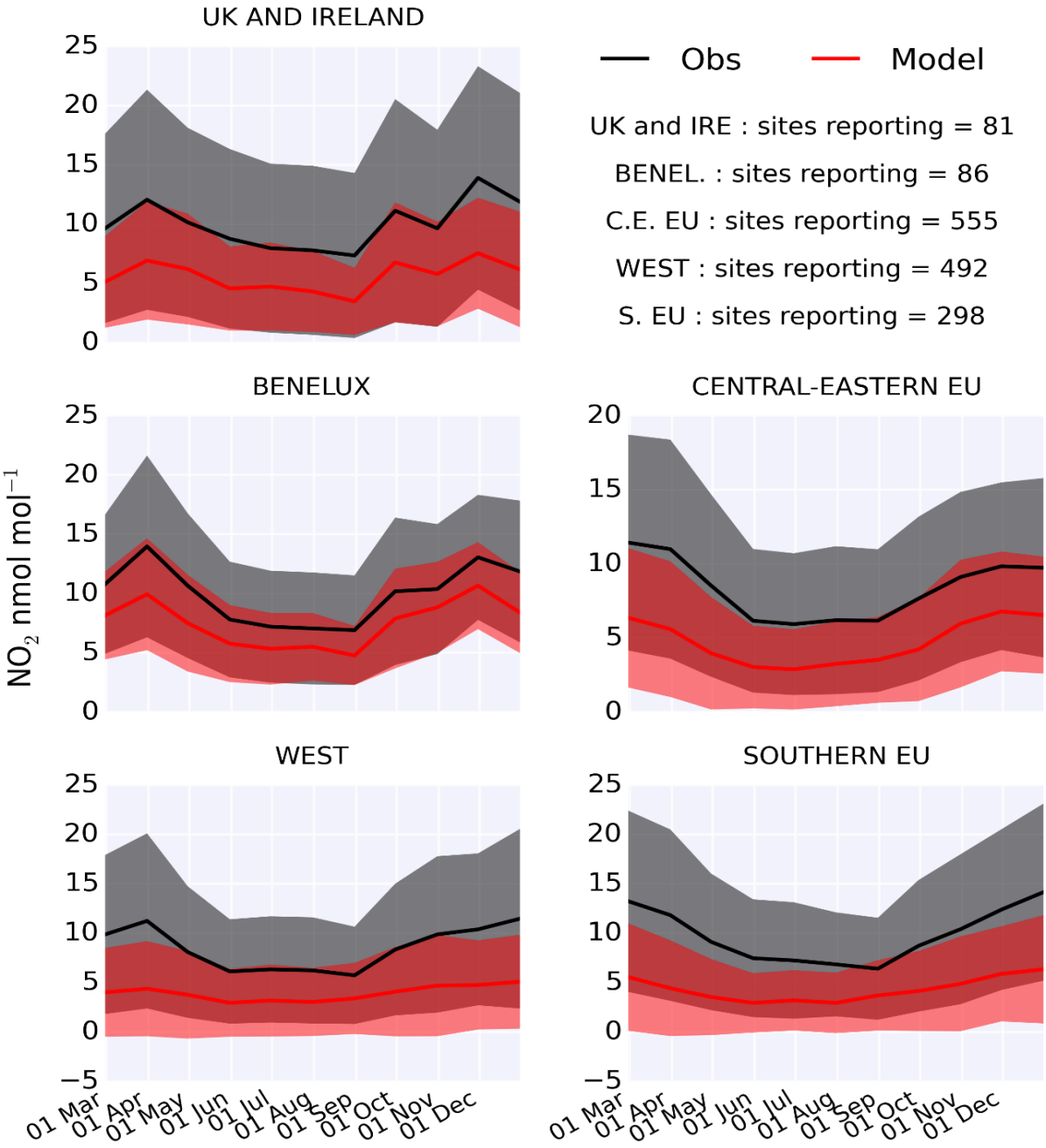

FIGURE 3 COMPARISON OF MONTHLY MEDIAN MODELLED AND OBSERVED NO_2 CONCENTRATIONS FOR REGIONS WITHIN EUROPE DURING THE OBSERVATIONAL PERIOD. THE SHADED AREAS GIVE THE MONTHLY STANDARD DEVIATION ACROSS THE SITES IN THE REGION.

4.1.2 Point by point (hourly) comparisons

Figure 4 shows a point by point comparison between the hourly model and observed site measurements averaged across the sites within each region. In all cases the model shows a degree of correlation with the observations however this correlation is in general relatively weak (R^2 ~ 0.4). As shown in the seasonality plot (Figure 3), model concentrations are underestimating observations by a factor of 1.3 – 3, with the largest factor in the Southern EU region. Across regions, the model best fit line is crosses near zero (between 0.7-1.9 nmol mol^{-1}) it is just that it appears to have too low a value of gradient (ranging

between 0.38 (Southern EU) and 0.71 (Benelux)). The model bias appears to be fractional for both high and low concentrations, which shows that this underestimate is likely a fractional bias.

4.1.3 Diurnal cycles

Figure 5 shows the annual NO_2 concentrations for all background sites averaged over a diurnal cycle. Observed NO_2 concentrations are highest during rush-hour periods of the day. This is likely due to the large increase in vehicle NO_X emissions from the transport sector (Guillaume et al., 2017). However, the model fails to capture this trend with little or no evidence for rush hour maxima. The model has the same diurnal scale that is applied in Sherwen et al., (2017).

A potential observational negative bias could explain some of the magnitude of some of the difference in the modelled underestimation in certain regions, but it does not explain why the model is not capturing the observational “rush-hour” rise

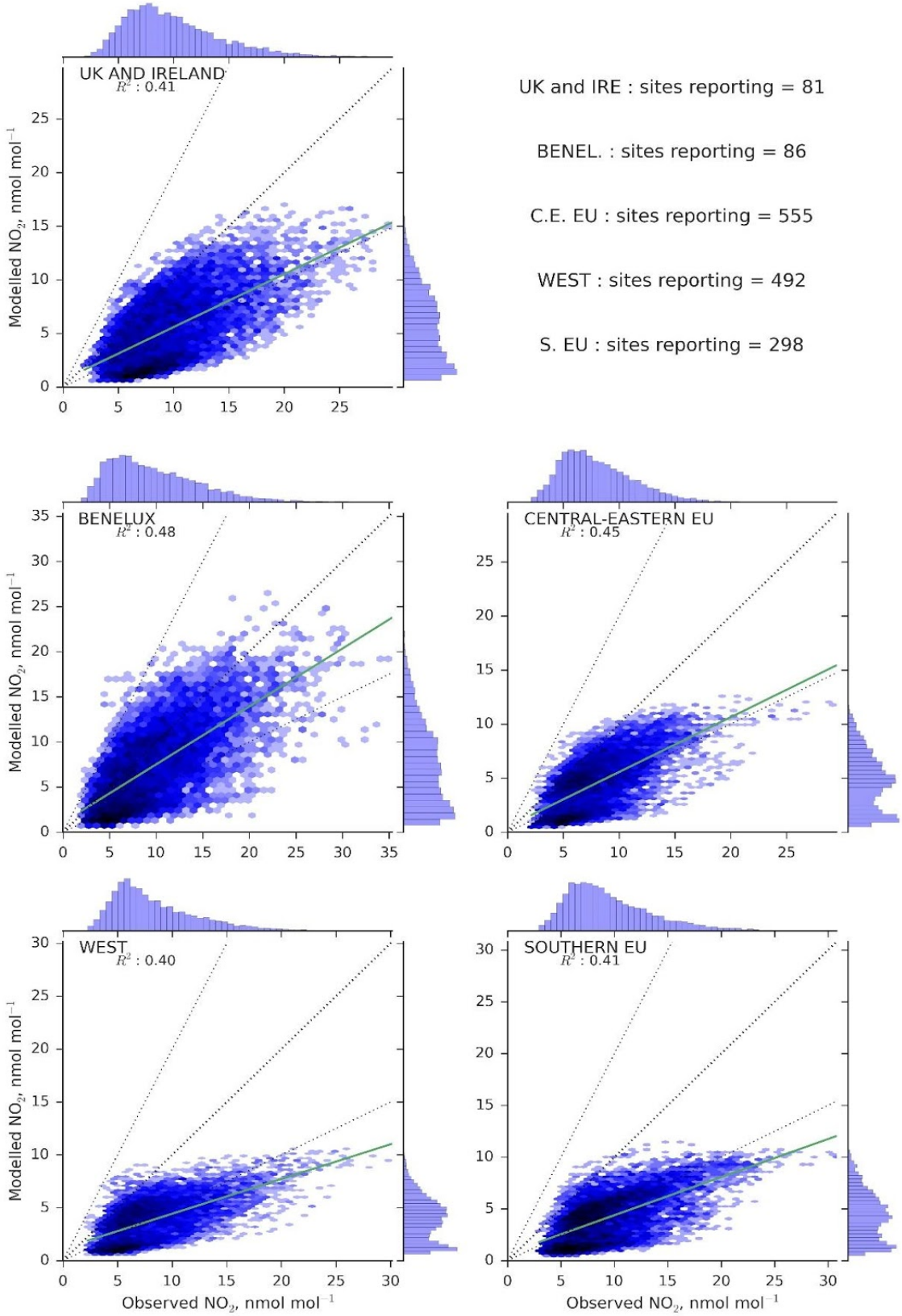

FIGURE 4 HOURLY NO_2 OBSERVED AND MODELLED CONCENTRATIONS FOR REGIONS WITHIN EUROPE DURING THE OBSERVATIONAL PERIOD. HEXAGON COLOUR SHADING IS ON A LOGARITHMIC SCALE WHICH REPRESENTS THE DENSITY OF SCATTER POINTS WITHIN THE HEXAGON AREA. GREEN LINE REPRESENTS THE LINE OF BEST FIT. DASHED LINES REPRESENT 1:2, 1:1 AND 2:1 RATIOS.

Figure 5 Comparison of modelled and observed median diurnal concentrations of NO_2 of background sites for regions within Europe during the observational period. Shaded regions give the hourly standard deviation across sites.

4.1.4 NO_2 conclusions

All of the analysis presented here in figures 3,4 and 5 show that the model is bias low compared to the observations.

However, NO_2 observations though are thought to be biased high (Steinbacher et al., 2007). Chemiluminescence analysers indirectly measure NO_2 by subtracting NO from total NO_x concentration via use of a molybdenum or photolytic converter which converts NO_2 to NO. The European monitoring network use both types of chemiluminescence instruments; molybdenum and photolytic. A conversion of nitrogen species other than NO_2 (e.g. HONO and PAN) to NO by these methods leads to a positive interference and so, a significant overestimation of NO_2 concentrations (Steinbacher et al., 2007). Steinbacher et al., (2007) compared two molybdenum analysers with two photolytic analysers at two rural sites in Switzerland. The molybdenum instruments were found to overestimate the "real" NO_2 by between 42-83% with the most interfering nitrogen compounds being nitrous acid (HONO) and peroxyacetyl nitrate (PAN). Photolytic analysers also showed a positive interference, with a 5% interference from PAN decomposition and a 5% interference from HONO to total NO_2 concentration (Gerboles et al., 2003). These interferences could explain some of the model's low measurement bias. However, more work needs to be done to quantify this bias more fully.

Also, given that the model failed to capture the "rush hour" rise in NO_2 (see Figure 5), rather than there being a continuous difference between the model and measurements, it would appear that the observational problems from the NO_2 instrumentation can not fully explain the model measurement disagreements alone. It appears likely that there is also a problem with the NO_2 emissions in the model.

Direct observations of NO_x emissions over London have pointed towards a factor of two difference between the inventories and emissions fluxes (Vaughan et al., 2016). Vaughan et al., (2016) attributed this bias mainly due to an underestimation of vehicle emissions in the inventory. Calculating these emissions is difficult and the uncertainties are large. The potential influence on the emissions inventory from emissions hidden using "defeat devices" are thought to be small as the highest estimate for VW NO_x is a 0.8% contribution of background urban NO_x in Germany (Guillaume et al., 2017), so it is likely a general underestimation of emissions is occuring.

The model significantly low bias for NO_2 could be explained by both an instrumental overestimate in NO_2 and by an underestimate in the modelled emissions. Future work will be needed to assess and address these problems.

4.2 NMHCs

NMHCs (non-methane hydrocarbons) were selected from the background AQER sites over the UK (as mentioned in Chapter 2.1) for an observational period of a year. Ethane, propane, lumped alkenes (which have more than 3 carbons (PRPE)) and alkanes (which have more than 4 carbons (ALK4)) were considered. Model comparison was made against 2 UK observational sites; Harwell, Auchencorth Moss. The only other AQER background site with NMHC observations is London Eltham. This site has been excluded from analysis as it showed high concentrations, which are highly likely indicative of very local sources.

4.2.1 Seasonal cycles

Figure 6 shows the monthly mean of hourly comparison between the model and the measurements for ethane, propane, PRPE and ALK4.

For ethane and propane the model underestimates concentrations, with a mean bias of ~ 0.7 nmol mol^{-1} and 0.5 nmol mol^{-1} in each case. The model performance for PRPE is much better, with near no bias ~0.02 nmol mol^{-1} for PRPE. For ALK4 there is a bias high of ~ 1 nmol mol^{-1}

The modelled underestimation for ethane and propane could be due to either a bias in the emissions used in the model or a bias generated from the modelled boundary conditions. There is no standard deviation for observations in the spring of 2015 as the Auchencorth Moss site is not showing observations, meaning a standard deviation across the two sites cannot be found.

The monthly observational fluctuation of PRPE is reduced with the exclusion of the London Eltham site, particularly for December. Even with the London site excluded, there is still a modelled overestimation of ALK4, implying a rural overestimation of emissions, although site coverage is limited. The model consistently overestimates observed ALK4 during all months of the year, indicating emissions are overestimated for longer alkanes.

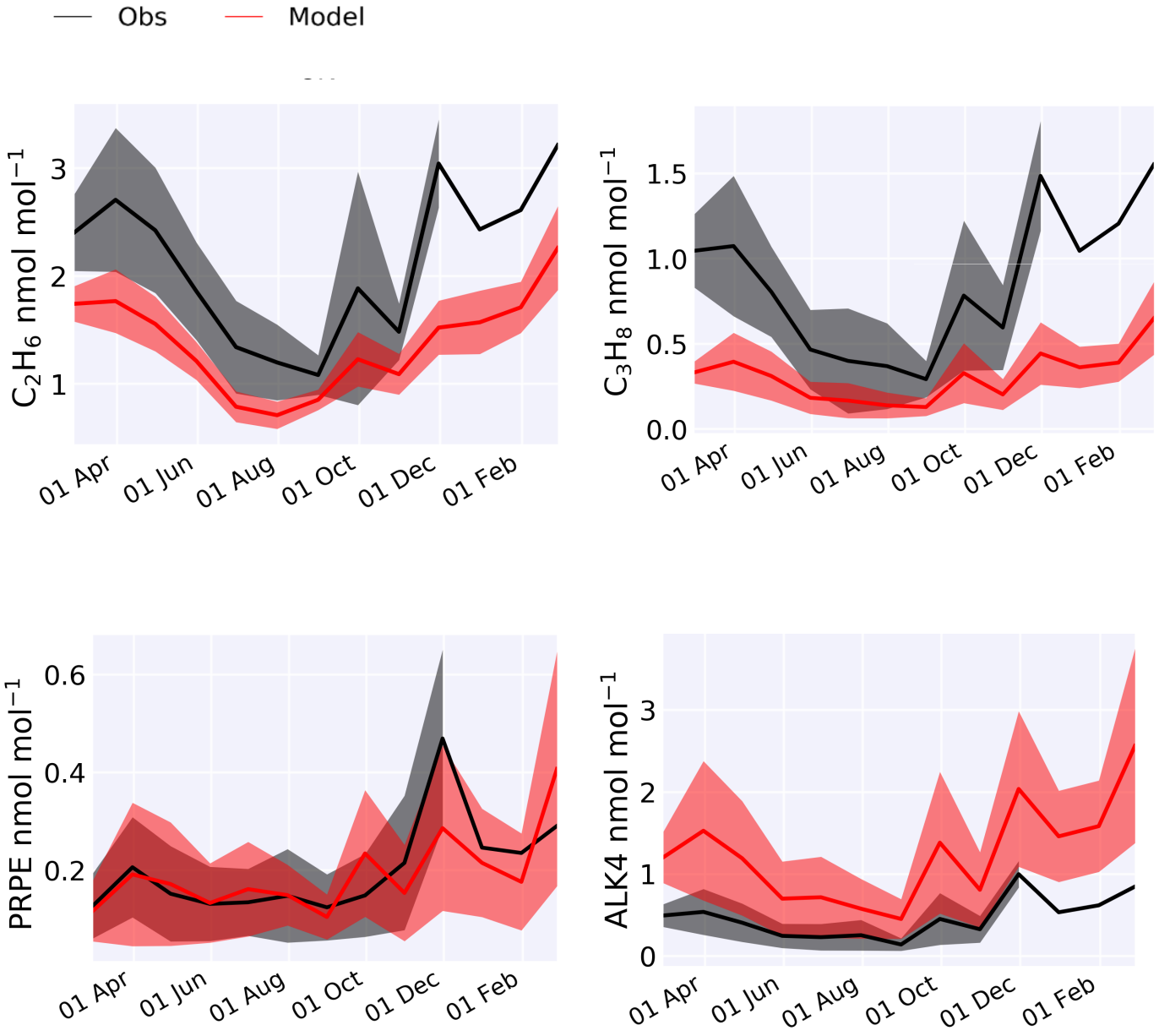

FIGURE 6 COMPARISON OF MONTHLY MEAN MODELLED AND OBSERVED ETHANE, PROPANE, PRPE AND ALK4 CONCENTRATIONS IN THE UK OVER THE OBSERVATION PERIOD. THE SHADED AREAS IS THE MONTHLY STANDARD DEVIATION

4.2.2 Point by point (hour) comparisons

Figure 7 shows a point by point comparison of the hourly values for the hydrocarbons averaged across the two sites. There is only a moderate correlation between the model and observations with significant biases in the gradient and y-intercept. This could reflect a range of issues with the model. The p-value is

calculated using the predefined calculation in the scipy library and indicate the results are statistically significant.

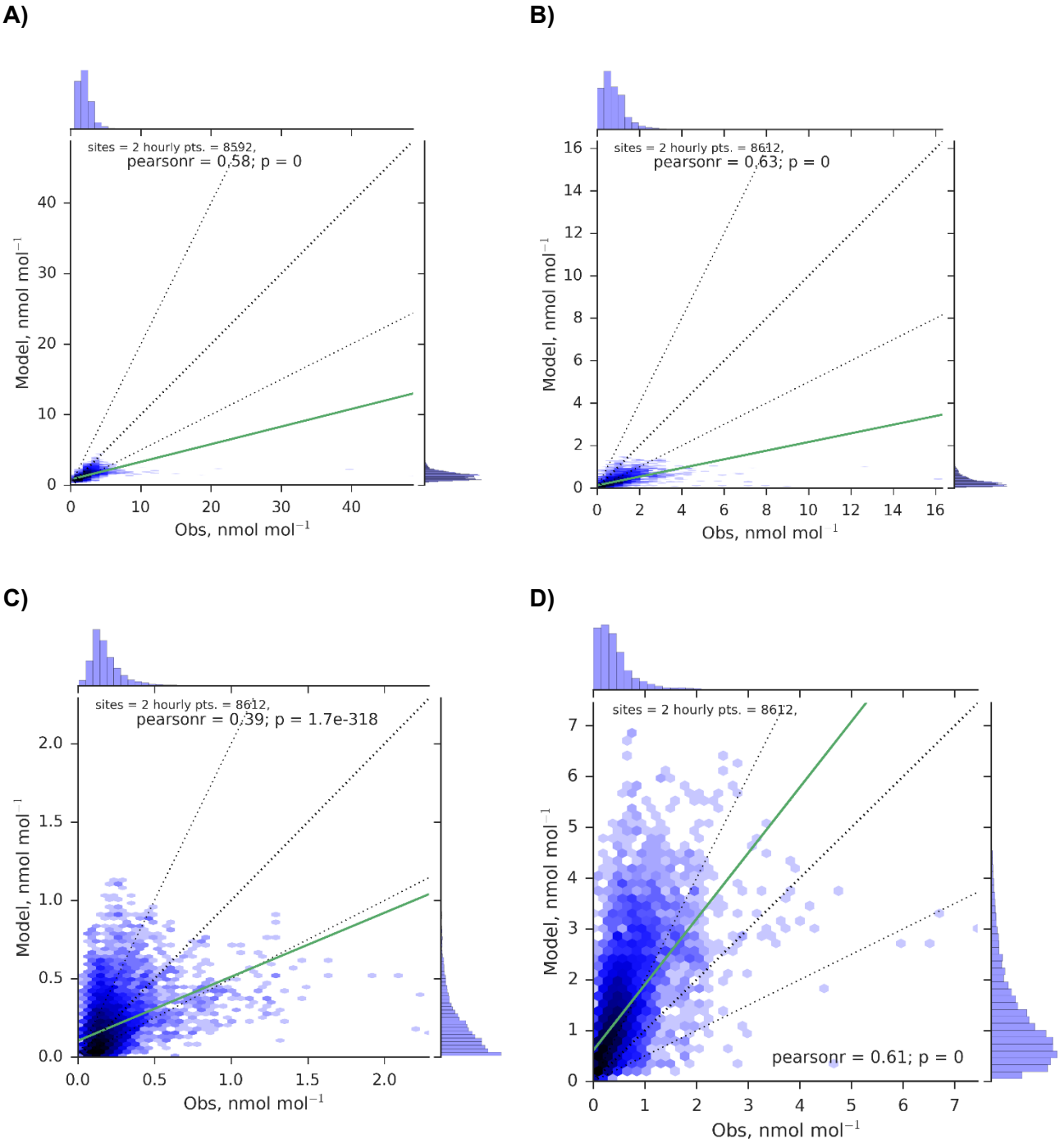

FIGURE 7 HOURLY A) ETHANE, B) PROPANE, C) PRPE AND D) ALK4 OBSERVED AND MODELLED CONCENTRATIONS OF BACKGROUND UK SITES DURING THE OBSERVATIONAL PERIOD. HEXAGON COLOUR

SHADING IS ON A LOGARITHMIC SCALE. GREEN LINE REPRESENTS THE LINE OF BEST FIT. DASHED LINES REPRESENT 1:1, 2:1 AND 1:2 RATIOS.

4.2.3 Diurnal cycles

Diurnal hourly average plots (Figure 8) show some curious properties. For all species, observations show little or no diurnal cycle whereas the model shows a much larger diurnal cycle for the shorter lived species (PRPE and ALK4). It is hard to reconcile the lack of a diurnal cycle with the known chemistry of these hydrocarbons. Explanations to this may be due to an issue with the timestamps on the observational data, in the processing of the data, or in the observations themselves. Although the diurnal cycles appear suspect the results here highlight the low bias in the modelled ethane and propane.

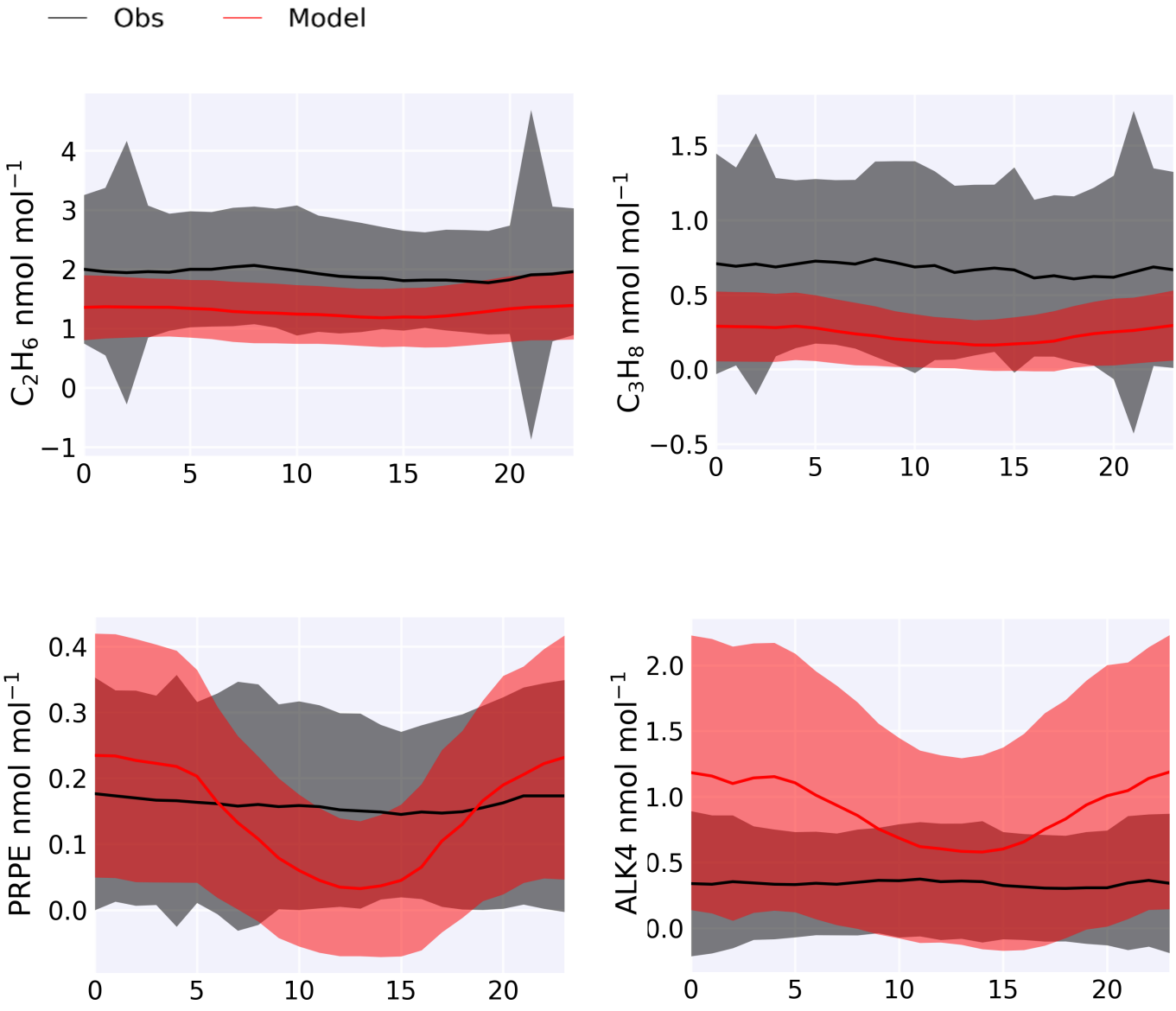

FIGURE 8 COMPARISON OF MEAN DIURNAL MODELLED AND OBSERVED ETHANE, PROPANE, PRPE AND ALK4 CONCENTRATIONS WITH FOR BACKGROUND SITES OVER THE UK IN THE OBSERVATIONAL PERIOD.

This bias seen in figure 8 may be due to local (UK scale) emissions or given the relatively long lifetime of ethane and propane there may be an issue with the boundary conditions used in the model.

The EMEP emissions do not currently account for ethane and propane emissions from gas network leakage emissions. It may be that this represents a significant missing source of ethane and propane to the emission inventories (Derwent et al., 2017).

In order to assess if boundary conditions (and not inventory emissions) are causing the underestimation in UK NMHC concentrations concentrations, observations and model results at Mace Head (west coast of Ireland) are now evaluated.

4.2.4 NMHCs comparison to Mace head Ireland

Averaged National Oceanic and Atmospheric Administration (NOAA) canister observations at Mace Head are shown in Figure 9. As mentioned in Chapter 2.3, Mace head is situated on the western coast of Ireland, which has minimal local and regional VOC influences. If there are elevated NMHCs in the UK relative to Mace head, this would indicate the magnitude of regional anthropogenic NMHC concentrations over the UK.

The NOAA canister observations at Mace Head were limited, with data collected at irregular ~weekly intervals between 10:00 and 16:00 (GMT). Alkenes are not stable in canisters, so no comparisons can be made with them. Alkane comparison is also provided for only a limited number of species (see Table 5). Figure 9 shows the monthly averaged comparison between ethane, propane and ALK4 species.

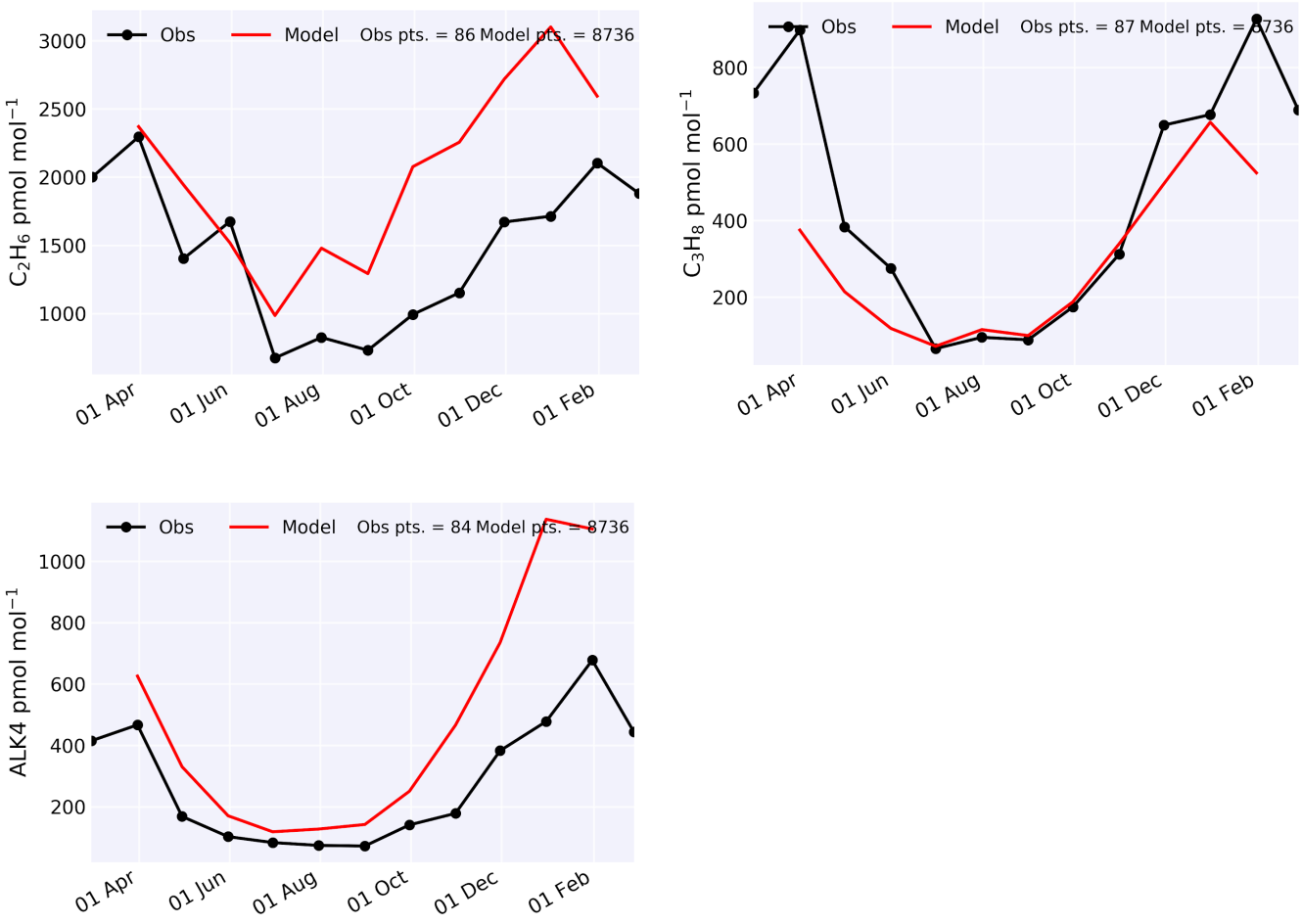

FIGURE 9 COMPARISON OF MONTHLY MEAN MODELLED AND OBSERVED ETHANE, PROPANE AND ALK4 CONCENTRATIONS AT MACE HEAD FOR THE OBSERVATIONAL PERIOD.

Figure 9 shows that modelled ethane at Mace head matches springtime observations well, but tends to overestimate summer, autumn and winter concentrations. This is in contrast to the UK NMHC network, (see Figure 6) where the model is underestimating ethane across the year. This suggests that the underestimation seen in ethane concentrations over the UK is likely due to a missing source rather than an issue with the western european boundary condition.

For propane the model is capturing summertime concentrations but underestimating concentrations in the spring, autumn and winter periods. Over the UK (see Figure 6), the model is also consistently underestimating NMHC surface monthly concentrations. Thus, the underestimation of the model at Mace Head signifies again missing source(s) and potentially an underestimation of the western european boundary conditions.

The model is capturing ambient ALK4 concentrations at Mace head well, with a slight overestimation ~100 pmol mol^{-1} across the time period. This is potentially due to longer chain alkanes (>C5) not being available for canister observations within the time period, accounting for the observed negative bias. At low and

high concentrations the model is consistently overestimating ALK4 concentrations, but considering the sparsity of observations, the model is performing well in comparison, indicating the model is capturing emissions reasonably.

4.2.5 VOC conclusions

For ethane it is likely that there is an underestimation of emissions in the UK. For propane, the model tends to underestimate UK concentrations to a larger extent than at Mace Head. It is likely that there is a significant underestimation/missing source(s) of emissions of these two species over the UK, which is not being captured by the model. Although for propane, boundary conditions may be contributing to this. Research in the field highlights the leakage emissions from the natural gas network, which are currently not accounted for sufficiently (Derwent et al, 2017) in the EMEP emissions inventory, could reduce the UK modelled negative bias. Further research into capturing the natural gas network emissions into the model sufficiently is required to quantify the impact of this source on the seen bias.

The modelled slight overestimation of ALK4, is possibly due to missing observed species not being available for comparison for the site in Mace head. Future readjustments to the diurnal scaling could also be a factor to mitigate the variance between the model and observations for these species.

4.3 Ozone

Ozone is a critical atmospheric species as it is both a pollutant and a key chemical in the wider oxidation chemistry of the atmosphere, as mentioned earlier in Chapter 1. It has a significant burden in public health.

Previous work by Yan et al., (2016) has compared ozone observations over Europe using the “two-way coupled” configuration, which differs from the “one-way coupled” simulation we use here as described in Chapter 3.2. Yan et al., (2016) showed ozone was overestimated by the model, which agrees with our study findings in Figures 10, 11 and 12. However, we cannot directly compare our results because their study used the 2005 EMEP NO_x emissions inventory, which were higher than the 2009 update used in this study. Furthermore Yan et al., (2016) compares a number of different site types (including road and kerbside sites) whereas this study compares all background site types only. Observations from over an 8.5 month period were compared to the model, with 1540 sites reporting ozone measurements in this section (see Chapter 2.1).

4.3.1 Seasonal cycles

Figure 10 shows the modelled and observed monthly / seasonal seasonal cycle of ozone. This shows the model does capture the seasonality seen in observations, with a summertime high and a wintertime low. The model particularly captures wintertime observations across all the regions. However, the model has a tendency to overestimate the mean concentrations, especially in the summer months.

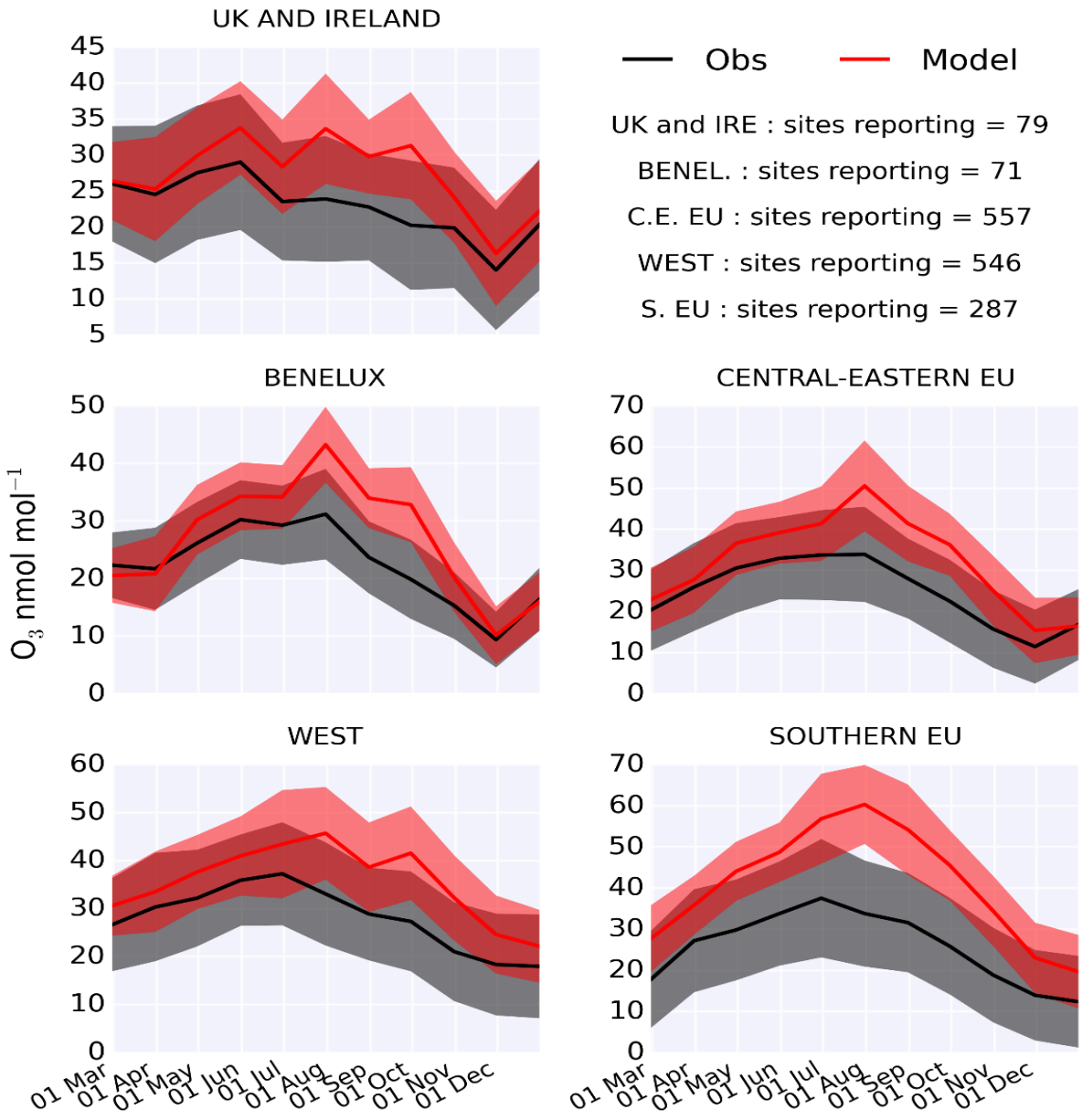

Figure 10 – Comparison of monthly mean modelled and observed ozone concentrations for regions within Europe during the observational period. The shaded areas give the monthly standard deviation across sites.

4.3.2 Point by point (hourly) comparisons

Figure 11 shows a point by point (hourly) comparison of the model performance across the sites within the regions of the European nested domain. The model shows some skill in capturing higher concentrations (>30 nmol mol-1), but does tend to have a positive bias at lower concentrations. The model high bias is more prominent in the southern regions of Europe (~20 nmol mol^{-1}) whereas in the northern regions it is as low as ~10 nmol mol^{-1}.

.

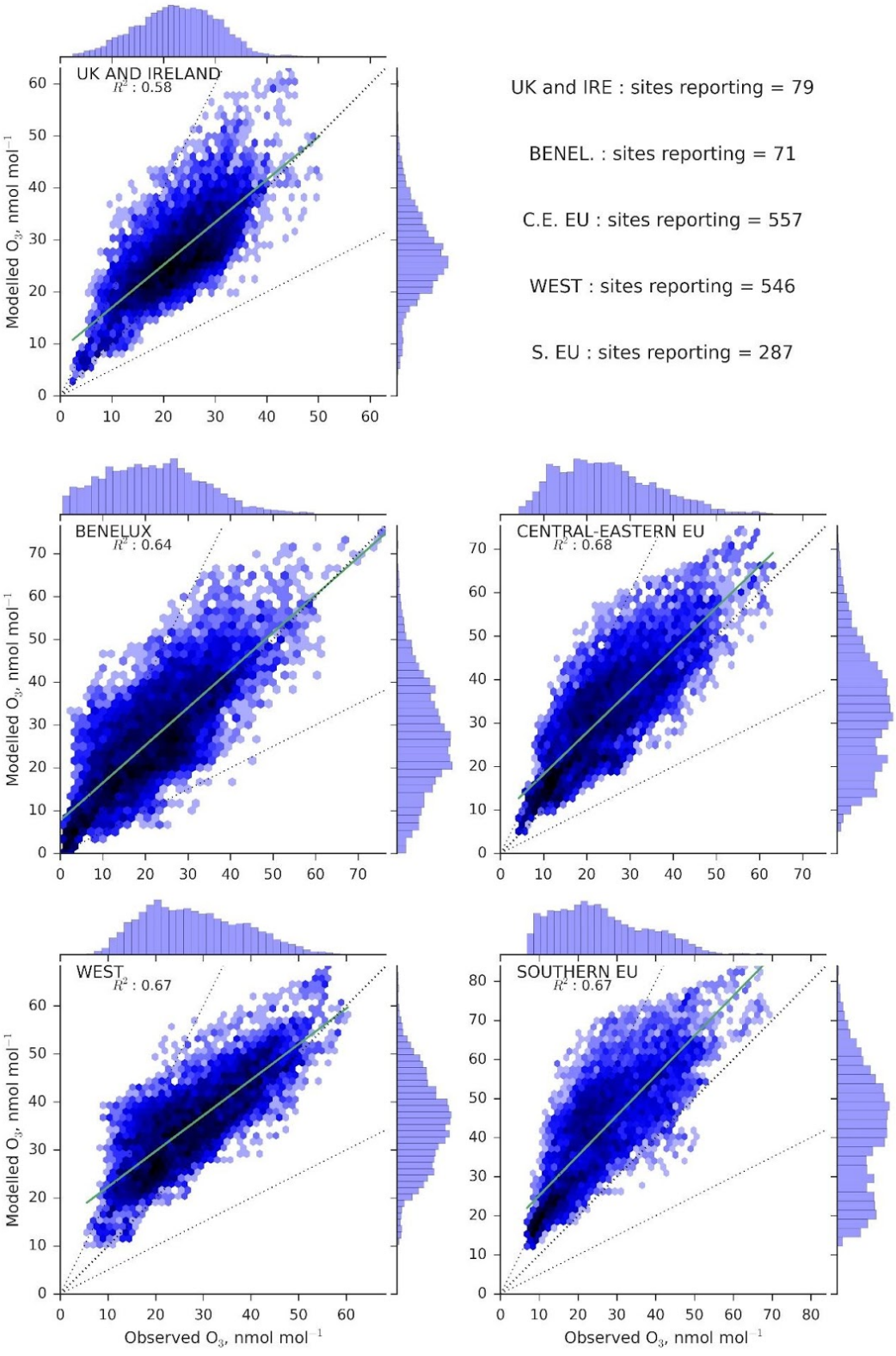

FIGURE 11 HOURLY OZONE OBSERVED AND MODELLED CONCENTRATIONS OF BACKGROUND SITES FOR REGIONS WITHIN EUROPE DURING THE OBSERVATIONAL PERIOD. HEXAGON COLOUR SHADING IS ON A LOGARITHMIC SCALE. GREEN LINE REPRESENTS THE LINE OF BEST FIT. DASHED LINES REPRESENT 1:1, 1:2 AND 2:1 RATIOS.

4.3.3 Diurnal cycles

Figure 12 shows the mean diurnal cycle in the model and in the measurements across all reporting background sites in five european regions. The model captures the general trend of ozone production during the day and ozone loss at night. However, during all times and across all locations, the model overestimates observations. The largest discrepancy is seen with night-time ozone, whereas the model broadly captures the observed afternoon maxima. The tendency for a notable observed minimum to occur at 05:00 is not visible in the model.

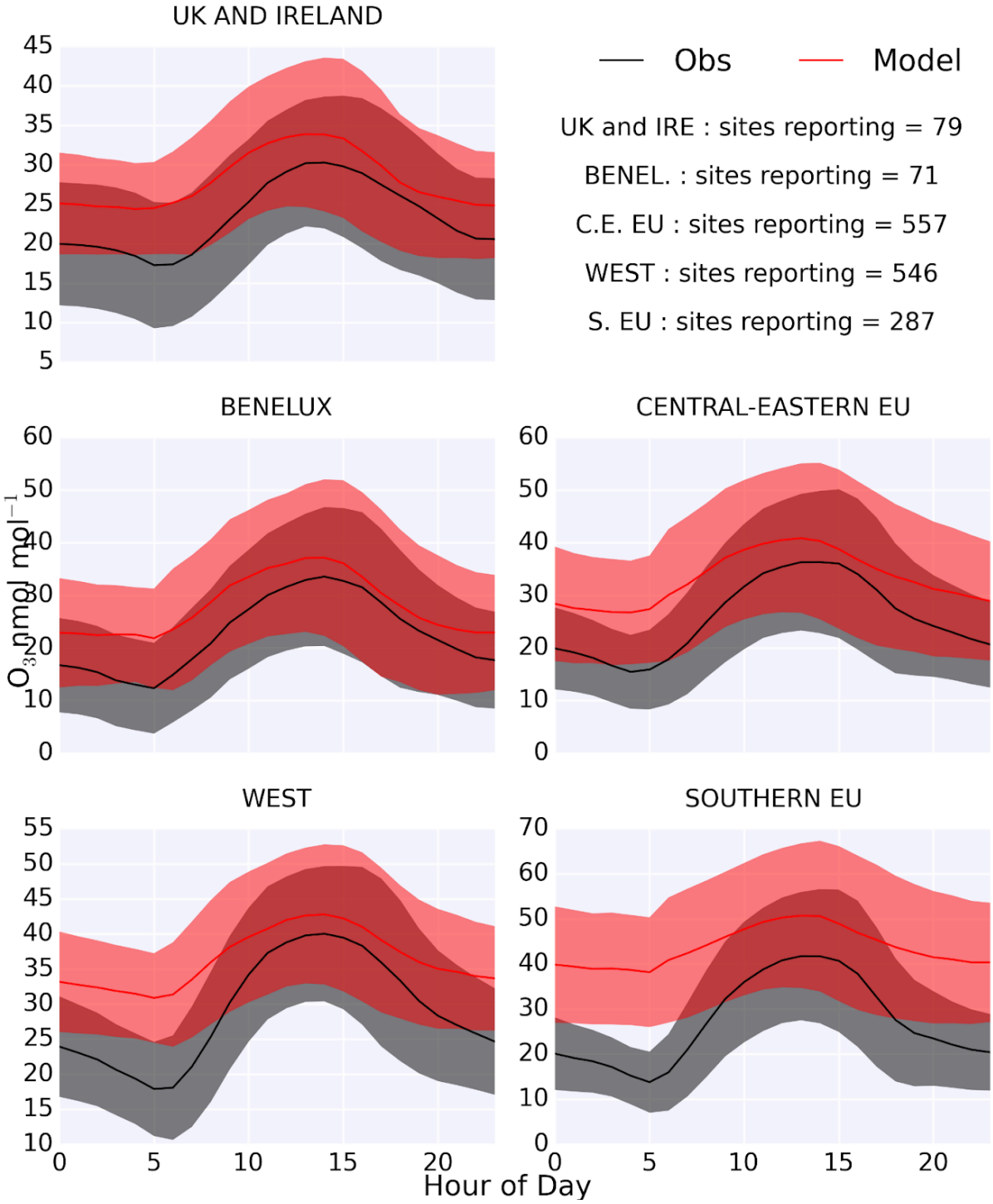

Figure 12 Comparison of modelled and observed median ozone concentrations of background sites within regions of Europe during the observational period. Shaded areas are the hourly standard deviation of site measurements.

4.3.4 Ozone conclusions

The modelled overestimation of ozone concentrations seen in figures 10, 11 and 12 could be due to problems in the ozone production or in its loss.

It is possible that the ozone production is overestimated in the model. However, the earlier comparisons made between observed NO_x and NMHCs (chapters 4.1 and 4.2 respectively) to the model seen earlier, suggest that if anything the model underestimates their concentrations. Although there may be non-linearities in the chemistry, this evidence would tend to suggest that the problem doesn't lie with the production of ozone, but due to ozone loss.

There may be issues with the modelled dry deposition rates of ozone. As mentioned earlier (in section 1.2.3), dry deposition accounts for a quarter of tropospheric ozone loss (Lelieveld and Dentener, 2000) and is accounted for with the "Wesley" dry deposition resistance-in-series scheme (Wang et al., 1998). In the summer, the area of vegetative surface is substantially increased, so if the rate of dry deposition from stomatal uptake is underestimated (Travis et al., 2016), this would lead to a modelled positive bias. This hypothesis is consistent with suggestions in Yan et al., (2016) and aligns to findings in this study.

The modelled surface overestimation could also indicate excessive vertical mixing of ozone, which has been proposed in Travis et al., (2016) as a potential factor for positive modelled bias over the US. During the months of higher ozone concentration, if vertical mixing was excessive, this would lead to a larger summertime "buildup" of ozone, leading to a larger modelled divergence to observations. Further research could investigate if this factor is significant to the overestimation seen by evaluation of modelled and observed vertical ozone profiles across Europe.

The comparisons presented in Figure 12 are consistent with recent work comparing the same european nested model model against UK observations (Sherwen et al., 2017). Sherwen et al., (2017) compared sites within the UK AURN air quality network, which showed a small positive bias, which also did not capture nighttime ozone loss sufficiently. These results reasonably correlate to findings for the UK and Ireland region in Figure 12. However, in the same paper, at the Weybourne coastal site, this was not the case. Here, the model has a low 9.2% bias and did sufficiently capture nighttime ozone loss. The differences between this study and the Weybourne site can be explained by the influence of halogen chemistry, which at the coast led to better approximation of night time ozone concentration. In figure 12 for the UK and Ireland region, the positive night-time bias is likely due to the inclusion of a large proportion of inland sites which ozone destruction is not influenced as much by halogen chemistry.

To conclude, there are three main potential causes to why the model is not capturing this loss in night time ozone concentrations in Europe. Firstly, night-time chemical loss of ozone to N_2O_5 may not be captured in the model sufficiently (in section 1.2.3.2, R 3.6 - R 3.8). Secondly, a potential cause could be an underestimation of ozone dry deposition. Finally, excessive mixing in the troposphere at night could explain the positive modelled night time bias, as highlighted earlier as a likely factor to modelled ozone positive bias in Travis et al., (2016). Further analysis is required to conclude if each of these factors are driving this night-time positive bias of modelled ozone.

If the nighttime loss of ozone was to be corrected, this would lead to an underestimation of modelled afternoon peak ozone concentrations. The difference in magnitude of between daily maximum and minimum of the modelled average line is of a smaller magnitude compared to the same observational comparison (figure 12). This disparity is worse in the more southern latitude regions. This subsequent issue, would likely be resolved with better increased concentrations of the underestimated modelled NO_2 and NMHCs (chapter 4.1 and 4.3), which would increase the rate of photochemical ozone production. This would increase the photochemical ozone production in the southern European regions, due to the higher intensity of light and therefore increase the magnitude of daily modelled ozone fluctuation.

In terms of an air quality perspective, the most important hours of the day are at peak ozone concentrations, between the late morning and late afternoon. Currently the model is performing particularly well between these times, and capturing the elevated ozone mixing ratios.

4.4 $PM_{2.5}$

This chapter evaluates the model's ability to simulate $PM_{2.5}$ over Europe. Individual hourly observations from 424 sites (see Chapter 2.1) are considered across Europe and are compared to the nearest model simulation point in space and time.

4.4.1 Seasonal cycles

The observed and modelled $PM_{2.5}$ is shown monthly/seasonally by region in Figure 13. Figure 13 shows the model is generally capturing monthly mixing ratios across regions but with a tendency towards being biased high in most locations, especially in the winter time across the 8.5 month period.

4.4.2 Point by point (hourly) comparisons

Figure 14 shows the same model overestimation seen in the seasonal analysis, with trend lines in all regions above the 1:1 line. The extent of the overestimation of the model to observations is similar (in terms of relative magnitude) in all regions, indicating a modelled issue which is not localised to certain regions. Notably, the north-west regions (UK and Ireland and the Benelux region) have a higher correlation (0.56 and 0.55) in comparison to the other EU regions (<0.47). Modelled $PM_{2.5}$ within the southern EU region has a particularly low correlation (0.05).

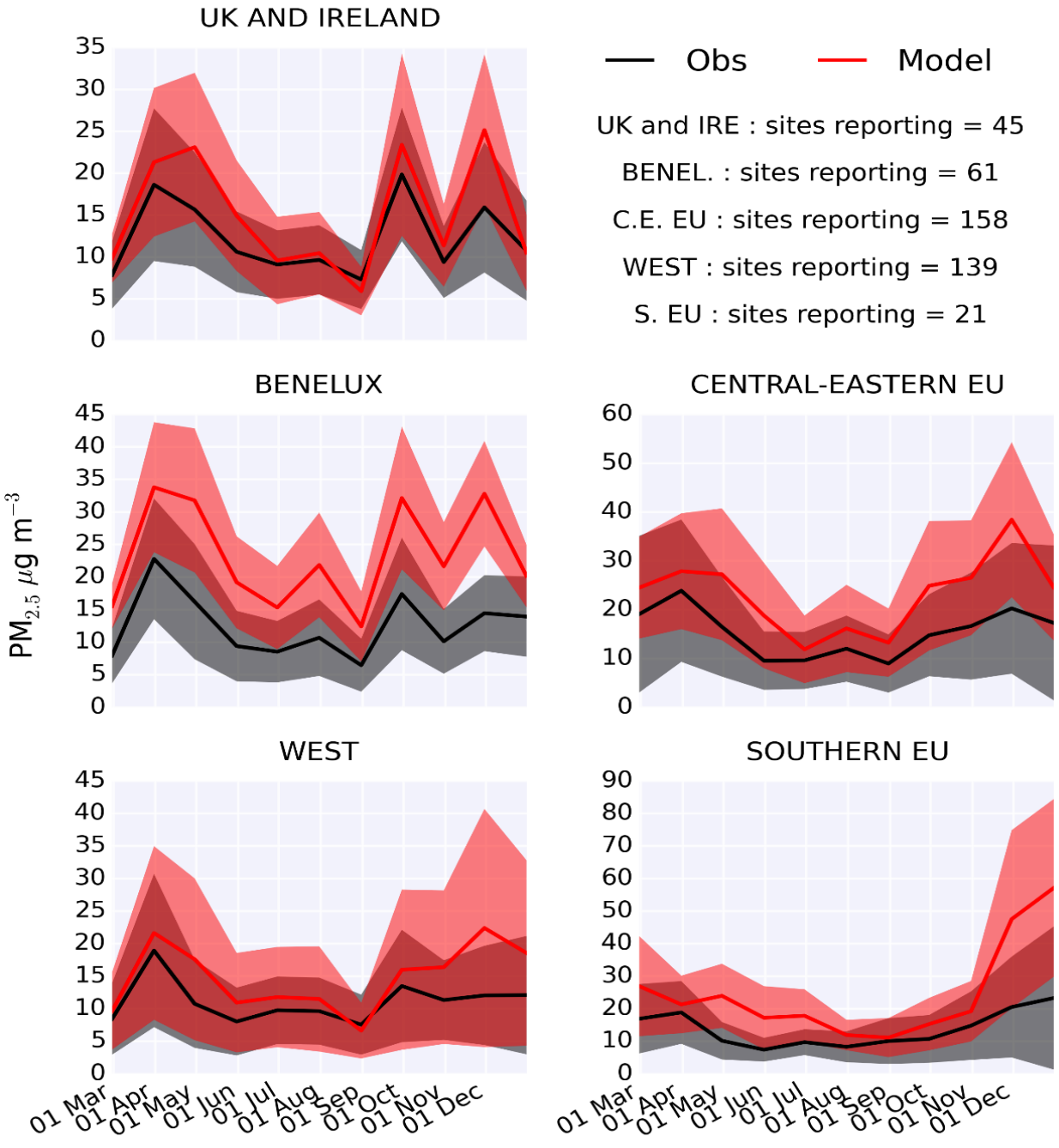

FIGURE 13 COMPARISON OF MONTHLY MEAN MODELLED AND OBSERVED $PM_{2.5}$ CONCENTRATIONS FOR REGIONS WITHIN EUROPE DURING THE OBSERVATIONAL PERIOD. THE SHADED AREAS GIVE THE MONTHLY STANDARD DEVIATION.

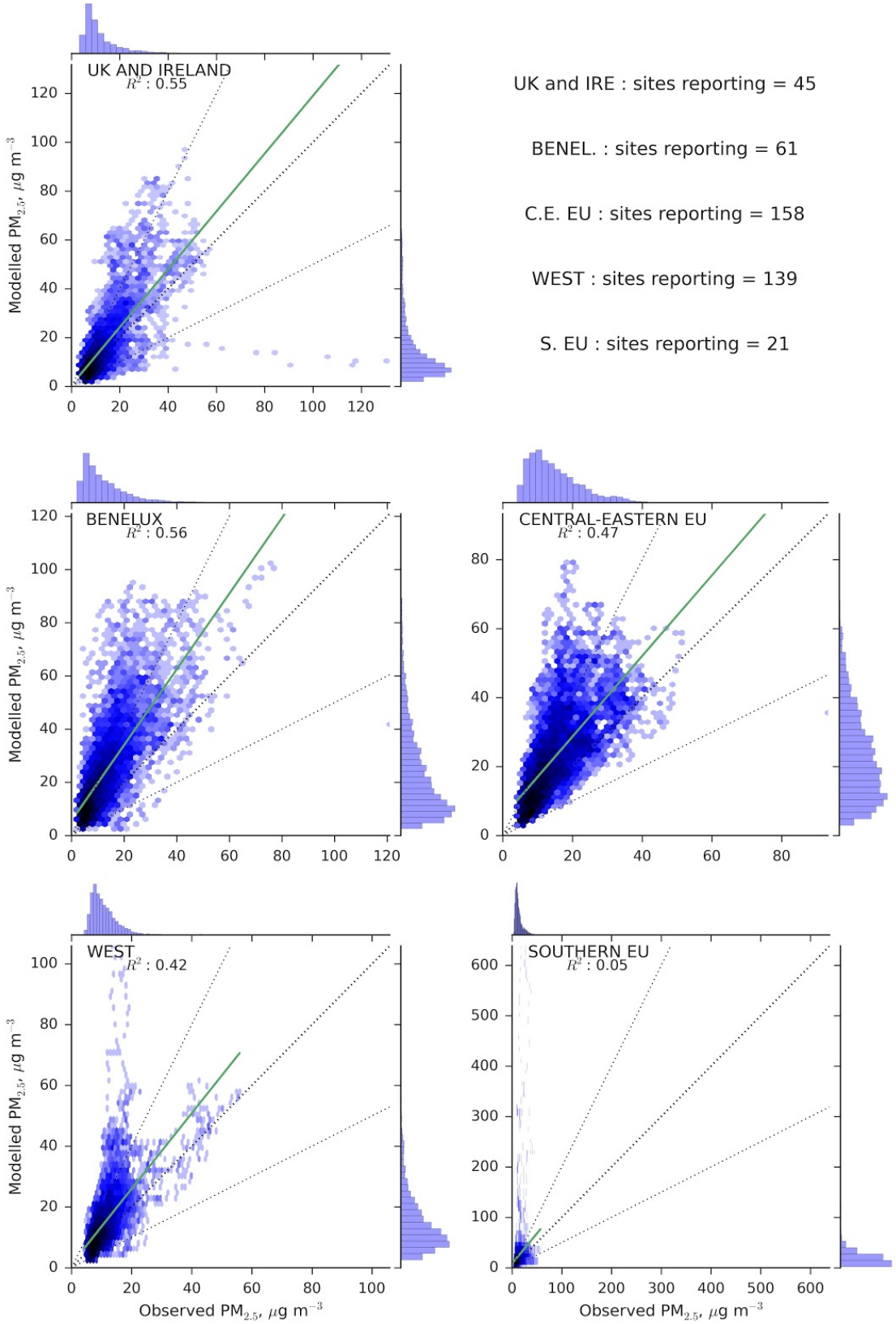

FIGURE 14 HOURLY $PM_{2.5}$ OBSERVED AND MODELLED CONCENTRATIONS FOR BACKGROUND SITES IN REGIONS OF EUROPE DURING THE OBSERVATIONAL PERIOD. HEXAGON COLOUR SHADING IS ON A

LOGARITHMIC SCALE. GREEN LINE REPRESENTS THE LINE OF BEST FIT. DASHED LINES REPRESENTS THE 1:1, 2:1 AND 1:2 RATIOS.

4.4.3 Diurnal cycles

Figure 15 shows average observed and modelled diurnal cycles for $PM_{2.5}$ for each chosen european region. The observations show relatively constant mixing ratios throughout the day with a small increase in concentrations during the “rush-hour” periods of the day. The model shows a tendency towards a positive bias, notably in the Benelux, Central-Eastern EU and Southern EU regions. The model also shows a much more significant diurnal cycle than is evident in the observations. This is in contrast to the diurnal comparison with NO_2 (Chapter 4.1.3) where the model underestimated the magnitude of the diurnal cycle.

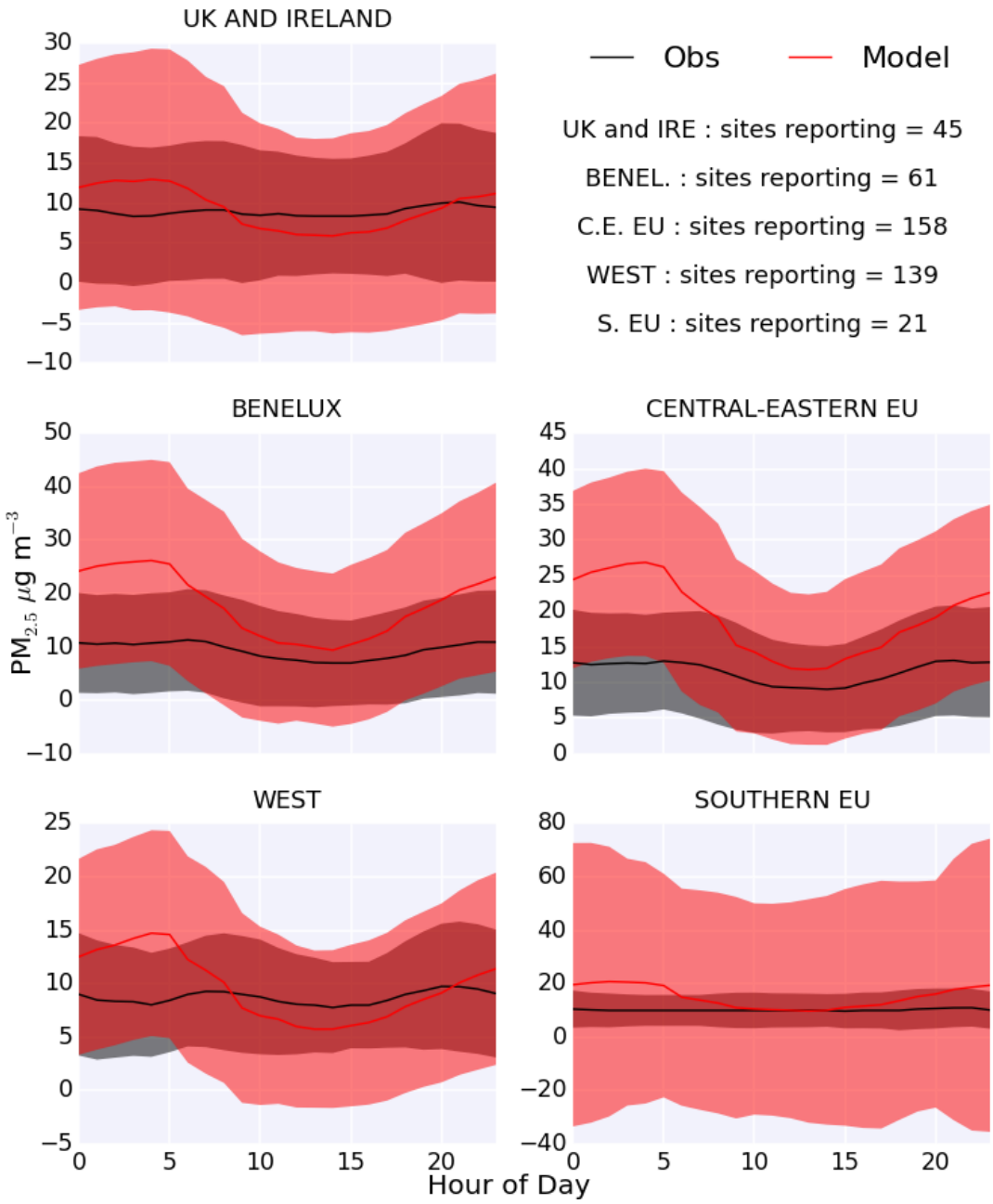

FIGURE 15 COMPARISON OF MODELLED AND OBSERVED MEDIAN DIURNAL $PM_{2.5}$ CONCENTRATIONS FOR BACKGROUND SITES FOR REGIONS WITHIN THE EU ACROSS THE OBSERVATIONAL TIME PERIOD. SHADED AREAS REPRESENT THE STANDARD DEVIATION ACROSS SITES WITHIN THE REGION.

4.4.4 $PM_{2.5}$ European conclusions

The monthly analysis in Figure 13 showed the months with higher observed $PM_{2.5}$, the model tended to have a more evident positive bias. This could indicate that during particular pollution events, there are $PM_{2.5}$ components being overestimated in the model leading to overall modelled overestimations depending pollution event conditions.

The point by point analysis (see Figure 14), along with the monthly analysis (see Figure 13) highlighted the model bias was in all regions. Southern Europe had the most significant modelled uncertainty. This could potentially be due to a modelled overestimation of a component which contributes significantly within the region and not in other regions. Possible explanations of this are (i) the close proximity of the Southern EU to the Saharan desert, this may indicate an overestimation of dust aerosol contributing to $PM_{2.5}$ composition, (ii) a photolytic sink of a significant $PM_{2.5}$ component being overestimated in the southern region and (iii) transport of $PM_{2.5}$ being miscalculated due to a difference with the atmospheric lifetime of certain $PM_{2.5}$ components.

The model tends to deviate more at higher mixing ratios, so during air mass stagnation, this effect could be exacerbated leading to a larger build-up of $PM_{2.5}$ than is observed. Investigation into modelled and observed meteorological conditions across the whole of Europe would be a way to evaluate this, but this analysis is beyond the time scope of this project.

In Figure 15, the model peaks at ~5am and has a minima at ~3pm, this coincides with solar intensity and air temperature. This indicates that diurnal scaling in the model is overestimated and driving the fluctuation in modelled daily $PM_{2.5}$ mixing ratios at a greater amplitude than observed. The amplitude of the diurnal scaling is of a factor ~>1.5, depending on the region. The largest deviance is in mainland European regions, particularly Southern EU. The diurnal scaling is driving the low correlation deviance seen in Figure 14 (between 0.47-0.05), and therefore the hypotheses of an overestimation of Saharan Dust driving the modelled deviance is unlikely when the variance between the model and emissions seem to be significant only over certain hours of the day.

However, the night-time rise in $PM_{2.5}$ could be due to the increase in production of Nitrate. As previously mentioned in Chapter 4.3 (Figure 12), ozone is overestimated in the model during the night, which leads to an overestimation N_2O_5 production (see section 1.2.3.2, R 3.6 - R 3.8). The N_2O_5 nighttime loss route on aerosol particles leads to nitrate formation (see section 1.2.4.1, R 4.8), which will lead to this rise in modelled night-time modelled $PM_{2.5}$ compared to observations.

Further research is needed to deduce if the nighttime production of N_2O_5 loss route is driving nitrate production is the primary reason for $PM_{2.5}$ nighttime modelled overestimation or whether it is the diurnal scaling of emissions being overestimated.

The analysis presented here tends to assume that $PM_{2.5}$ is composed of a single material. It is however made up of a complicated mix of material. The next section investigates the model's ability to simulate this mix focussing over the UK.

4.5 UK $PM_{2.5}$ composition

$PM_{2.5}$ is in general composed of inorganic ions (sulfate, nitrate, ammonium), organic material, black carbon, sea-salt and dust (see chapter 1.2.4). Any chemical transport model needs to be able to partition between these types. Thus, in this section the modelled composition of $PM_{2.5}$ is compared to observations

from the UK AQER and MARGA networks (see sections 2.1 and 2.2) with a focus on the secondary inorganic aerosol sources.

4.5.1 $PM_{2.5}$ stacked vs line time series and the $PM_{2.5}$ composition vs total $PM_{2.5}$ plots

In this section we initially look at how the model captures $PM_{2.5}$ composition at different observed mixing ratios before comparison to the MARGA network in section 4.5.2.

Figure 16 shows the time series of $PM_{2.5}$ measured (black line) across the 45 AQER sites in the UK compared to that simulated by the model showing the modelled different components. This highlights that the model captures the general trend of observed $PM_{2.5}$ mixing ratios (see Chapter 4.4), including capturing all days of elevated observed $PM_{2.5}$.

The change in composition with $PM_{2.5}$ concentration is shown in Figure 17. Here the modelled fractional $PM_{2.5}$ composition is plotted as a function of the $PM_{2.5}$ concentration. At low $PM_{2.5}$ concentrations (say below 15 μg m^{-3}), sea-salt makes up almost 10% of the total mass. However, as $PM_{2.5}$ concentration increases this fraction drops rapidly as the concentration of secondary compounds, most notably SO_4^{2-}. NO_3^-, $NH4^+$ increase. In polluted air (say $PM_{2.5}$ > the 25 μg m^{-3} WHO daily exposure limit) sea-salt plays a trivial role. It is these secondary inorganic compounds that the model attributes to high $PM_{2.5}$ events. The high secondary aerosol contribution to composition at high concentrations is typically ~75%, which is similar to conclusions in similar studies (Vieno et al., 2016, Malley et al., 2016, Yin and Harrison, 2008).

Desert dust can play a role at any $PM_{2.5}$ concentration. Even at 80 μg m^{-3} of $PM_{2.5}$ dust can provide 5-15% of the load.

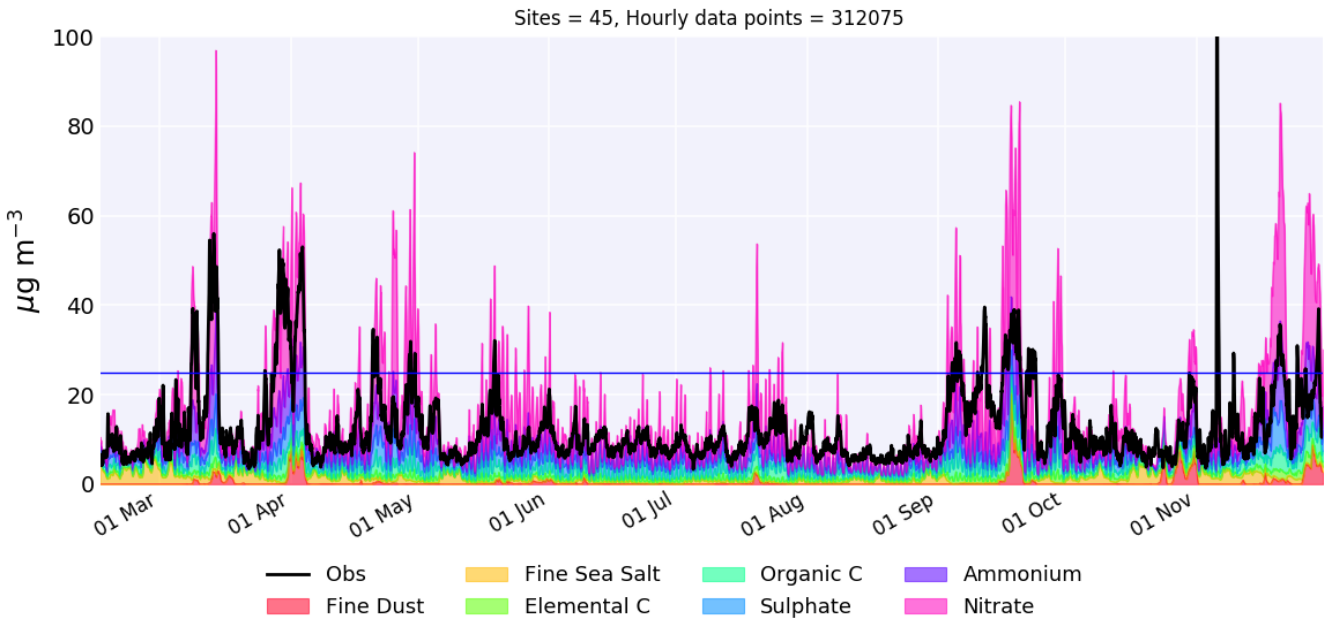

FIGURE 16 HOURLY AVERAGED MEAN SURFACE $PM_{2.5}$ CONCENTRATION OBSERVED OVER THE UK COMPARED TO MODELLED CONCENTRATION AND THE MODEL CONTRIBUTIONS ACROSS THE OBSERVATION PERIOD. 25 μG M^{-3} HORIZONTAL LINE REPRESENTS THE WHO MAX DAILY EXPOSURE LIMIT.

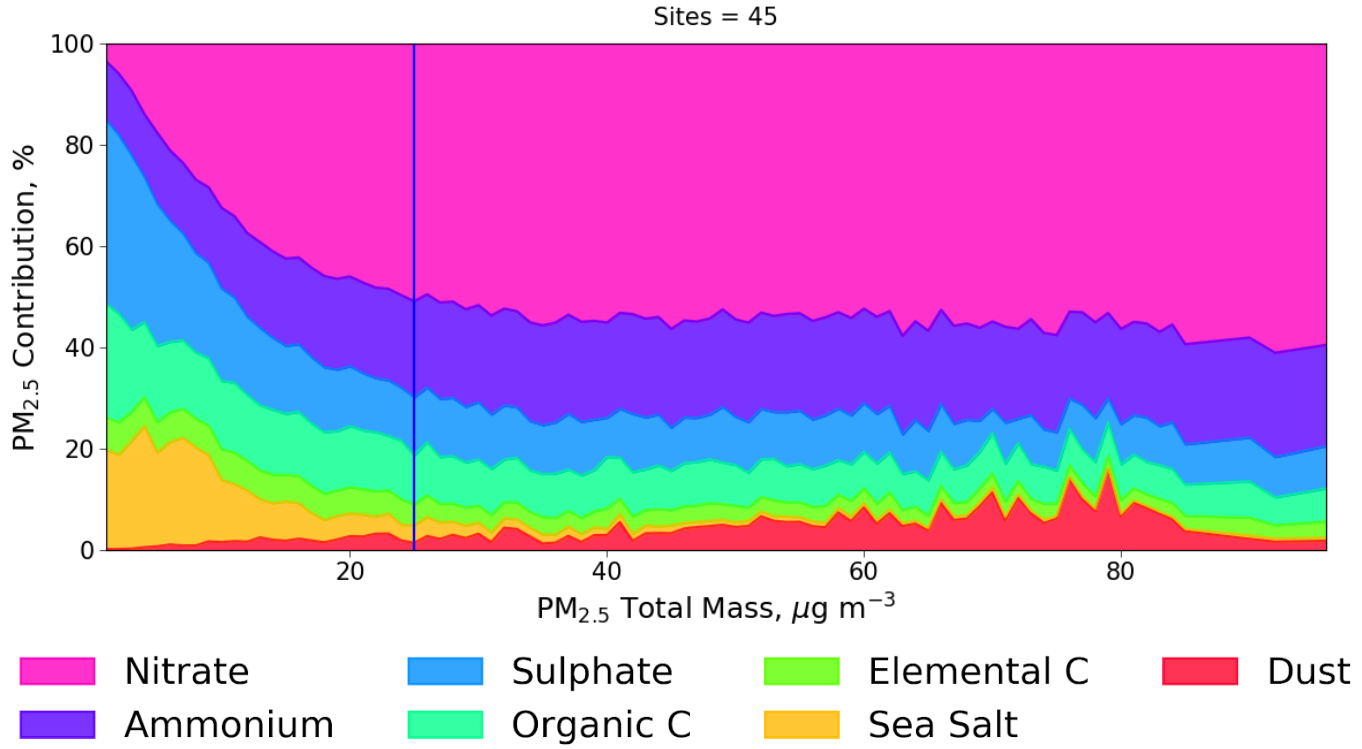

FIGURE 17 THE MODELLED STACKED RELATIVE CONTRIBUTIONS OF $PM_{2.5}$ AGAINST THE TOTAL MODELLED $PM_{2.5}$ CONCENTRATIONS OVER THE UK, ACROSS THE OBSERVATIONAL PERIOD. 25 μG M^{-3} VERTICAL LINE REPRESENTS THE WHO MAX DAILY EXPOSURE LIMIT.

Thus to evaluate the model performance in greater detail the model's ability to simulate the sulfate, nitrate and ammonium in the aerosol needs to be examined. This is what is achieved in the next section.

4.5.2 Comparisons with observations from the MARGA network.

Figure 18 compares the model to the measurements for sulphate, nitrate and ammonium made at the Monitor for AeRosols and Gases (MARGA, 2017) network at the Auchencorth Moss and Harwell sites in the UK. The measurements made there are described in more detail in Section (see Chapter 2.3).

In general the model simulates the sulfate observations better than the ammonium and the nitrate(<10% bias compared to biases of upto 350%). At some times the model is biased high and at other biased low but it appears to capture most of the events and gives a credible performance. Both the simulation of nitrate and ammonium appear to be biased high.

There are multiple explanations for these biases. As discussed in Chapter 4.1 the model underestimates the NO_2 concentrations. This may represent an underestimates in the NO_x emissions or potentially an overestimate in the NO_x sinks (potentially from N_2O_5 hydrolysis, see section 1.2.1.2, R 1.6 - R1.8). An overestimate in the NO_x sink would lead to increased nitric acid (HNO_3) production. However, for HNO_3 to be converted in to aerosol phase nitrate, there needs to be ammonia present. It would therefore seem most likely that the model overestimate in the nitrate is a result of an overestimate in the ammonium with therefore appearing to be a fairly consistent relationship between the model overestimate in the nitrate and in the ammonium.

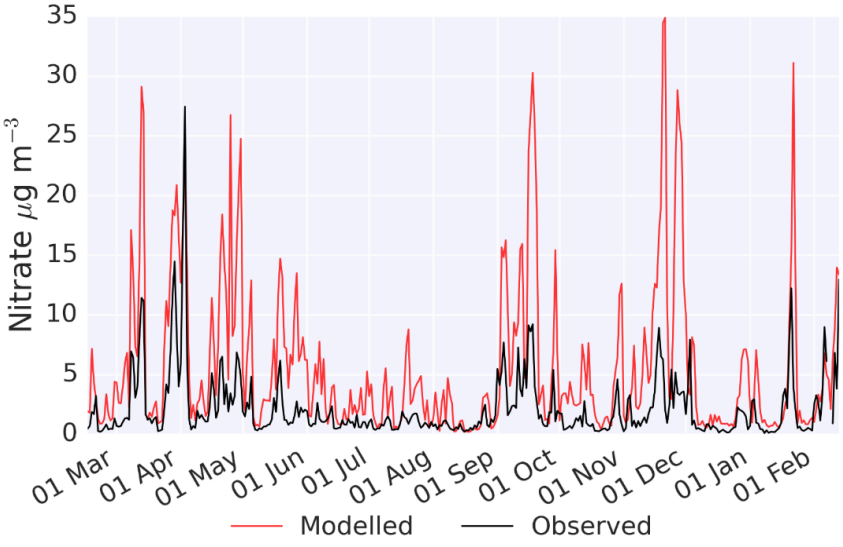

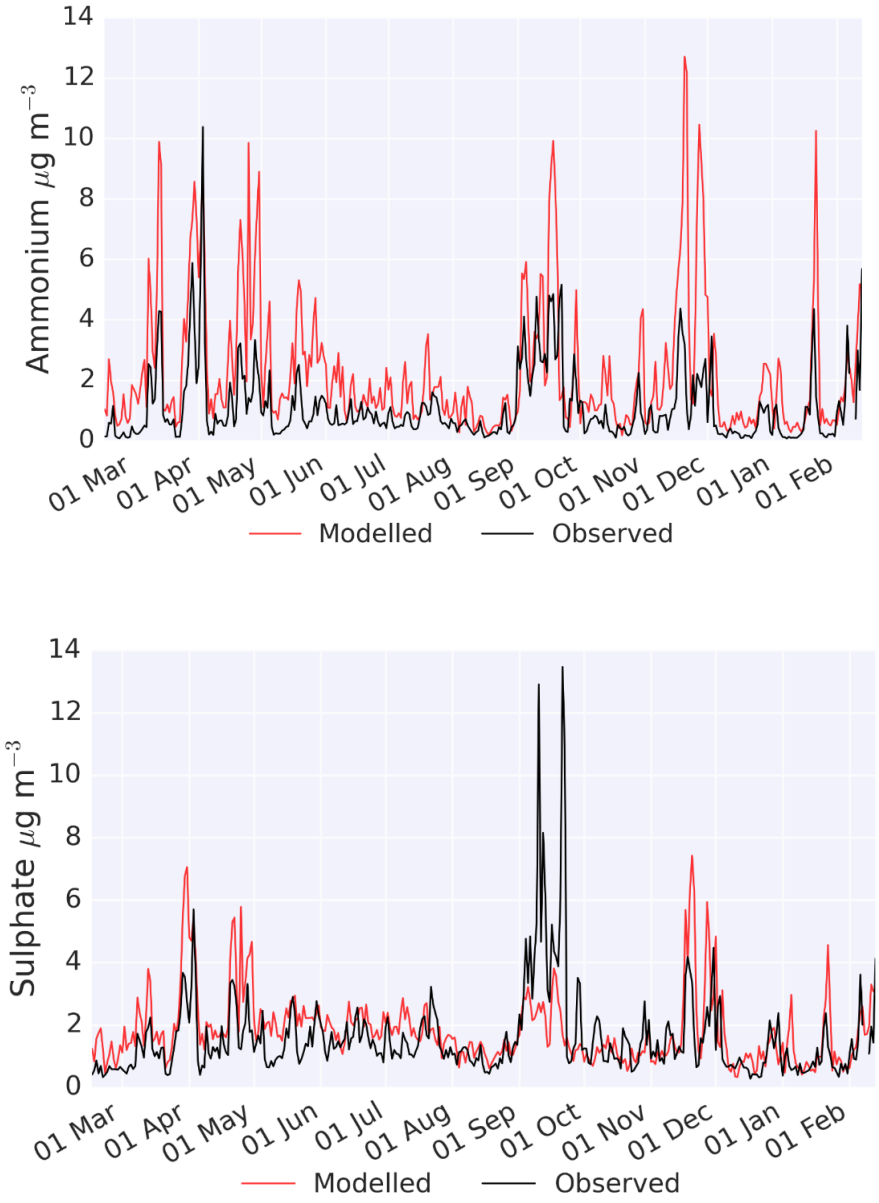

FIGURE 18 DAILY AVERAGED NITRATE, AMMONIUM AND SULPHATE MODELLED AND OBSERVED CONCENTRATIONS ACROSS THE OBSERVATIONAL PERIOD WHERE OBSERVATIONS ARE FROM THE MARGA UK NETWORK.

The model shows ability to capture observed days of elevated sulphate, ammonium and nitrate mixing ratios in Figure 18. The model is particularly good at capturing elevated sulphate observations, but has a positive bias for elevated nitrates and ammonium.

4.5.3 Conclusions

The model has ability to capture sulphate observations well but to overestimate nitrates and ammonium is potentially caused by multiple factors. As mentioned earlier, the overestimation of modelled ozone leads to increased night-time N_2O_5 concentration and hydrolysis of N_2O_5 which would cause an overestimation of nitrates (see section 1.2.3.2, R 3.6 - 3.8). So, the large modelled contribution of nitrates to $PM_{2.5}$

composition could be linked to the high bias in night-time ozone, increasing the rate of nitrate aerosol production. The ozone concentration could therefore explain the high bias in modelled nitrate. However this doesn't explain the positive model bias for ammonium.

A factor that is potentially causing modelled over estimation of ammonium is an overestimation of ammonia in the EMEP emission inventory. As mentioned earlier, emitted ammonia will typically react in the atmosphere with sulphates in preference to nitrates. Sulphuric acid is relatively nonvolatile in respect to nitrates so more readily partitions into the aerosol phase, so there is more sulphuric acid available to be neutralised by ammonia to form sulphates. Therefore any excess ammonia, once sulphuric acid is neutralised, will then go on to react with nitrates. The model reflects this chemistry capturing observed sulphate well, but not ammonium. The overestimation of ammonia in the model is likely due to the large uncertainties in ammonia emissions, as Xu et al., (2016) states is due to variances in ambient temperatures, planting practices, soil composition, and other factors going into emissions scaling, which has led to an overestimation of ammonium. One significant sector with a high level of uncertainty is agriculture, where it is hard to quantify with certainty livestock, manure and fertilizer based ammonia emissions.

Previous three year analysis on the both the UK sites between 2010 and 2013 attributed the largest fraction of $PM_{2.5}$ composition was from secondary aerosol with an annual average sum between 48 and 52% (Malley et al., 2016). This agreed with findings from Figure 17, confirming the importance of secondary aerosols.

The MARGA UK observations may be underestimating concentrations due to the experimental approach taken. It is reported over a range of meteorological conditions, that MARGA observations have a negative bias for nitrate and sulphate, which is more severe at lower concentrations (Chen et al., 2017, Stieger et al., 2017). An example of this underestimation is nitric acid absorption along the sampling tube inlet which has a 30% underestimation in comparison with aerosol mass spectrometry sampling (Rumsey et al., 2014). The 30% underestimation was attributed to the length of the inlet tube (Chen et al., 2017), and using chemically inert materials (Rumsey et al., 2014). In Chen et al, (2017) a used a 4m inlet tube, whereas the MARGA UK inlet tubes are 1 meter in length which will partially compensate for this instrumentation underestimation, meaning this underestimation will not be as severe in this study.

A further issue is that the rural site may not be capturing the local pollution from the nearby cities, which is within the extent of the modelled grid box. This is because Harwell is within 15 km of Oxford, Swindon and Reading, and the the model was run at ~25 km resolution. The hourly average will therefore be capturing some of the urban pollution from the region. The model would need to be run at a higher resolution, to see if this mitigates the models positive bias due to urban $PM_{2.5}$ emission influences at Harwell. The same applies to Auchencorth Moss, which is 17 km south of Edinburgh. So a future comparison at higher resolution may reduce the model bias, but this analysis is beyond the remit and the time constraint of this project.

Chapter 5: The Ability of the Model to Capture UK $PM_{2.5}$ Events

As discussed in Chapter 1.4, elevated $PM_{2.5}$ concentrations usually occur during the winter and spring months in the UK during a series of "events". This chapter focuses on two such events, on 8th-14th March 2014 and the 27th March to 4th April 2014.

5.1 Comparison with the AQER network

The sites reporting in the UK from the Air Quality e-Reporting (AQER) network, are compared to the model (see chapter 2.1). Figure 19 shows hourly observations (black line) of observed UK averaged $PM_{2.5}$ along with the modelled simulation of $PM_{2.5}$ composition during the two springtime events. The average observed $PM_{2.5}$ value is the mean of upto 43 sites measurements taken across the country during the observational period. The model is the equivalent values obtained from averaging from the same location grid boxes in the model.

Figure 19 shows the model captures much of the variability observed in these periods, i.e. it captures the timings of the pollution events. It also has some skill in simulating the synoptic variability seen in these events. There is however a tendency of the model to have a slight positive bias to observations during these periods The model is however bias high of 3.2 μg m^{-3} (model mean is 15.8 μg m^{-3} and observations is 12.6 μg m^{-3})

Figure 19 also shows the speciation (sulfate, nitrate, ammonium, seasalt, dust, organic carbon and black carbon) of the $PM_{2.5}$ with Figure 20 showing the fractional modelled speciation.

Figure 20 shows that during the same days of the background periods of $PM_{2.5}$ pollution as seen in figure 19 (say $PM_{2.5}$ less than 15 μg m^{-3}), between a 20-60% proportion of modelled $PM_{2.5}$ aerosol is from natural sources (sea-salt and desert dust). During high concentrations of $PM_{2.5}$ in figure 19 (say above 25 μg m^{-3}) the fraction of natural sources decreases and the concentration of sulphates, ammonium and nitrates increases often making up to 90% of total modelled aerosol composition. Increases in the nitrate and ammonium fractions are particularly apparent. For example on the 12th March there is a 35% rise in modelled secondary aerosol in comparison to the previous day. Primary emissions from combustion (NO_x) and agriculture (NH_3) therefore play a significant role in forming these secondary aerosols. The model contribution of ammonium and nitrate levels is indicative of high ammonium nitrates concentrations, which is also concluded to be a large contributor to PM concentrations in the UK by Vieno et al., (2014). The relatively small contribution of Saharan dust (<20%) across both pollution events is seen, has already been reported previously (Vieno et al., 2016) and is discussed in detail in Chapter 1.4.

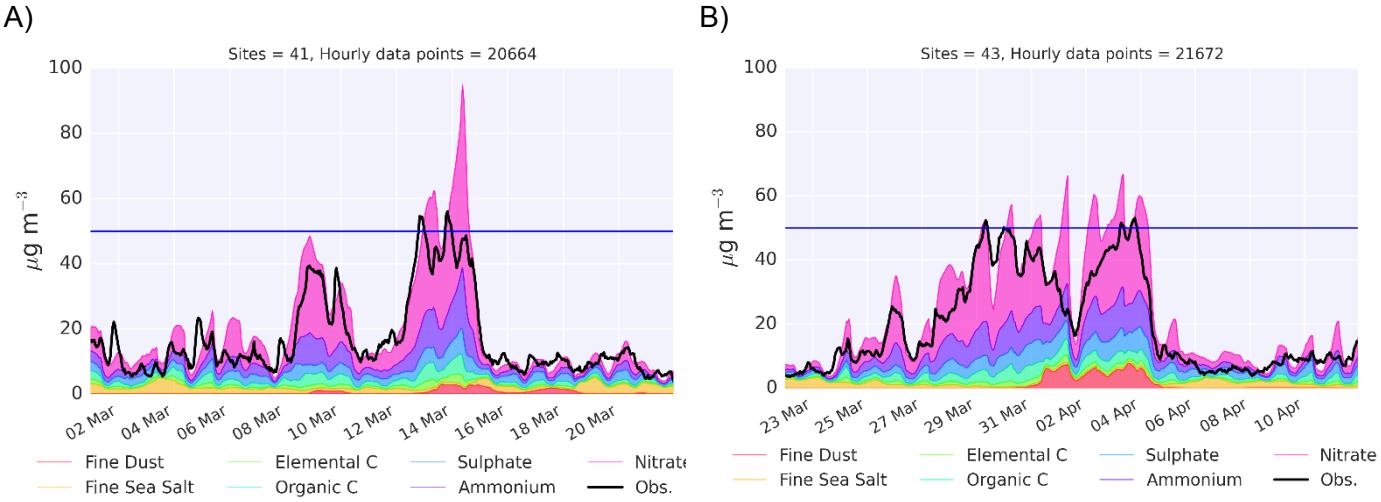

Figure 19 Mean surface $PM_{2.5}$ concentration observed over the UK compared to modelled concentration and the model contributions for two pollution events in March and April 2014. 50 µg m^{-3} horizontal lines represents "severe" levels of $PM_{2.5}$

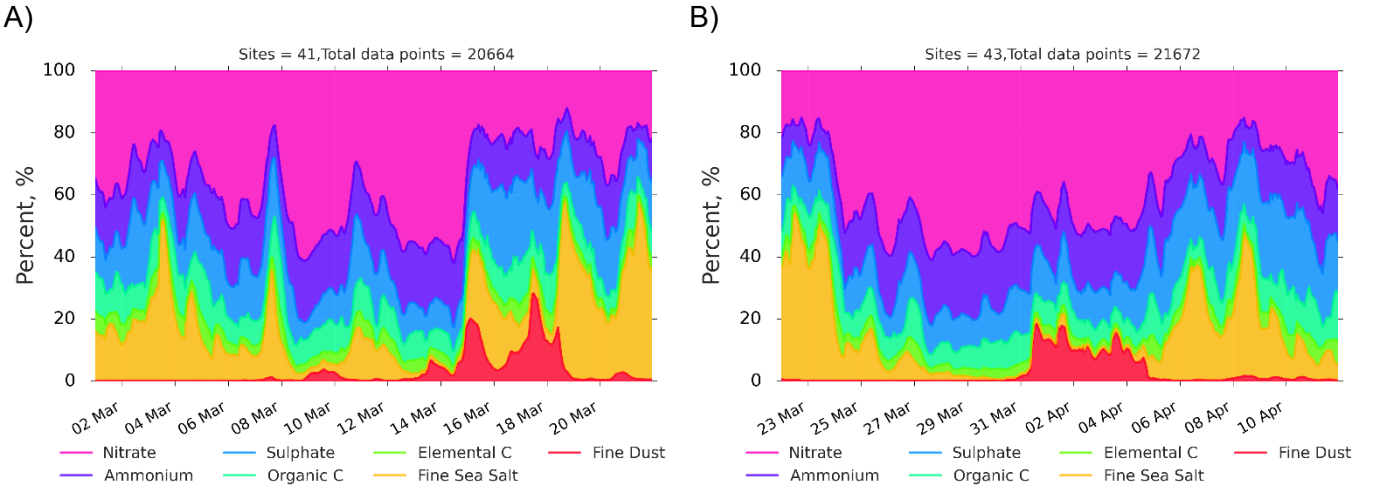

Figure 20 Mean modelled $PM_{2.5}$ surface contributions over the UK, normalised as a percentage for the two pollution "events" March - April 2014. (events 8-14th March and 27th March - 4th April).

This analysis in figures 19 and 20 shows that the model can capture the daily variability of $PM_{2.5}$, but it does not show whether or not the model captures the increase in the secondary (sulphate, nitrate and ammonium) contributions during these periods. Speciated measurements are needed for this comparison.

5.2 Comparison to the MARGA Network

The Monitor for AeRosols and Gases (MARGA) instrumentation (see Chapter 2.3) provides UK aerosol ion observations which are comparable to model $PM_{2.5}$ composition results.

Figure 21 shows modelled sulfate, nitrate and ammonia for the two events, and the corresponding observations with Figure 22 showing the comparison species by species. Figure 21 shows the the model overestimates the total mass of sulfate, nitrate and ammonia by a factor of 2 for the 1st event but performs better for the 2nd event as model overestimates by a factor of 1.5. The sulfate is relatively well (10% bias) simulated but the model overestimates the concentration of ammonia and nitrate in Figure 22.

MARGA Sulphate, Ammonia and Nitrate

Model Sulphate, Ammonia and Nitrate

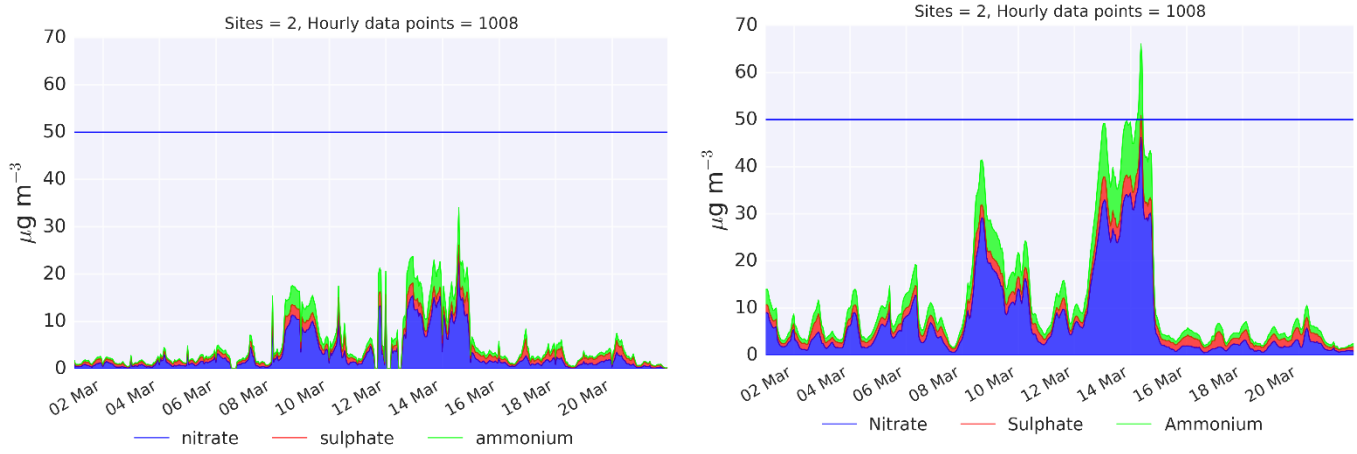

MARGA Sulphate, Ammonia and Nitrate

Model Sulphate, Ammonia and Nitrate

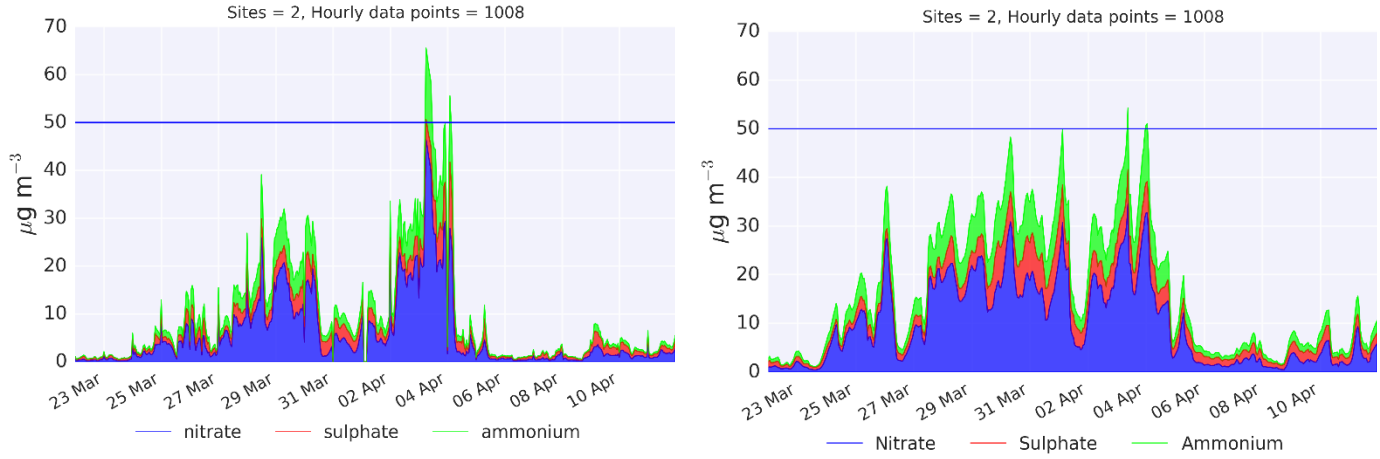

FIGURE 21 THE MODELLED AND OBSERVED $PM_{2.5}$ STACKED RELATIVE CONTRIBUTIONS OF SECONDARY AEROSOL ACROSS BOTH POLLUTION EVENTS IN THE SPRING OF 2014. 50 μG M^{-3} HORIZONTAL LINES REPRESENTS "SEVERE" LEVELS OF $PM_{2.5}$.

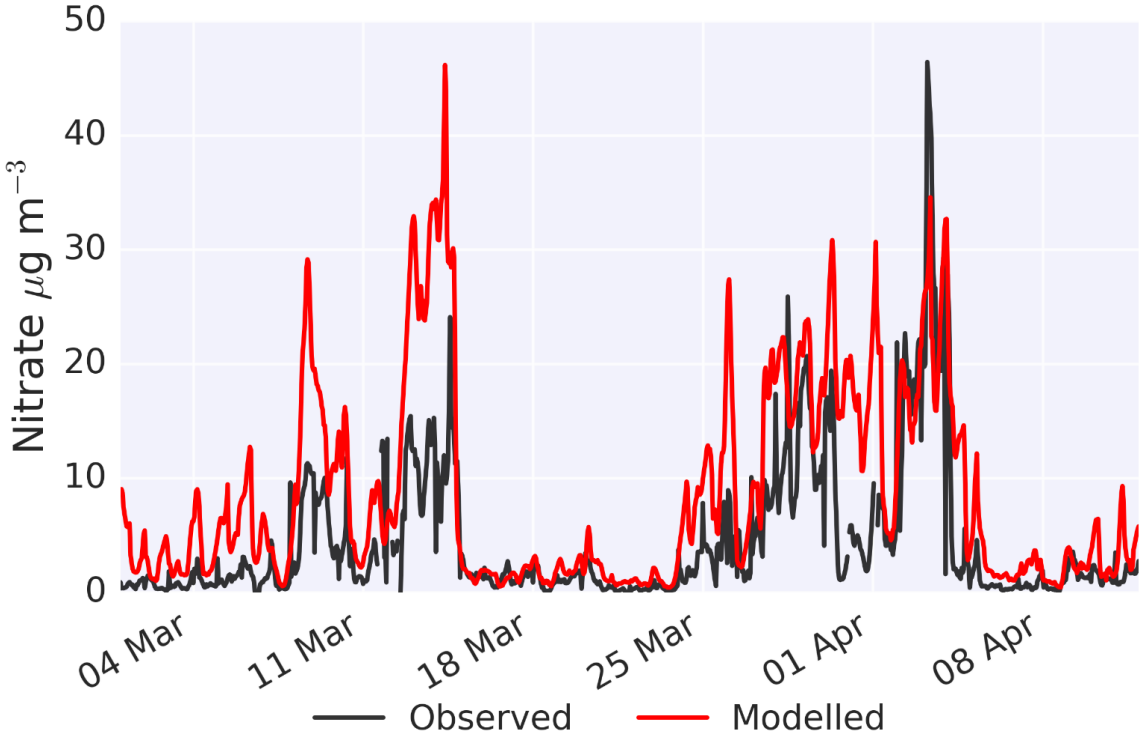
Nitrate μg m^{-3}
50
40
30
20
10
0
04 Mar
11 Mar
18 Mar
25 Mar
01 Apr
08 Apr
Observed
Modelled

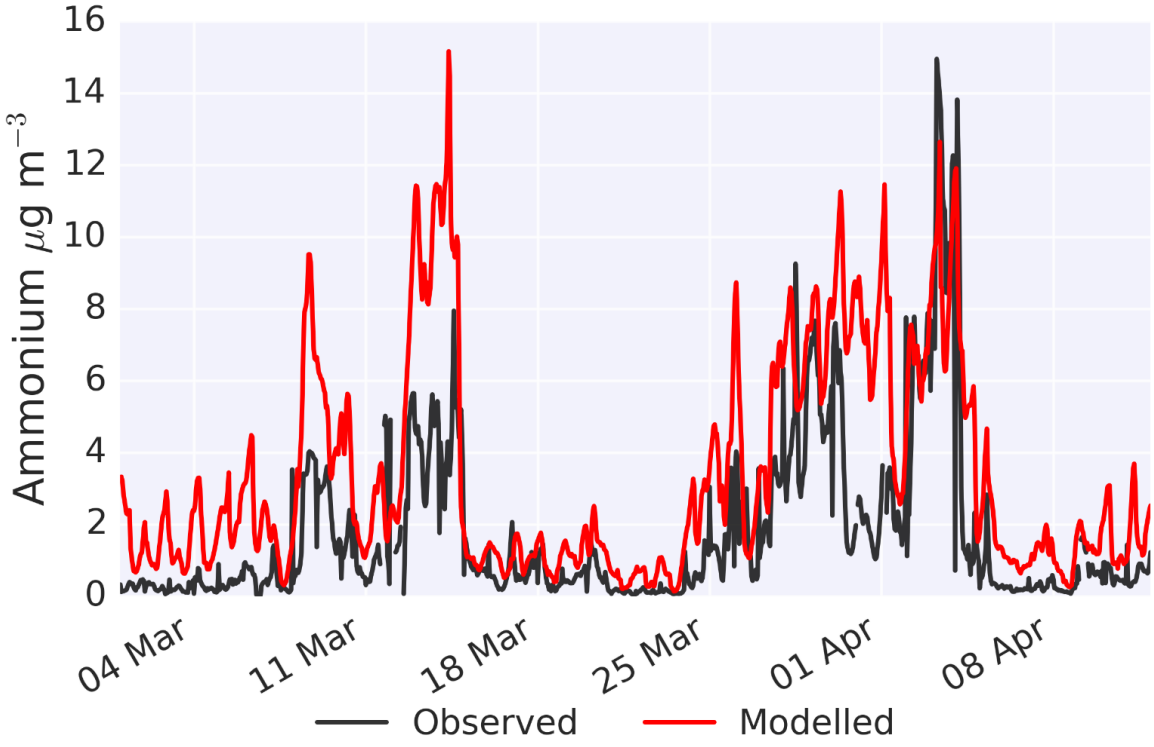
Ammonium μg m^{-3}
16
14
12
10
8
6
4
2
0
04 Mar
11 Mar
18 Mar
25 Mar
01 Apr
08 Apr
Observed
Modelled

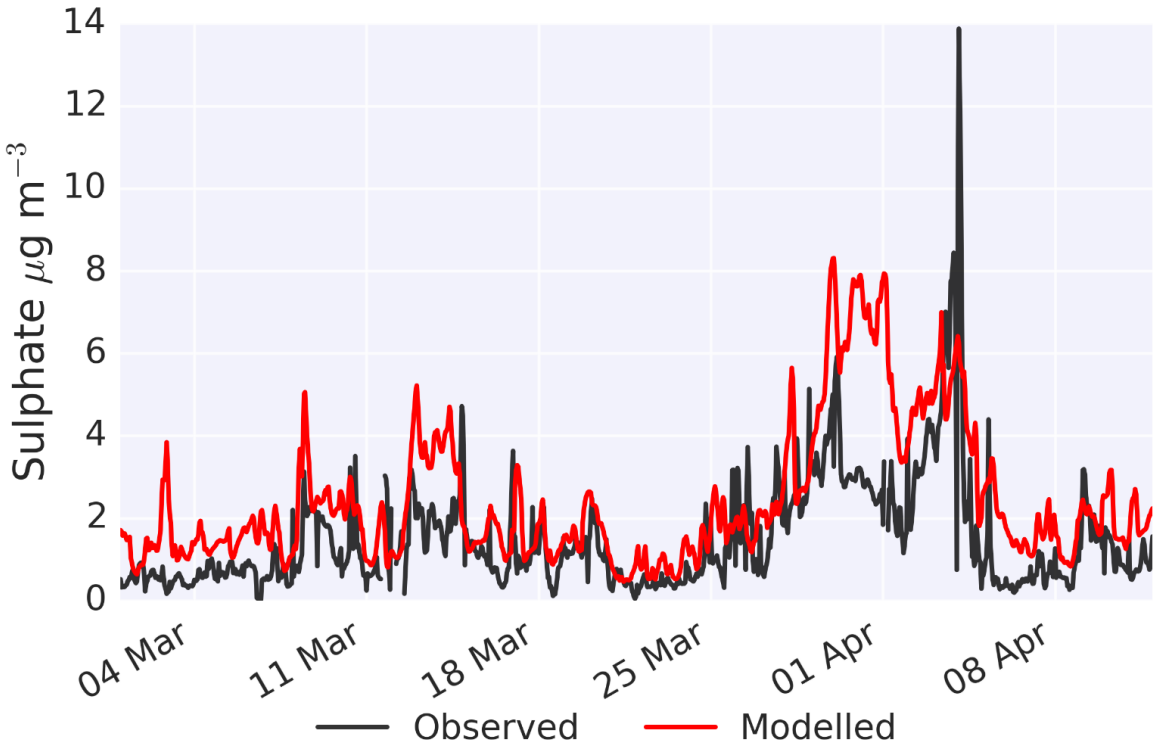

FIGURE 22 MODELLED AND OBSERVED UK NITRATE, AMMONIUM AND SULPHATE CONCENTRATIONS DURING BOTH POLLUTION EVENTS IN THE SPRING OF 2014 (MARCH - APRIL 2014).

Overall the model does a reasonable job in attributing most of the aerosol to nitrate in these “events”, which is consistent with previous work (Vieno et al 2014). The cause of the overestimate could be for multiple reasons. Firstly, an overestimate in the emissions of NO_x, which is needed to make the nitrate, would lead to too rapid a conversion of NO_x to nitrate, due to excessive ozone which drives nighttime N_2O_5 formation and subsequent nitrate formation. Secondly, issues with the MARGA observations such as loss of ion on the inlet tube either due to the length of the inlet tube or inertia of the tube (Rumsey et al., 2014) could account for an observational negative bias. Thirdly, the modelled ammonia emissions are likely to be too high as ammonia is needed to stabilize nitrate in the aerosol phase, which is overestimated, along with ammonium concentrations. Finally, a too long a lifetime for nitrate aerosol could cause the nitrate overestimation.

5.3 Summary

The model shows capability in simulating the speciation of the sulfate, nitrate and ammonia aerosol during pollution events. It does however show that the model overestimates the nitrate and ammonia fraction. A common source of ammonium is the agricultural sector (see section 1.2.4.1) and nitrates vehicle emissions. However, this analysis does not conclude which of these sectors is the predominant contributor to each pollutional event. Source appointment from the EMEP inventory over the same period might allow an indication of the main sector contributors across the region (see Table 6) to these events, however time restraints meant that this was not investigated.

Chapter 6: Influence of the Agricultural Sector on $PM_{2.5}$

Agricultural emissions have been implicated in the creation of significant amounts of European $PM_{2.5}$ (Lelieveld et al., 2015). This has a tangible impact on the focus of future air quality policy. Chapter 5 showed that ammonium (predominantly from agriculture) makes up a significant fraction of total $PM_{2.5}$ and also has a significant impact on the nitrate concentrations. This chapter specifically investigates the contribution of the agricultural sectors to overall $PM_{2.5}$ concentrations in Europe, with comparison to the "base" run in chapter 4,4 for the same year time period span (Feb 2014 - Feb 2015). We also look at the burden of the agricultural sector on the same pollution "events" over the UK in the spring of 2014, as described in chapter 5.

In order to explore the influence of the agricultural sector on European $PM_{2.5}$, emissions from the agricultural sector are switched off in the model simulations described as the "AgriOff" run and compared to the base run. The setup of the model AgriOff and the base runs is explained in chapter 3.7.

6.1 The European agricultural burden on $PM_{2.5}$

This section assesses the burden of the agricultural sector in Europe, where the "base" run was conducted in Chapter 4.4

Figure 23 shows the annual mean concentration of $PM_{2.5}$ in the "base" case simulation, in the "AgriOff" simulation, the concentration difference between the two and the ratio of the two concentrations. There is a significant reduction in $PM_{2.5}$ when the agricultural sector emissions are switched off (a 28% drop). The domain-mean surface $PM_{2.5}$ concentration of 16.17 μg m^{-3} (for the base run) drops to 11.48 μg m^{-3} (for the AgriOff run) when agricultural emissions are switched off. Regional $PM_{2.5}$ showa large fractional reduction when agricultural emissions are removed, with a fractional difference drop of typically between 0.25 and 0.65. Over the Po Valley region of Italy, annual mean $PM_{2.5}$ concentrations are reduced by over 25 μg m^{-3}. Also notably, fractionally $PM_{2.5}$ drops by around 60% over virtually all of the northern Europe, which is in agreement with findings in Vieno et al., (2014). The central European region area is also profoundly affected by emissions from the agricultural sector (a fractional difference drop upto 0.65).

Base run, EU mean = 16.17 µg m^{-3}

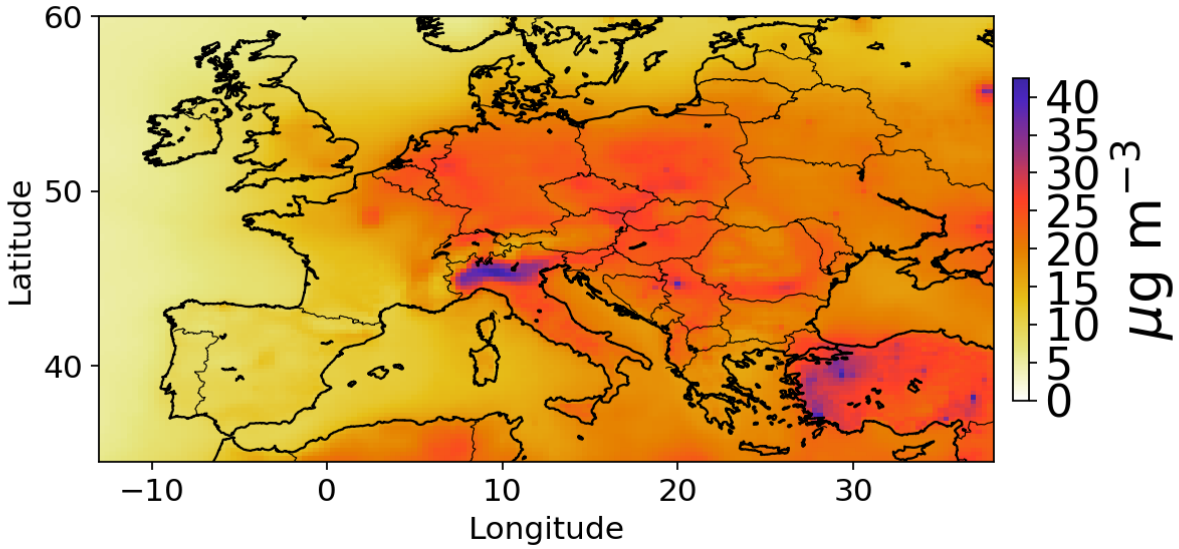

AgriOff run, EU mean = 11.48 µg m^{-3}

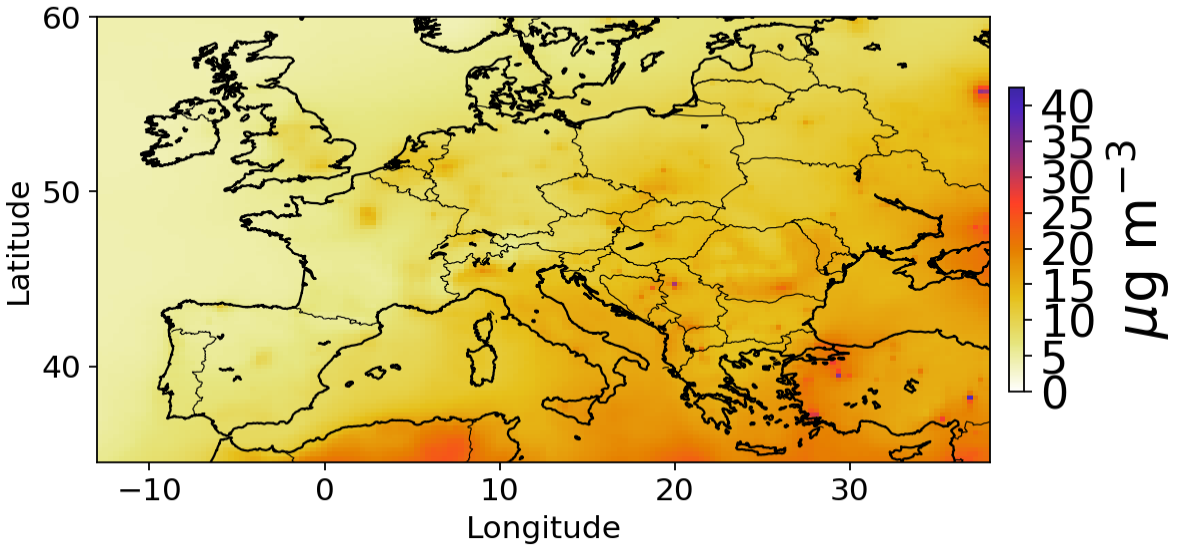

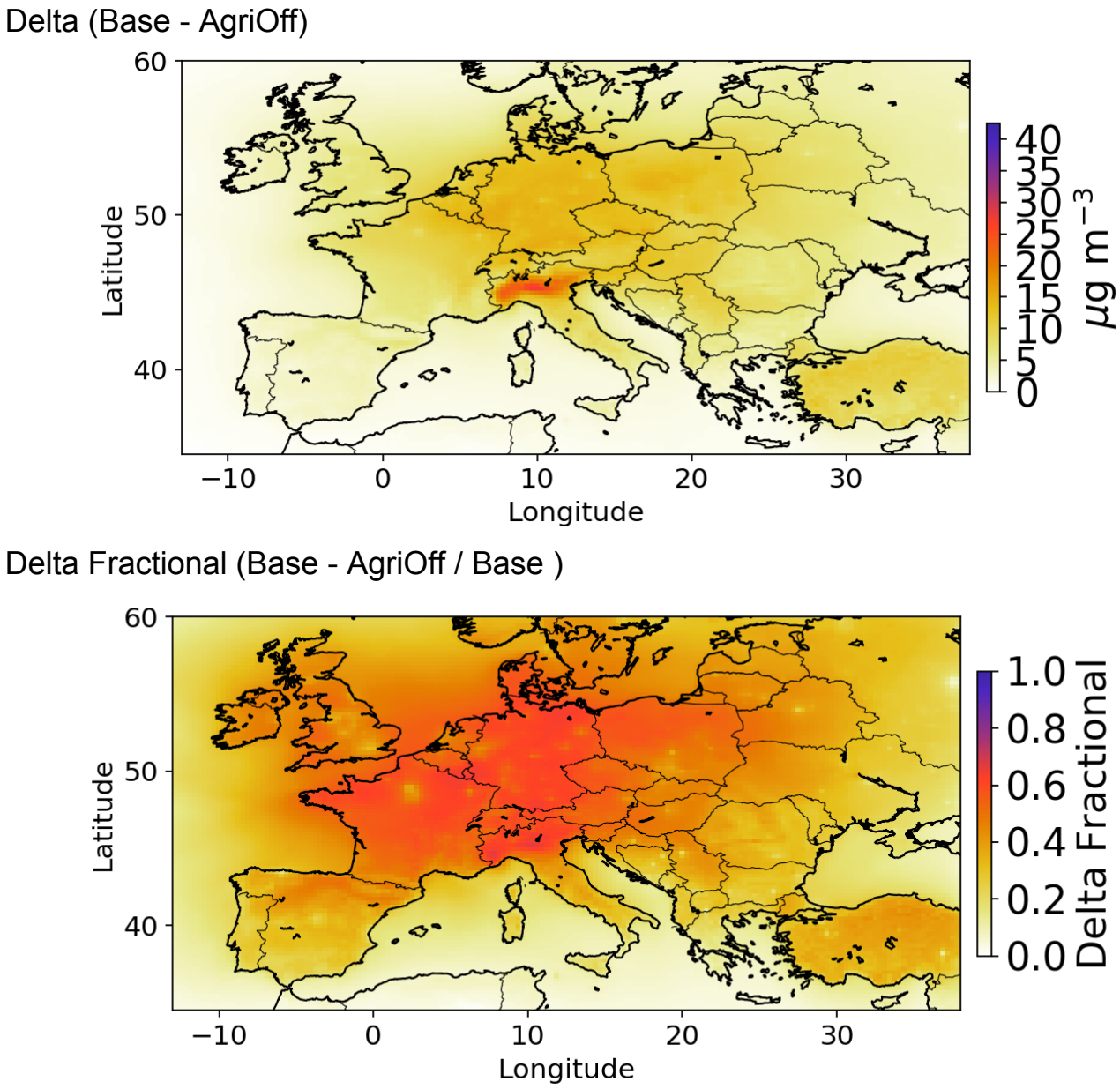

FIGURE 23 THE AVERAGE $PM_{2.5}$ MIXING RATIO ACROSS THE YEAR OBSERVATIONAL PERIOD FOR THE "BASE" RUN (TOP PANEL), THE "AGRIOFF" RUN (2ND TOP PANEL) AND THE DIFFERENCE IN MIXING RATIO BETWEEN THE TWO RUNS (3RD PANEL). THE BOTTOM PANEL SHOWS THE FRACTIONAL DIFFERENCE BETWEEN THE BASE RUN AND AGRIOFF RUN MIXING RATIOS (BOTTOM PANEL).

Figure 24 shows the number of days that modelled $PM_{2.5}$ concentrations are on average above the WHO 25 μg m^{-3} daily limit, for every grid box within the nested European domain. The top pane shows how many days the daily averaged $PM_{2.5}$ exceeds the WHO limit for the "Base" run, the middle pane is the same analysis but for the "AgriOff" run and the bottom pane is the delta in days between these two runs.

In the base run, for some regions (e.g The Po Valley in northern Italy, eastern Europe, Turkey, central Europe and parts of north western Europe) a high number of days of the year in 2014 exceed the 25 μg m^{-3} limit, An example seen, could be north western Europe, which exceeds the WHO limit by 100 days a year.

Switching off the agricultural emissions has a profound impact on the number of days exceeding the limit. There are very large decreases in the number of days exceeding the WHO daily exceedance limit, with almost all areas showing fewer than 75 days in exceedance of the limit and many areas only exceeding the limit between 0 and 25 days. For example, some regions (i.e. The Po Valley, central Europe, Turkey, and parts of north western Europe) there are large decreases (deltas) in the number of days $PM_{2.5}$ exceeds the WHO 25 μg m^{-3} limit (upto ~225 days, ~125 days, ~110 days and ~90 days in the Po Valley, central Europe, Turkey and parts of north western Europe respectively). These results highlight similar to conclusions found by Vieno et al., (2014) and Lelieveld et al., (2015) on the importance of the agricultural emissions from the agricultural sector on “high” $PM_{2.5}$ levels (say above the WHO limit).

Base run

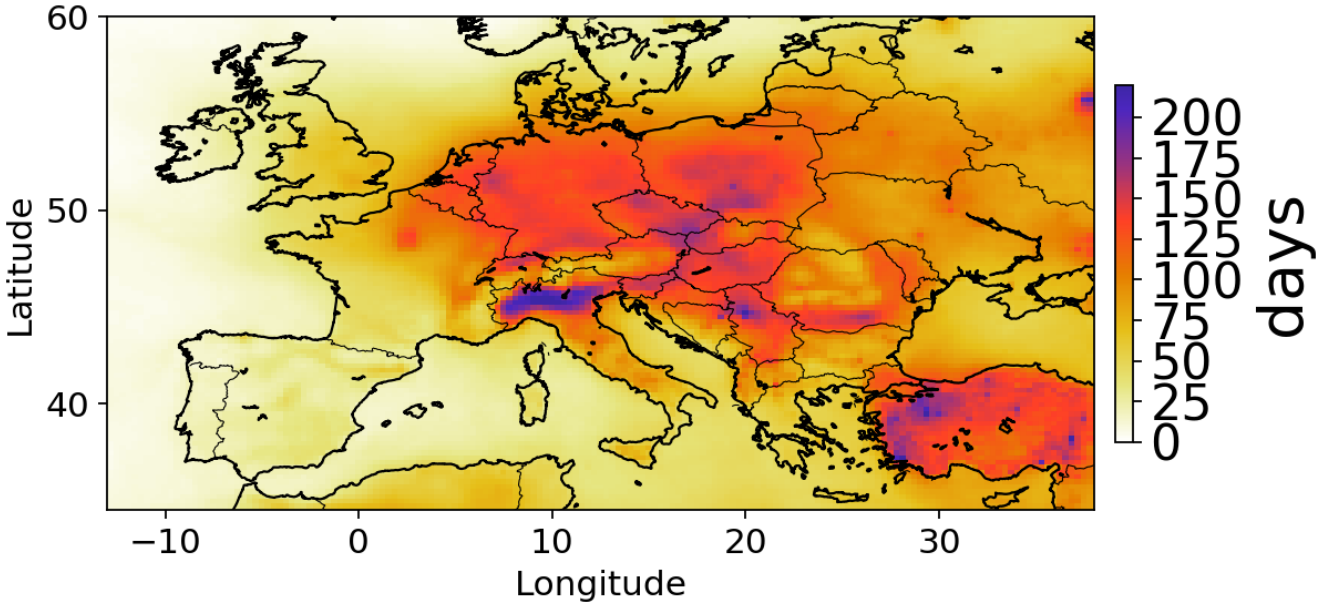

AgriOff run

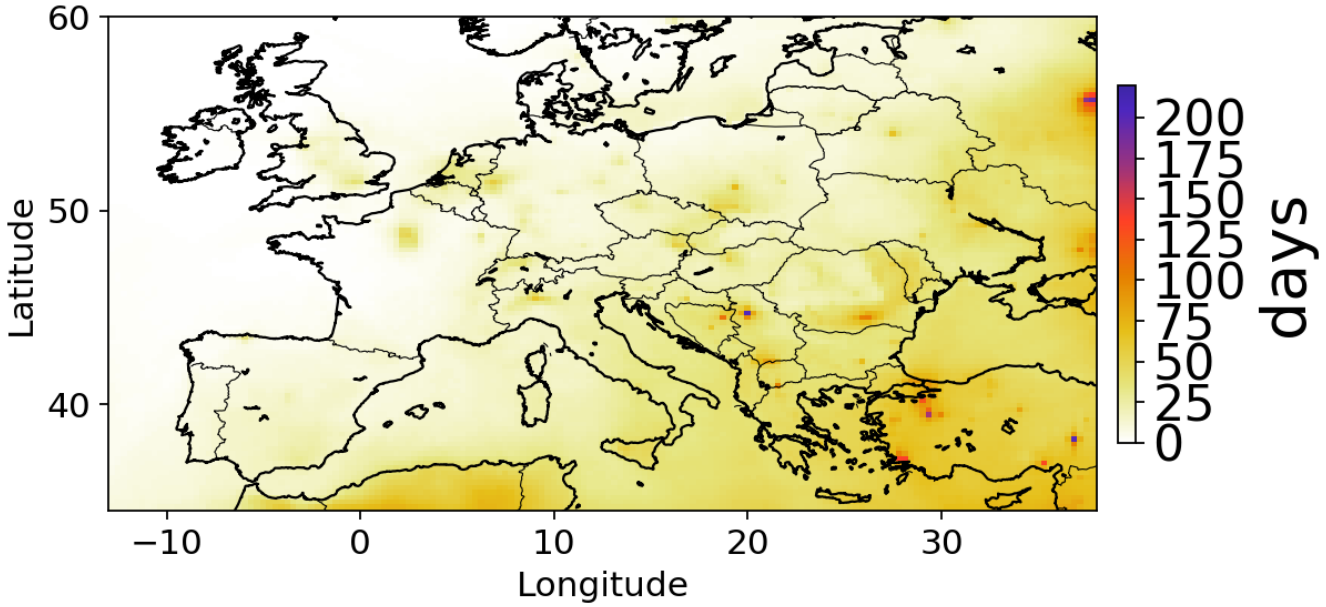

Delta (Base - AgriOff run)

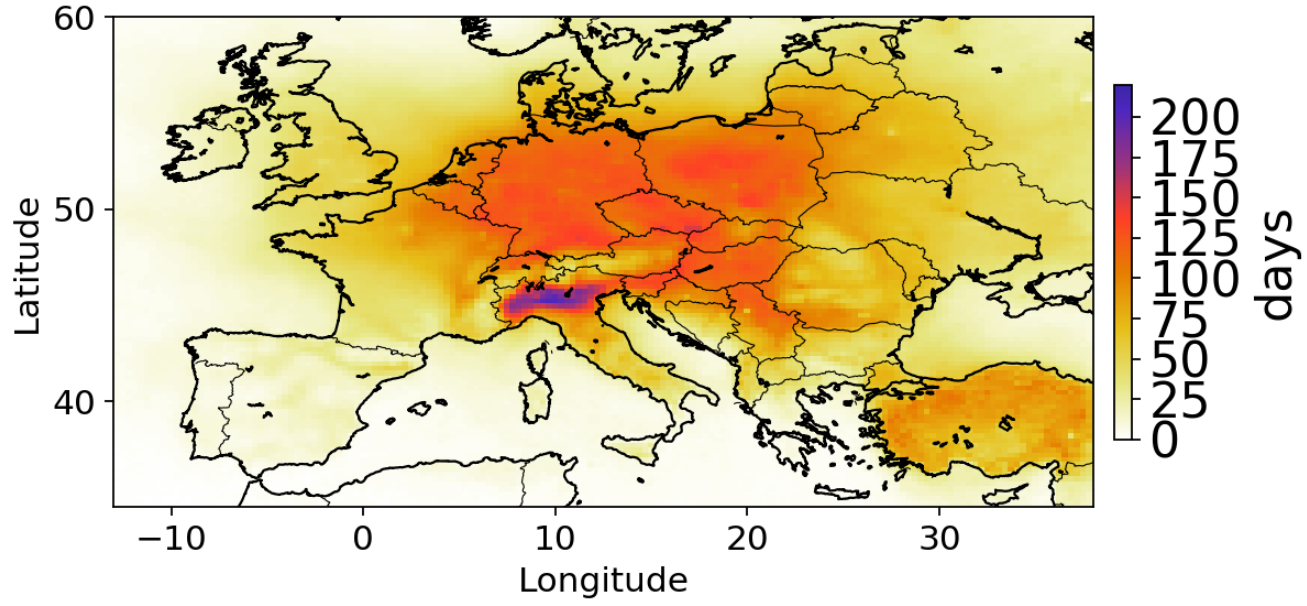

FIGURE 24 THE NUMBER OF DAYS $PM_{2.5}$ MIXING RATIOS ARE ABOVE THE WHO DAILY RECOMMENDED MAXIMUM (25 µG M^{-3}), ACROSS THE OBSERVATIONAL PERIOD FOR THE NORMAL RUN, THE AGRIOFF RUN AND THE DELTA (THE DIFFERENCE IN DAYS BETWEEN THE RUNS).

6.2 The agricultural burden on UK Spring PM episodes

This section is evaluating the burden of the agricultural sector on the same $PM_{2.5}$ spring 2014 events which were studied in chapter 5.

Figure 25 shows both the base simulation and the “Agri-run” simulations for the two springtime ‘events’ (8th - 14th March 2014 and the 27th March - 4th April 2014). The black line is the average of $PM_{2.5}$ observations captured across the observational period with the modelled $PM_{2.5}$ speciated into the different components. There is a large drop in the modelled $PM_{2.5}$ concentration when the agricultural emissions are switched off. The only modelled PM components that are affected when agricultural emissions are switched off is ammonium, nitrates and sulphates. The “agri-run” $PM_{2.5}$ concentration are now typically well below the daily observational $PM_{2.5}$ (black line), unlike in the base run in Chapter 5, where the model tended to have a positive bias during polluto events. Although the modelled ammonium concentration has dropped significantly, its concentration is still comparable to that of nitrate or sulfate. This reflects non-agricultural sources of ammonia (e.g. transport) and the advection of ammonia from outside of the domain.

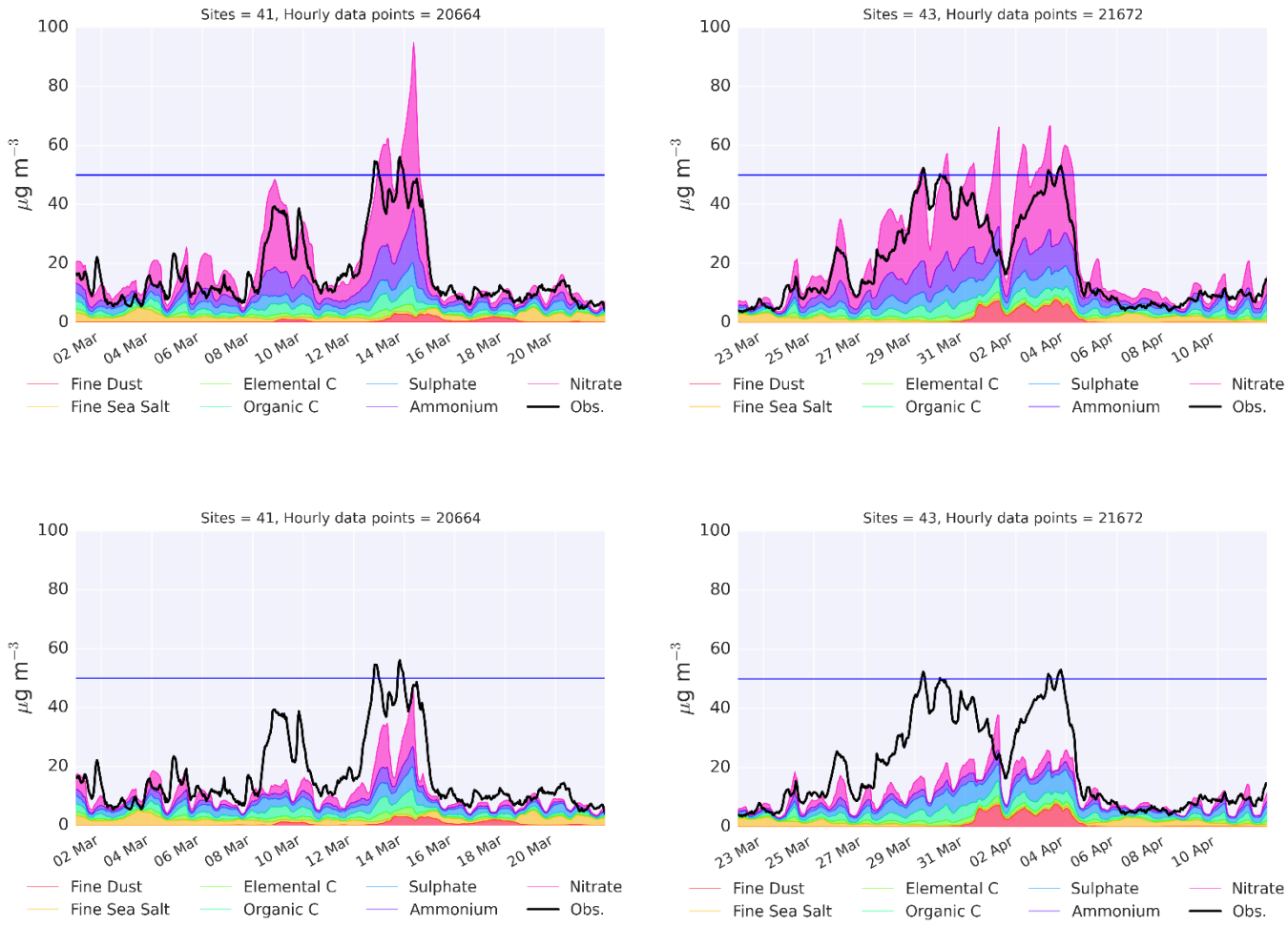

FIGURE 25 MEAN SURFACE $PM_{2.5}$ CONCENTRATION OBSERVED OVER THE UK DURING THE TWO POLLUTION 'EVENTS' COMPARED TO MODELLED CONCENTRATION AND THE MODEL CONTRIBUTIONS FOR THE BASE SIMULATION (UPPER) AND THE "AGRIOFF" SIMULATION. (LOWER). RUNS ARE OVER THE 2 SPRING POLLUTION EVENTS BETWEEN THE 1ST MARCH AND THE 14TH APRIL 2014. THE BLUE HORIZONTAL LINE AT 50 μG M^{-3} "SEVERE" LEVELS OF $PM_{2.5}$

Figure 26 shows the comparison of the hourly concentrations for the base run and AgriOff run during the pollution episodes for the inorganic aerosol components. The components that show a significant reduction between the Base and AgriOff runs were; nitrates and ammonium, with sulfates barely changing. During the two pollution events the ammonium and nitrates drop by >50% across the UK. For most of the observation period the sulphate concentration remains relatively constant (within 10%) between the AgriOff and base runs. As mentioned earlier, this is due sulphuric acid being relatively nonvolatile in respect to nitrates so more readily partitions into the aerosol phase. Hence, more sulphuric acid is available to be neutralised by ammonia to form sulfates, so typically there is enough ammonia to react all of the sulphuric acid away. However, with less ammonia, less ammonium ions are less ammonium can associate and neutralise nitrate to react and stabilise all the nitrate which is captured in the reduced nitrates and ammonium seen in the AgriOff runs.

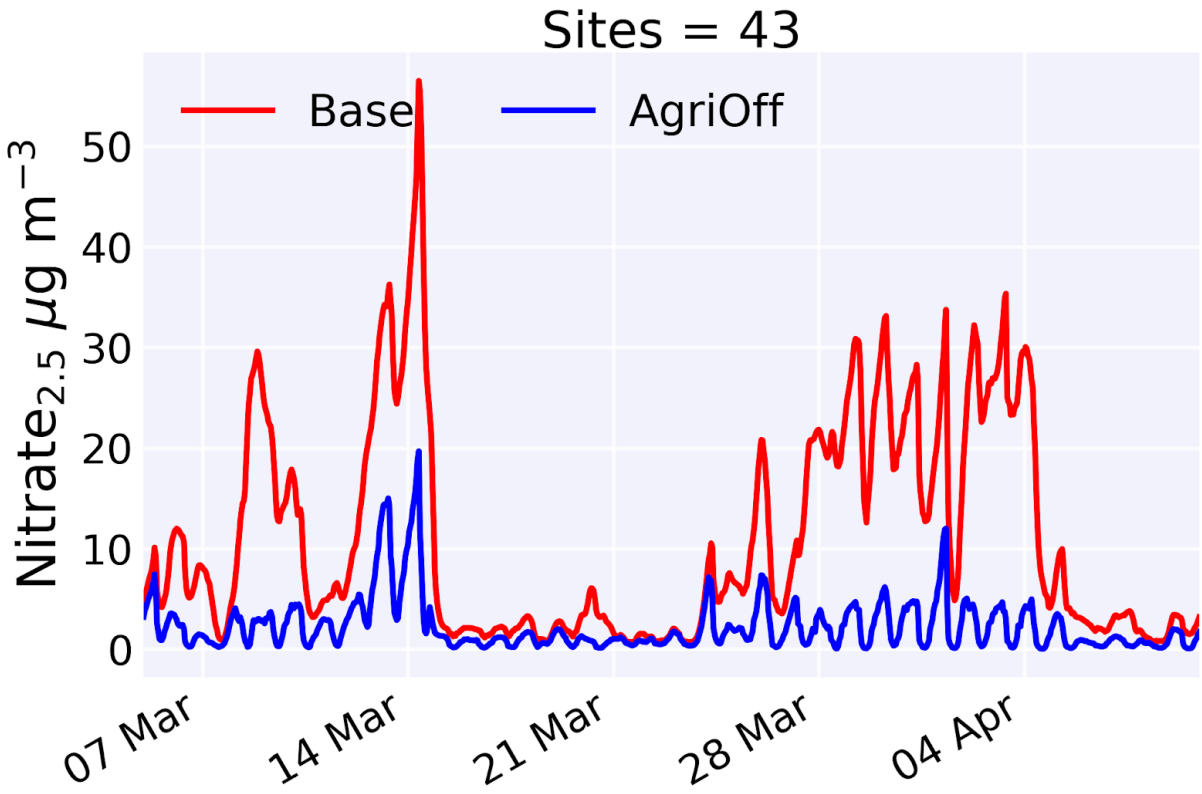
Sites = 43
Base
AgriOff
Nitrate$_{2.5}$ μg m^{-3}
50
40
30
20
10
0
07 Mar
14 Mar
21 Mar
28 Mar
04 Apr

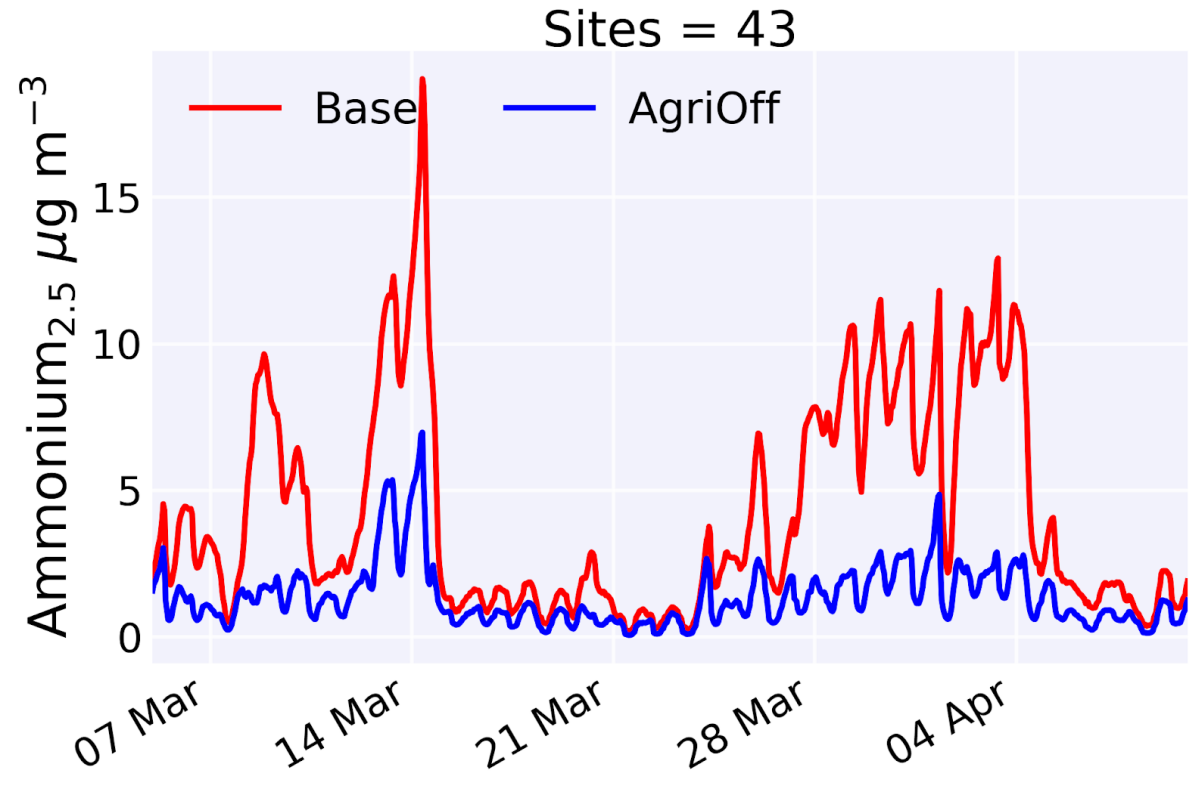
Sites = 43
Base
AgriOff
Ammonium$_{2.5}$ μg m^{-3}
15
10
5
0
07 Mar
14 Mar
21 Mar
28 Mar
04 Apr

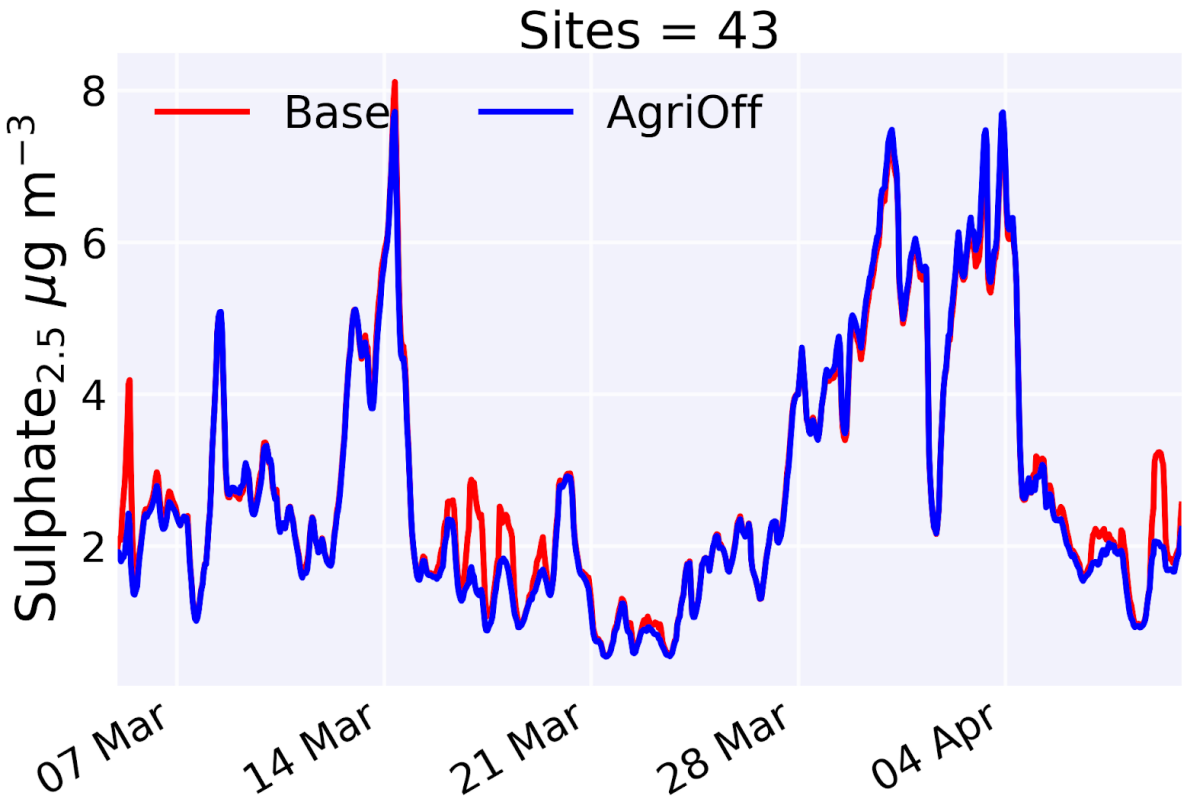

FIGURE 26 UK HOURLY SURFACE LEVELS OF NITRATE AMMONIUM AND SULPHATE FOR $PM_{2.5}$ FOR THE "BASE" RUN MODEL OUTPUT AND "AGRI-OFF" MODEL RUN CONCENTRATIONS BETWEEN THE 1ST MARCH AND THE 14TH APRIL.

Figure 26 is looking at the question to how these $PM_{2.5}$ secondary components influence the difference in $PM_{2.5}$ concentrations over time between the runs. Figure 27 shows the change in concentration for ammonium, sulphate and nitrate as a percentage of the total change in $PM_{2.5}$ between the base run and the AgriOff run. Across the two pollution periods nitrates accounts for ~71% of the total drop in $PM_{2.5}$ for the AgriOff run in comparison to the base run. Whereas ~29% of the $PM_{2.5}$ concentration drop is accounted to ammonium contributions. Sulphates have a sporadic influence on the contribution to the drop in $PM_{2.5.}$ This confirms that in the model ammonia will typically react with sulfates in preference to nitrates as sulphates between runs are mostly unchanged whereas nitrates are reduced. As ammonia emissions are reduced in the AgriOff run, less ammonia is available after any ammonia neutralised sulphates, meaning lower concentrations of nitrates and ammonium forming. But during days of relatively low ammonia emissions, sulphuric acid contributes to the percentage drop in $PM_{2.5}$. As there is not enough ammonia to neutralise all the aerosol phase sulphuric acid, therefore lower concentrations of sulphates form, hence it contributes to the drop in $PM_{2.5}$ concentration.

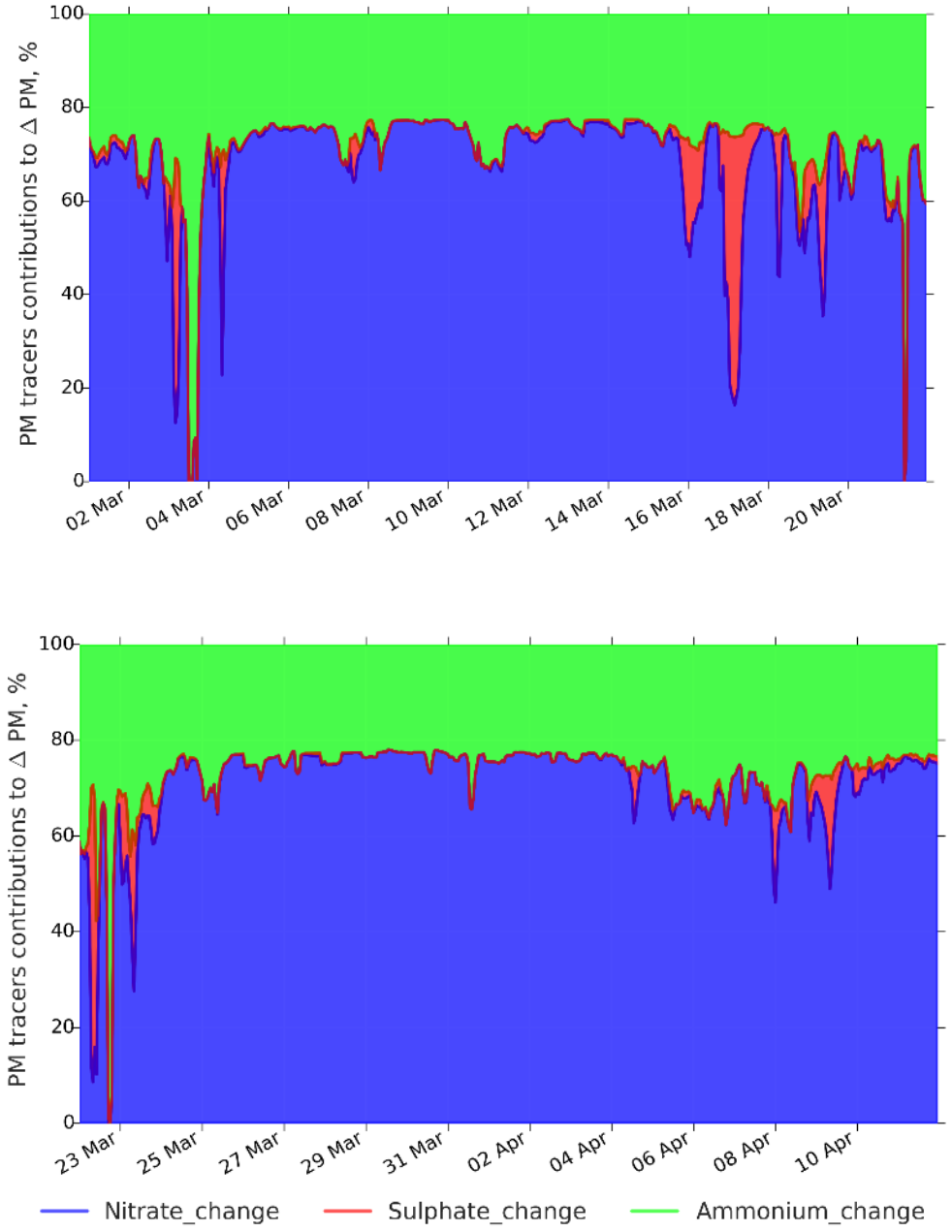

FIGURE 27 THE CHANGE IN CONCENTRATION OF AMMONIUM, SULPHATE AND NITRATE AS A PERCENTAGE OF TOTAL CHANGE IN PM2.5 BETWEEN THE "BASE RUN" AND THE "AGRIOFF" RUN BETWEEN THE 1ST MARCH 2014 AND THE 14TH APRIL 2014.

6.3 Summary

Agricultural emissions have a profound impact on the concentrations of surface $PM_{2.5}$ over Europe. In the simulations shown here total $PM_{2.5}$ drops by ~60% over much of Europe when agricultural emissions are removed. This leads to a significant reduction in the number of days when $PM_{2.5}$ exceeds the 25 μg m^{-3} daily mean recommended limit across all regions (upto 225 days). These large reductions are due to the reduction in ammonium and also nitrate in the aerosol. The reduction in nitrate is due to the aerosol

thermodynamics which leads to sulfate preferentially neutralizing with the ammonia before nitrate can be incorporated into the aerosol phase. This leads to a significant fraction of the $PM_{2.5}$ over Europe being due to agricultural emissions.

Policies that target the reduction in agricultural ammonia emissions are likely to result in a significant reduction in the concentration of surface $PM_{2.5}$ over Europe. However, there is also scope for reduction in the other components of the aerosol which would also benefit air quality.

The removal of agricultural emissions have highlighted that $PM_{2.5}$ concentrations are subject to a complex system, with non-linearities in the results of this study. This scenario is an extreme case where all emissions have been switched off in the model. More work is needed to draw clear quantitative conclusions about the efficacy of a policy targeting emissions from the agricultural sector.

Chapter 7: Conclusions

For the first time the European nested grid version of the GEOS-Chem model of chemistry and transport has been compared to European wide observations. The main findings show that:

The model performed well in capturing seasonal fluctuation in NO_2 concentrations. The model however tended to have a negative bias. This low bias is most notable during the “rush hour” when the observations show large increases in NO_2 concentrations but the model shows little or no change. This is likely a combination of an underestimation of anthropogenic NO_x emissions in the emissions inventory, issues with its diurnal emissions and/or issues with interference on molybdenum based chemiluminescence analysers. This, together with other evidence i.e. the underestimate in anthropogenic NO_x emissions from transport sources (Vaughan et al., 2016) would suggest that a re-evaluation of the transport NO_x source in Europe is needed.

For smaller NMHCs (ethane and propane) in the UK, the model captured the season cycle but tended to underestimate concentrations. However, the model did better in comparison with observations at Mace head (a site of indicative of the wider hemispheric background condition). This tends to suggest a missing anthropogenic source of ethane and propane is not being captured in emissions. Leaks from the natural gas network is a potential emission source which is not accounted for (Derwent et al., 2017) in the model which could account for this modelled negative bias.

For the larger NMHCs (PRPE and ALK4), the model captured much of the seasonal variability of PRPE and ALK4, however diurnal analysis proved that the model was not capturing the fluctuation of these species well within the given hours of a day.

The model captures seasonal variations in ozone concentrations, though with a positive bias. Although the model is biased high at all times of the day the bias is worst during the night time. This is a common feature of models and reflects a combination of difficulty in representing the dynamics of the night time boundary layer, difficulties in representing night time NOx-HOx chemistry, ozone deposition rates, etc. The afternoon diurnal ozone peak is better represented by the model which is what is important for most AQ applications. It in not obvious whether correcting for the issue in NOx and NMHCs outlined earlier would make this night-time ozone problem better or worse.

The model captures the seasonal variations in $PM_{2.5}$ well. It tends to have a small positive bias compared to observations which is exacerbated during months with higher $PM_{2.5}$ concentrations. The model has a much larger diurnal cycle than the observations which is hard to reconcile with the opposite trends in NO_2 and ozone.

The model captured the UK $PM_{2.5}$ events well, being sensitive to hourly changes in observations, though with a positive bias. This positive bias was mainly due to an overestimation of nitrates and sulphates

The model simulates the sulfate concentration of $PM_{2.5}$ reasonably well compared to the MARGA network but tends to overestimate nitrate and sulfate. This may be due to an overestimate of ammonia emissions which would lead to increases in both components.

Removing agricultural emissions from the model has a profound impact on the european $PM_{2.5}$, the results are in agreeance with findings in Vieno et al., (2014) and Lelieveld et al., (2015). The domain-mean surface $PM_{2.5}$ concentration dropped 28%, from 16.17 μg m^{-3} to 11.48 μg m^{-3} . In terms of breaches of the WHO daily exposure limit (25 μg m^{-3}), For some regions (Po valley, Eastern Europe, Turkey and northern Europe and parts of north western Europe) there are very large decreases in the number of days $PM_{2.5}$ exceeds this limit (upto 225 days). Policies that target the reduction in agricultural ammonia emissions are likely to result in a significant reduction in the concentration of surface $PM_{2.5}$ over Europe, as this study highlights the large burden the agricultural sector plays on $PM_{2.5}$ concentrations.

Overall the model shows many positive traits, particularly capturing in Ozone and $PM_{2.5}$. However, it requires more extensive evaluation and comparison to observations before it is able to capture the above species correctly for different temporal scales.

List of Abbreviations

ALK4	Alkanes >= 4 carbon atoms
AQER	Air Quality e-Reporting
CMAQ	Community Multi-Scale Air Quality (model)
CTM	Chemical Transport Model
EMEP	European Monitoring and Evaluation Programme
GEOS	Goddard Earth Observing System
HNO_3	Nitric acid
MARGA	Monitor for AeRosols and Gases in Air
N_2O_5	Dinitrogen Pentoxide
NH_3	Ammonia
NOAA	National Oceanic and Atmospheric Administration
NMHC	Non-methane hydrocarbon
NO_x	The sum of Nitrogen Oxide (NO) and Nitrogen Dioxide (NO_2)
PAN	Peroxyacetyl Nitrates
$PM_{2.5}$	Particulate matter with a diameter of 2.5 μm or less (μm m-3)
PM_{10}	Particulate matter with diameter of 10 μm or less (μm m-3)
PM	$PM_{2.5}$ and PM_{10}
PMN	Peroxymethacroyl Nitrate
PRPE	Alkenes >= 3 carbon atoms
SO_x	Sulphur Oxides
SO_2	Sulphur Dioxide
SA	Secondary Aerosol
VOCs	Volatile Organic Compounds

References

ALEXANDER, B., PARK, R. J., JACOB, D. J., LI, Q. B., YANTOSCA, R. M., SAVARINO, J., LEE, C. C. W. & THIEMENS, M. H. C. D. 2005. Sulfate formation in sea-salt aerosols: Constraints from oxygen isotopes. *Journal of Geophysical Research: Atmospheres,* 110**,** n/a-n/a.

AQEG 2004. Nitrogen Dioxide in the UK. Available: http://www.defra.gov.uk/environment/airquality/aqeg

ATKINSON, R. W., BARRATT, B., ARMSTRONG, B., ANDERSON, H. R., BEEVERS, S. D., MUDWAY, I. S., GREEN, D., DERWENT, R. G., WILKINSON, P., TONNE, C. & KELLY, F. J. 2009. The impact of the congestion charging scheme on ambient air pollution concentrations in London. *Atmospheric Environment,* 43**,** 5493-5500.

ATKINSON, R. W., KANG, S., ANDERSON, H. R., MILLS, I. C. & WALTON, H. A. 2014. Epidemiological time series studies of PM 2.5 and daily mortality and hospital admissions: a systematic review and meta-analysis. *Thorax***,** 600-665.

AYRES, J. 2010. COMEAP Long-Term Exposure to Air Pollution: Effect on Mortality. *gov.uk.*

BBC. 2014. *Air pollution: High levels to spread across England* [Online]. Available: http://www.bbc.co.uk/news/uk-26844425 [Accessed 10/06/17].

BEY, I., JACOB, D. J., YANTOSCA, R. M., LOGAN, J. A., FIELD, B. D., FIORE, A. M., LI, Q., LIU, H. Y., MICKLEY, L. J. & SCHULTZ, M. G. 2001. Global modeling of tropospheric chemistry with assimilated meteorology: Model description and evaluation. *Journal of Geophysical Research: Atmospheres,* 106**,** 23073-23095.

BUCKLAND, T., BUSH, T., EATON, S., KILROY, E., KENT, A., LOADER, A., MORRIS, R., NORRIS, J., STEDMAN, J., VINCENT, V., WILLIS, P., NEWINGTON, J., WATERMAN, D. 2015. Air pollution in the uk 2014. DEFRA.

CHEN, D., WANG, Y., MCELROY, M. B., HE, K., YANTOSCA, R. M. & LE SAGER, P. 2009. Regional CO pollution and export in China simulated by the high-resolution nested-grid GEOS-Chem model. *Atmospheric Chemistry and Physics,* 9**,** 3825-3839.

CHEN, X., WALKER, J. & GERON, C. 2017. Chromatography related performance of the Monitor for AeRosols and GAses in ambient air (MARGA): laboratory and field-based evaluation. *Atmos. Meas. Tech.,* 10.

CHIN, A. T. H. 1996. Containing air pollution and traffic congestion: Transport policy and the environment in Singapore. *Atmospheric Environment,* 30**,** 787-801.

CROPPER, P. M., HANSEN, J. C. & EATOUGH, D. J. 2013. Measurement of light scattering in an urban area with a nephelometer and PM2.5 FDMS TEOM monitor: Accounting for the effect of water. *Journal of the Air & Waste Management Association,* 63**,** 1004-1011.

DE MEIJ, A., THUNIS, P., BESSAGNET, B. & CUVELIER, C. 2009. The sensitivity of the CHIMERE model to emissions reduction scenarios on air quality in Northern Italy. *Atmospheric Environment,* 43**,** 1897-1907.

DEBELL, L. J., TALBOT, R. W., DIBB, J. E., MUNGER, J. W., FISCHER, E. V. & FROLKING, S. E. 2004. A major regional air pollution event in the northeastern United States caused by

extensive forest fires in Quebec, Canada. *Journal of Geophysical Research-Atmospheres,* 109.

DEFRA 2011. Review of Transboundary Air Pollution: Acidification, Eutrophication, Ground Level Ozone and Heavy Metals in the UK.

DEFRA 2015. Valuing impacts on air quality: Updates in valuing changes in emissions of Oxides of Nitrogen (NOX) and concentrations of Nitrogen Dioxide (NO2).

DERWENT, R. G., DERNIE, J. I. R., DOLLARD, G. J., DUMITREAN, P., MITCHELL, R. F., MURRELLS, T. P., TELLING, S. P. & FIELD, R. A. 2014. Twenty years of continuous high time resolution volatile organic compound monitoring in the United Kingdom from 1993 to 2012. *Atmospheric Environment,* 99**,** 239-247.

DERWENT, R. G., FIELD, R. A., DUMITREAN, P., MURRELLS, T. P. & TELLING, S. P. 2017. Origins and trends in ethane and propane in the United Kingdom from 1993 to 2012. *Atmospheric Environment,* 156**,** 15-23.

DERWENT, R. G., SIMMONDS, P. G., O'DOHERTY, S., GRANT, A., YOUNG, D., COOKE, M. C., MANNING, A. J., UTEMBE, S. R., JENKIN, M. E. & SHALLCROSS, D. E. 2012. Seasonal cycles in short-lived hydrocarbons in baseline air masses arriving at Mace Head, Ireland. *Atmospheric Environment,* 62**,** 89-96.

EEA 2012. Particulate matter from natural sources and related reporting under the EU Air Quality Directive in 2008 and 2009.

EEA 2015. Air Quality In Europe - 2015 Report. *In:* UNION., P. O. O. T. E. (ed.). Luxembourg: European Environment Agency.

EEA. 2016. Development in emissions of different air pollutants [Online]. Available: https://www.eea.europa.eu/data-and-maps/daviz/development-emissions-of-pm2-1#tab-chart_3 [Accessed 10/11/2017].

EEA. 2017. *Air Quality e-Reporting (AQ e-Reporting)* [Online]. Available: https://www.eea.europa.eu/data-and-maps/data/aqereporting-2 [Accessed 29/12/2017].

FAIRLIE, D., DANIEL, J. & ROKJIN, P. 2007. The impact of transpacific transport of mineral dust in the United States. *Atmospheric Environment,* 41**,** 1251-1266.

FRIEDMAN, C. L. & SELIN, N. E. 2012. Long-Range Atmospheric Transport of Polycyclic Aromatic Hydrocarbons: A Global 3-D Model Analysis Including Evaluation of Arctic Sources. *Environmental Science & Technology,* 46**,** 9501-9510.

FRIEDMAN, C. L., ZHANG, Y. & SELIN, N. E. 2014. Climate Change and Emissions Impacts on Atmospheric PAH Transport to the Arctic. *Environmental Science & Technology,* 48**,** 429-437.

GAO, Y. & ZHANG, M. G. 2014. Modeling study on seasonal variation in aerosol extinction properties over China. *Journal of Environmental Sciences,* 26**,** 97-109.

GERBOLES, M., LAGLER, F., REMBGES, D. & BRUN, C. 2003. Assessment of uncertainty of NO2 measurements by the chemiluminescence method and discussion of the quality objective of the NO2 European Directive.: Journal of Environmental Monitoring.

GINOUX, P., PROSPERO, J., TORRES, O. & CHIN, M. 2004. Long-term simulation of global dust distribution with the GOCART model: correlation with North Atlantic Oscillation. Environmental Modelling & Software.

GINOUX, P., PROSPERO, J. M., GILL, T. E., HSU, N. C. & ZHAO, M. 2012. Global-scale attribution of anthropogenic and natural dust sources and their emission rates based on MODIS deep blue aerosol products. *Reviews of Geophysics,* 50.

GONG, L., LEWICKI, R., GRIFFIN, R. J., TITTEL, F. K., LONSDALE, C. R., STEVENS, R. G., PIERCE, J. R., MALLOY, Q. G. J., TRAVIS, S. A., BOBMANUEL, L. M., LEFER, B. L. & FLYNN, J. H. 2013. Role of atmospheric ammonia in particulate matter formation in Houston during summertime. *Atmospheric Environment,* 77**,** 893-900.

GRANGE, S. 2016. *Framework and a collection of functions to allow for maintenance of air quality monitoring data* [Online]. Available: https://github.com/skgrange/smonitor [Accessed 06/06/2017].

GRANGE, S. 2017. *Technical note: smonitor Europe (Version 1.0.1)* [Online]. [Accessed].

GRIGORATOS, T. & MARTINI, G. 2014. Non-exhaust traffic related emissions. Brake and tyre wear PM. European commission: JRC science and policy report.

GUENTHER, A., KARL, T., HARLEY, P., WIEDINMYER, C., PALMER, P. I. & GERON, C. 2006. Estimates of global terrestrial isoprene emissions using MEGAN (Model of Emissions of Gases and Aerosols from Nature). *Atmos. Chem. Phys.,* 6**,** 3181-3210.

GUERREIRO, C., FOLTESCU, V. & DE LEEUW, F. 2014. Air quality status and trends in Europe. *Atmospheric Environment,* 98**,** 376-384.

GUILLAUME, P., MALINA, C., MALINA, R., ASHOK, A., DEDOUSSI, I., EASTHAM, S., SPETH, R. & BARRETT, S. 2017. Public health impacts of excess NO x emissions from Volkswagen diesel passenger vehicles in Germany. *Environmental Research Letters,* 12**,** 034014.

GUILLAUME, P. C. A. R. M. A. A. A. A. I. C. D. A. S. D. E. A. R. L. S. A. S. R. H. B. 2017. Public health impacts of excess NO x emissions from Volkswagen diesel passenger vehicles in Germany. *Environmental Research Letters,* 12**,** 034014.

HARRISON, R. H., R 1995. *Volatile Organic Compounds in the Atmosphere*.

HELMIG, D., BOTTENHEIM, J., LEWIS, A., MILTON, M., PLASS, C., REIMANN, S., TANS, P. & THIEL, S. 2009. Volatile Organic Compounds in the Global Atmosphere. *EOS.*

HOLMES, C. D., JACOB, D. J., CORBITT, E. S., MAO, J., YANG, X., TALBOT, R. & SLEMR, F. 2010. Global atmospheric model for mercury including oxidation by bromine atoms. *Atmos. Chem. Phys.,* 10**,** 12037-12057.

HOU, P. & WU, S. 2016. Long-term Changes in Extreme Air Pollution Meteorology and the Implications for Air Quality. 6**,** 23792.

HU, L., JACOB, D. J., LIU, X., ZHANG, Y., ZHANG, L., KIM, P. S., SULPRIZIO, M. P. & YANTOSCA, R. M. 2017. Global budget of tropospheric ozone: Evaluating recent model advances with satellite (OMI), aircraft (IAGOS), and ozonesonde observations. *Atmospheric Environment,* 167**,** 323-334.

INDEPENDENT 2014. Smog expert: Worsening Saharan dust storms to become an annual Spring fixture as climate changes.

JACOB, D. 1999. *Introduction to Atmospheric Chemistry*, Princeton University Press.

JAEGLÉ, L., QUINN, P. K., BATES, T. S., ALEXANDER, B. & LIN, J. T. 2011. Global distribution of sea salt aerosols: new constraints from in situ and remote sensing observations. *Atmos. Chem. Phys.,* 11**,** 3137-3157.

JAENICKE, R. 2005. Abundance of cellular material and proteins in the atmosphere. *Science,* 308**,** 73-73.

JENNINGS, S. G., SPAIN, T. G., DODDRIDGE, B. G., MARING, H., KELLY, B. P. & HANSEN, A. D. A. 1996. Concurrent measurements of black carbon aerosol and carbon monoxide at Mace Head. *Journal of Geophysical Research: Atmospheres,* 101**,** 19447-19454.

JHUN, I. C., B. ZANOBETTI, A. KOUTRAKIS, P. 2015. The impact of nitrogen oxides concentration decreases on ozone trends in the USA.

JOHNSON, M. S., MESKHIDZE, N. & PRAJU KILIYANPILAKKIL, V. C. M. 2012. A global comparison of GEOS-Chem-predicted and remotely-sensed mineral dust aerosol optical depth and extinction profiles. *Journal of Advances in Modeling Earth Systems,* 4**,** n/a-n/a.

KANSAL, A. 2009. Sources and reactivity of NMHCs and VOCs in the atmosphere: A review. *Journal of Hazardous Materials,* 166**,** 17-26.

KELLER, A., LONG , M., YANTOSCA , R., DA SILVA, A., PAWSON, S. & JACOB, D. 2014. HEMCO v1.0: a versatile, ESMF-compliant component for calculating emissions in atmospheric models. *Geosci. Model Dev.* 1417 ed.

LEE, J. D., LEWIS, A. C., MONKS, P. S., JACOB, M., HAMILTON, J. F., HOPKINS, J. R., WATSON, N. M., SAXTON, J. E., ENNIS, C., CARPENTER, L. J., CARSLAW, N., FLEMING, Z., BANDY, B. J., ORAM, D. E., PENKETT, S. A., SLEMR, J., NORTON, E., RICKARD, A. R., WHALLEY, L. K., HEARD, D. E., BLOSS, W. J., GRAVESTOCK, T., SMITH, S. C., STANTON, J., PILLING, M. J. & JENKIN, M. E. 2006. Ozone photochemistry and elevated isoprene during the UK heatwave of August 2003. *Atmospheric Environment,* 40**,** 7598-7613.

LELIEVELD, J. & DENTENER, F. J. 2000. What controls tropospheric ozone? *Journal of Geophysical Research: Atmospheres,* 105**,** 3531-3551.

LELIEVELD, J., EVANS, J. S., FNAIS, M., GIANNADAKI, D. & POZZER, A. 2015. The contribution of outdoor air pollution sources to premature mortality on a global scale. *Nature,* 525**,** 367-371.

LIU, H., CRAWFORD, J. H., PIERCE, R. B., NORRIS, P., PLATNICK, S. E., CHEN, G., LOGAN, J. A., YANTOSCA, R. M., EVANS, M. J., KITTAKA, C., FENG, Y. & TIE, X. C. D. 2006. Radiative effect of clouds on tropospheric chemistry in a global three-dimensional chemical transport model. *Journal of Geophysical Research: Atmospheres,* 111**,** n/a-n/a.

LIU, H., JACOB, D. J., BEY, I. & YANTOSCA, R. M. 2001. Constraints from 210Pb and 7Be on wet deposition and transport in a global three-dimensional chemical tracer model driven by assimilated meteorological fields. *Journal of Geophysical Research: Atmospheres,* 106**,** 12109-12128.

MAIONE, M., FOWLER, D., MONKS, P. S., REIS, S., RUDICH, Y., WILLIAMS, M. L. & FUZZI, S. 2016. Air quality and climate change: Designing new win-win policies for Europe. *Environmental Science & Policy,* 65**,** 48-57.

MALLEY, C. S., HEAL, M. R., BRABAN, C. F., KENTISBEER, J., LEESON, S. R., MALCOLM, H., LINGARD, J. J. N., RITCHIE, S., MAGGS, R., BECCACECI, S., QUINCEY, P., BROWN, R. J. C. & TWIGG, M. M. 2016. The contributions to long-term health-relevant particulate matter at the UK EMEP supersites between 2010 and 2013: Quantifying the mitigation challenge. *Environment International,* 95**,** 98-111.

MAO, J. Q., PAULOT, F., JACOB, D. J., COHEN, R. C., CROUNSE, J. D., WENNBERG, P. O., KELLER, C. A., HUDMAN, R. C., BARKLEY, M. P. & HOROWITZ, L. W. 2013. Ozone and

organic nitrates over the eastern United States: Sensitivity to isoprene chemistry. *Journal of Geophysical Research-Atmospheres,* 118**,** 11256-11268.

MARGA. 2017. *Continuous monitoring of aerosols and gases in ambient air* [Online]. Available: https://www.metrohm.com/en-gb/products-overview/process-analyzers/applikon-marga/ [Accessed 14/08/2017].

MARTIN, R. V., JACOB, D. J., YANTOSCA, R. M., CHIN, M. & GINOUX, P. C. 2003. Global and regional decreases in tropospheric oxidants from photochemical effects of aerosols. *Journal of Geophysical Research: Atmospheres,* 108**,** n/a-n/a.

MONKS, P., APSIMON, H., CARUTTHERS, D., CARSLAW, D., DERWENT, D., HARRISON, R., LAXEN, D. & STEDMAN, J. 2012. Fine Particulate Matter (PM2.5) in the United Kingdom. DEFRA.

MORÁN, M., FERREIRA, J., MARTINS, H., MONTEIRO, A., BORREGO, C. & GONZÁLEZ, J. A. 2016. Ammonia agriculture emissions: From EMEP to a high resolution inventory. *Atmospheric Pollution Research,* 7**,** 786-798.

NASSAR, R., NAPIER-LINTON, L., GURNEY, K. R., ANDRES, R. J., ODA, T., VOGEL, F. R. & DENG, F. 2013. Improving the temporal and spatial distribution of CO2 emissions from global fossil fuel emission data sets. *Journal of Geophysical Research: Atmospheres,* 118**,** 917-933.

NOAA. 2013. *GAW - Data Access* [Online]. Available: https://www.ncdc.noaa.gov/gaw-data-access [Accessed 06/06/2017].

PARLIAMENT, E. 2008. DIRECTIVE 2008/50/EC OF THE EUROPEAN PARLIAMENT AND OF THE COUNCIL on ambient air quality and cleaner air for Europe.

PLATT, U. F., WINER, A. M., BIERMANN, H. W., ATKINSON, R. & PITTS, J. N. 1984. Measurement of nitrate radical concentrations in continental air. *Environmental Science & Technology,* 18**,** 365-369.

READ, K. A., MAHAJAN, A. S., CARPENTER, L. J., EVANS, M. J., FARIA, B. V. E., HEARD, D. E., HOPKINS, J. R., LEE, J. D., MOLLER, S. J., LEWIS, A. C., MENDES, L., MCQUAID, J. B., OETJEN, H., SAIZ-LOPEZ, A., PILLING, M. J. & PLANE, J. M. C. 2008. Extensive halogen-mediated ozone destruction over the tropical Atlantic Ocean. *Nature,* 453**,** 1232.

REINHART, W. & MILLET, D. 2011. Implementation of the RETRO Anthropogenic Emission Inventory into the GEOS-Chem Model.

RIEDER, H. E., FIORE, A. M., HOROWITZ, L. W. & NAIK, V. 2015. Projecting policy-relevant metrics for high summertime ozone pollution events over the eastern United States due to climate and emission changes during the 21st century. *Journal of Geophysical Research-Atmospheres,* 120**,** 784-800.

ROCHETTE, P., ANGERS, D. A., CHANTIGNY, M. H., GASSER, M.-O., MACDONALD, J. D., PELSTER, D. E. & BERTRAND, N. 2013. NH3 volatilization, soil concentration and soil pH following subsurface banding of urea at increasing rates. *Canadian Journal of Soil Science,* 93**,** 261-268.

RUMSEY, I. C., COWEN, K. A., WALKER, J. T., KELLY, T. J., HANFT, E. A., MISHOE, K., ROGERS, C., PROOST, R., BEACHLEY, G. M., LEAR, G., FRELINK, T. & OTJES, R. P. 2014. An assessment of the performance of the Monitor for AeRosols and GAses in ambient air (MARGA): a semi-continuous method for soluble compounds. *Atmos. Chem. Phys.,* 14**,** 5639-5658.

SAARIKOSKI, S. K., SILLANPÄÄ, M. K., SAARNIO, K. M., HILLAMO, R. E., PENNANEN, A. S. & SALONEN, R. O. 2008. Impact of Biomass Combustion on Urban Fine Particulate Matter in Central and Northern Europe. *Water, Air, and Soil Pollution,* 191**,** 265-277.

SHERWEN, T., EVANS, M. J., SOMMARIVA, R., HOLLIS, L. D. J., BALL, S. M., MONKS, P. S., REED, C. P., CARPENTER, L. J., LEE, J. D., FORSTER, G., BANDY, B. J., REEVES, C. E. & BLOSS, W. J. 2017. Effects of halogens on European air-quality. *FARADAY DISCUSSIONS*.

SHERWEN, T., SCHMIDT, J. A., EVANS, M. J., CARPENTER, L. J., GROSSMANN, K., EASTHAM, S. D., JACOB, D. J., DIX, B., KOENIG, T. K., SINREICH, R., ORTEGA, I., VOLKAMER, R., SAIZ-LOPEZ, A., PRADOS-ROMAN, C., MAHAJAN, A. S. & ORDONEZ, C. 2016a. Global impacts of tropospheric halogens (Cl, Br, I) on oxidants and composition in GEOS-Chem. *Atmospheric Chemistry and Physics,* 16**,** 12239-12271.

SHERWEN, T., SCHMIDT, J. A., EVANS, M. J., CARPENTER, L. J., GROßMANN, K., EASTHAM, S. D., JACOB, D. J., DIX, B., KOENIG, T. K., SINREICH, R., ORTEGA, I., VOLKAMER, R., SAIZ-LOPEZ, A., PRADOS-ROMAN, C., MAHAJAN, A. S. & ORDÓÑEZ, C. 2016b. Global impacts of tropospheric halogens (Cl, Br, I) on oxidants and composition in GEOS-Chem. *Atmos. Chem. Phys.,* 16**,** 12239-12271.

SKJØTH, C. A., GEELS, C., BERGE, H., GYLDENKÆRNE, S., FAGERLI, H., ELLERMANN, T., FROHN, L. M., CHRISTENSEN, J., HANSEN, K. M., HANSEN, K. & HERTEL, O. 2011. Spatial and temporal variations in ammonia emissions – a freely accessible model code for Europe. *Atmos. Chem. Phys.,* 11**,** 5221-5236.

SOFEN, E. D., BOWDALO, D., EVANS, M. J., APADULA, F., BONASONI, P., CUPEIRO, M., ELLUL, R., GALBALLY, I. E., GIRGZDIENE, R., LUPPO, S., MIMOUNI, M., NAHAS, A. C., SALIBA, M. & TØRSETH, K. 2016. Gridded global surface ozone metrics for atmospheric chemistry model evaluation. *Earth Syst. Sci. Data,* 8**,** 41-59.

STAVRAKOU, T., MÜLLER, J. F., BOERSMA, K. F., VAN DER A, R. J., KUROKAWA, J., OHARA, T. & ZHANG, Q. 2013. Key chemical NO_x sink uncertainties and how they influence top-down emissions of nitrogen oxides. *Atmos. Chem. Phys.,* 13**,** 9057-9082.

STEINBACHER, M., ZELLWEGER, C., SCHWARZENBACH, B., BUGMANN, S., BUCHMANN, B., ORDÓÑEZ, C., PREVOT, A. S. H. & HUEGLIN, C. C. D. 2007. Nitrogen oxide measurements at rural sites in Switzerland: Bias of conventional measurement techniques. *Journal of Geophysical Research: Atmospheres,* 112**,** n/a-n/a.

STEVENSON, D. S., DENTENER, F. J., SCHULTZ, M. G., ELLINGSEN, K., VAN NOIJE, T. P. C., WILD, O., ZENG, G., AMANN, M., ATHERTON, C. S., BELL, N., BERGMANN, D. J., BEY, I., BUTLER, T., COFALA, J., COLLINS, W. J., DERWENT, R. G., DOHERTY, R. M., DREVET, J., ESKES, H. J., FIORE, A. M., GAUSS, M., HAUGLUSTAINE, D. A., HOROWITZ, L. W., ISAKSEN, I. S. A., KROL, M. C., LAMARQUE, J. F., LAWRENCE, M. G., MONTANARO, V., MÜLLER, J. F., PITARI, G., PRATHER, M. J., PYLE, J. A., RAST, S., RODRIGUEZ, J. M., SANDERSON, M. G., SAVAGE, N. H., SHINDELL, D. T., STRAHAN, S. E., SUDO, K. & SZOPA, S. C. D. 2006. Multimodel ensemble simulations of present-day and near-future tropospheric ozone. *Journal of Geophysical Research: Atmospheres,* 111**,** n/a-n/a.

STIEGER, B., SPINDLER, G., FAHLBUSCH, B., MÜLLER, K., GRÜNER, A., POULAIN, L., THÖNI, L., SEITLER, E., WALLASCH, M. & HERRMANN, H. 2017. Measurements of

PM10 ions and trace gases with the online system MARGA at the research station Melpitz in Germany – A five-year study. *Journal of Atmospheric Chemistry*.

STREETS, D., FU, J., JANG, C., HAO, J., HE, K., TANG, X., ZHANG, Y., WANG, Z., LI, Z., ZHANG, Q., WANG, L., WANG, B. & YU, C. 2007. Air quality during the 2008 Beijing Olympic Games. *Atmospheric Environment,* 41**,** 480-492.

SUAREZ, M., RIENECKER, M., TODLING, R., BACMEISTER, J., TAKACS, L., LIU, H., GU, W., SIENKIEWICZ, M., KOSTER, R. & GELARO, R. 2008. The GEOS-5 Data Assimilation System - Documentation of Versions 5.0.1, 5.1.0, and 5.2.0.

TEGEN, I. & FUNG, I. 1995. CONTRIBUTION TO THE ATMOSPHERIC MINERAL AEROSOL LOAD FROM LAND-SURFACE MODIFICATION. *Journal of Geophysical Research-Atmospheres,* 100**,** 18707-18726.

TORSETH, K., AAS, W., BREIVIK, K., FJAERAA, A. M., FIEBIG, M., HJELLBREKKE, A. G., MYHRE, C. L., SOLBERG, S. & YTTRI, K. E. 2012. Introduction to the European Monitoring and Evaluation Programme (EMEP) and observed atmospheric composition change during 1972-2009. *Atmospheric Chemistry and Physics,* 12**,** 5447-5481.

TRAVIS, K. R., JACOB, D. J., FISHER, J. A., KIM, P. S., MARAIS, E. A., ZHU, L., YU, K., MILLER, C. C., YANTOSCA, R. M., SULPRIZIO, M. P., THOMPSON, A. M., WENNBERG, P. O., CROUNSE, J. D., ST CLAIR, J. M., COHEN, R. C., LAUGHNER, J. L., DIBB, J. E., HALL, S. R., ULLMANN, K., WOLFE, G. M., POLLACK, I. B., PEISCHL, J., NEUMAN, J. A. & ZHOU, X. L. 2016. Why do models overestimate surface ozone in the Southeast United States? *Atmospheric Chemistry and Physics,* 16**,** 13561-13577.

TWIGG, M. M., DI MARCO, C. F., LEESON, S., VAN DIJK, N., JONES, M. R., LEITH, I. D., MORRISON, E., COYLE, M., PROOST, R., PEETERS, A. N. M., LEMON, E., FRELINK, T., BRABAN, C. F., NEMITZ, E. & CAPE, J. N. 2015. Water soluble aerosols and gases at a UK background site – Part 1: Controls of PM_{2.5} and PM₁₀ aerosol composition. *Atmos. Chem. Phys.,* 15**,** 8131-8145.

VAUGHAN, A. R., LEE, J. D., MISZTAL, P. K., METZGER, S., SHAW, M. D., LEWIS, A. C., PURVIS, R. M., CARSLAW, D. C., GOLDSTEIN, A. H., HEWITT, C. N., DAVISON, B., BEEVERS, S. D. & KARL, T. G. 2016. Spatially resolved flux measurements of NOx from London suggest significantly higher emissions than predicted by inventories. *Faraday Discussions,* 189**,** 455-472.

VIENO, M., HEAL, M. R., HALLSWORTH, S., FAMULARI, D., DOHERTY, R. M., DORE, A. J., TANG, Y. S., BRABAN, C. F., LEAVER, D., SUTTON, M. A. & REIS, S. 2014. The role of long-range transport and domestic emissions in determining atmospheric secondary inorganic particle concentrations across the UK. *Atmospheric Chemistry and Physics,* 14**,** 8435-8447.

VIENO, M., HEAL, M. R., TWIGG, M. M., MACKENZIE, I. A., BRABAN, C. F., LINGARD, J. J. N., RITCHIE, S., BECK, R. C., MORING, A., OTS, R., DI MARCO, C. F., NEMITZ, E., SUTTON, M. A. & REIS, S. 2016. The UK particulate matter air pollution episode of March-April 2014: more than Saharan dust. *Environmental Research Letters,* 11**,** 12.

WALTON, H., DAJNAKM D, BEEVERS, S., WILLIAMS, M., WATKISS, P. & HUNT, A. 2015. *Understanding the Health Impacts of Air Pollution in London* . Understanding the Health Impacts of Air Pollution in London .

WANG, S. X., ZHAO, M., XING, J., WU, Y., ZHOU, Y., LEI, Y., HE, K. B., FU, L. X. & HAO, J. M. 2010. Quantifying the Air Pollutants Emission Reduction during the 2008 Olympic Games in Beijing. *Environmental Science & Technology,* 44**,** 2490-2496.

WANG, Y., JACOB, D. & LOGAN, J. 1998. Global simulation of tropospheric O_3-NO_x-hydrocarbon chemistry. Journal of Geophysical Research.

WANG, Y. S., YAO, L., WANG, L. L., LIU, Z. R., JI, D. S., TANG, G. Q., ZHANG, J. K., SUN, Y., HU, B. & XIN, J. Y. 2014. Mechanism for the formation of the January 2013 heavy haze pollution episode over central and eastern China. *Science China-Earth Sciences,* 57**,** 14-25.

WANG, Y. X., MCELROY, M. B., JACOB, D. J. & YANTOSCA, R. M. C. D. 2004. A nested grid formulation for chemical transport over Asia: Applications to CO. *Journal of Geophysical Research: Atmospheres,* 109.

WHO 2006. Air Quality Guidelines Global Update 2005 Guidelines Particulate matter, ozone, nitrogen dioxide and sulfur dioxide.

WHO 2016. Ambient air pollution: A global assessment of exposure and burden of disease.

XING, Y. X., Y. SHI, M. LIAN, Y. 2016. The impact of PM2.5 on the human respiratory system.

XU, P., LIAO, Y., LIN, Y., ZHAO, C., YAN, C., CAO, M., WANG, G. & LUAN, S. 2016. High-resolution inventory of ammonia emissions from agricultural fertilizer in China from 1978 to 2008. ACP.

YAN, Y., LIN, J., CHEN, J. & HU, L. 2016. Improved simulation of tropospheric ozone by a global-multi-regional two-way coupling model system. *Atmos. Chem. Phys.,* 16**,** 2381-2400.

YAN, Y. Y., LIN, J. T., KUANG, Y., YANG, D. & ZHANG, L. 2014. Tropospheric carbon monoxide over the Pacific during HIPPO: two-way coupled simulation of GEOS-Chem and its multiple nested models. *Atmos. Chem. Phys.,* 14**,** 12649-12663.

YIN, J. & HARRISON, R. M. 2008. Pragmatic mass closure study for PM1.0, PM2.5 and PM10 at roadside, urban background and rural sites. *Atmospheric Environment,* 42**,** 980-988.

YOUNG, P. J., ARCHIBALD, A. T., BOWMAN, K. W., LAMARQUE, J. F., NAIK, V., STEVENSON, D. S., TILMES, S., VOULGARAKIS, A., WILD, O., BERGMANN, D., CAMERON-SMITH, P., CIONNI, I., COLLINS, W. J., DALSØREN, S. B., DOHERTY, R. M., EYRING, V., FALUVEGI, G., HOROWITZ, L. W., JOSSE, B., LEE, Y. H., MACKENZIE, I. A., NAGASHIMA, T., PLUMMER, D. A., RIGHI, M., RUMBOLD, S. T., SKEIE, R. B., SHINDELL, D. T., STRODE, S. A., SUDO, K., SZOPA, S. & ZENG, G. 2013. Pre-industrial to end 21st century projections of tropospheric ozone from the Atmospheric Chemistry and Climate Model Intercomparison Project (ACCMIP). *Atmos. Chem. Phys.,* 13**,** 2063-2090.

ZHANG, B., WANG, Y. & HAO, J. 2015. Simulating aerosol–radiation–cloud feedbacks on meteorology and air quality over eastern China under severe haze conditions in winter. *Atmos. Chem. Phys.,* 15**,** 2387-2404.

ZHANG, L., GONG, S., PADRO, J. & BARRIE, L. 2001. A size-segregated particle dry deposition scheme for an atmospheric aerosol module. *Atmospheric Environment,* 35**,** 549-560.

ZHANG, L., JACOB, D. J., DOWNEY, N. V., WOOD, D. A., BLEWITT, D., CAROUGE, C. C., VAN DONKELAAR, A., JONES, D. B. A., MURRAY, L. T. & WANG, Y. 2011. Improved estimate of the policy-relevant background ozone in the United States using the GEOS-Chem global model with 1/2° × 2/3° horizontal resolution over North America. *Atmospheric Environment,* 45**,** 6769-6776.

ZHANG, L., SHAO, J. Y., LU, X., ZHAO, Y. H., HU, Y. Y., HENZE, D. K., LIAO, H., GONG, S. L. & ZHANG, Q. 2016. Sources and Processes Affecting Fine Particulate Matter Pollution over North China: An Adjoint Analysis of the Beijing APEC Period. *Environmental Science & Technology,* 50**,** 8731-8740.